Ocean response to offshore wind farms off the Coast of New England

César Sauvage & Co-Authors

University of Hawai’i at Manoa, HI,USA

Oceanography Seminar
May 7, 2026

Contact: csauvage@hawaii.edu

Introduction

Offshore wind resources map (~100 m height)

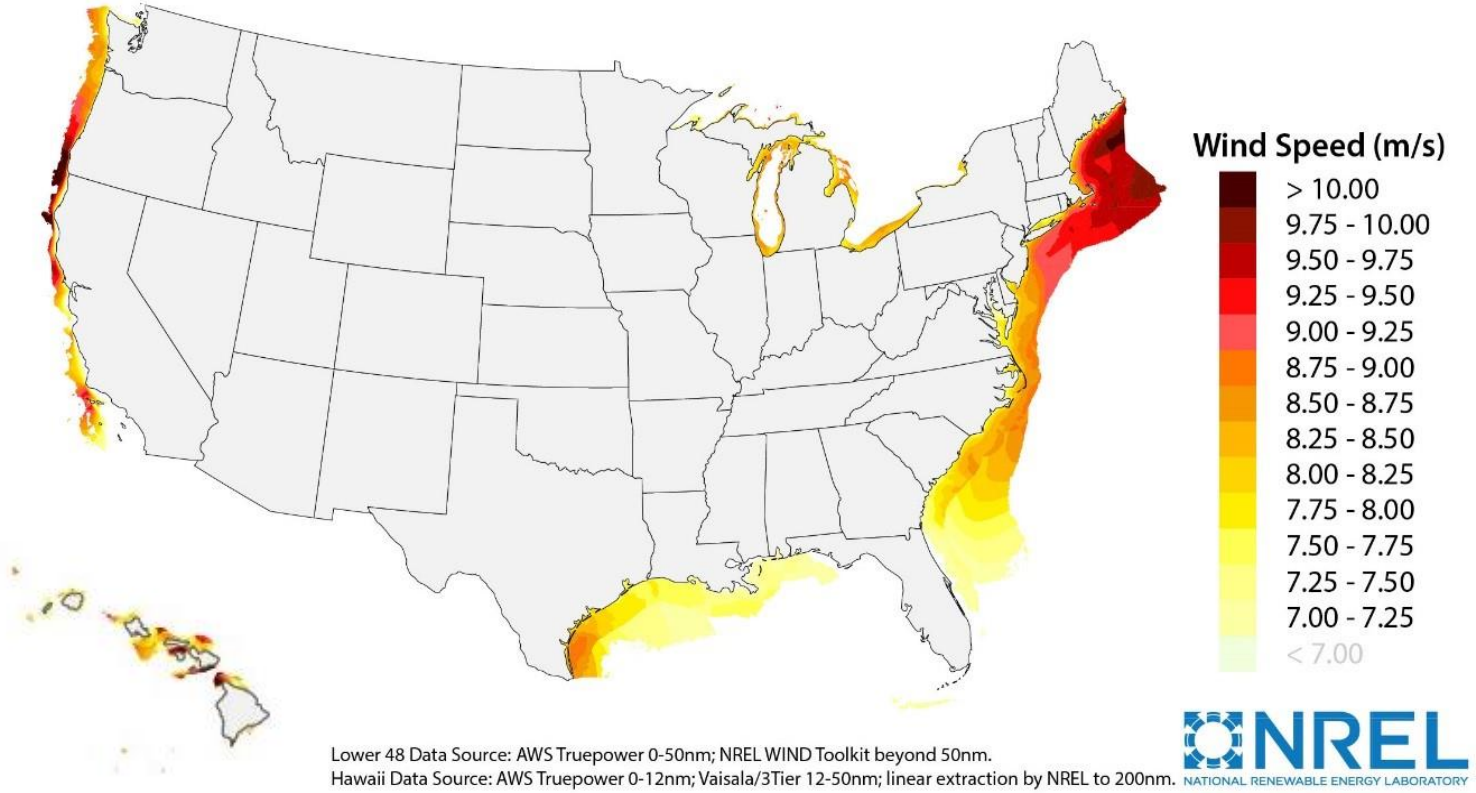

Introduction

Offshore wind resources map (~100 m height)

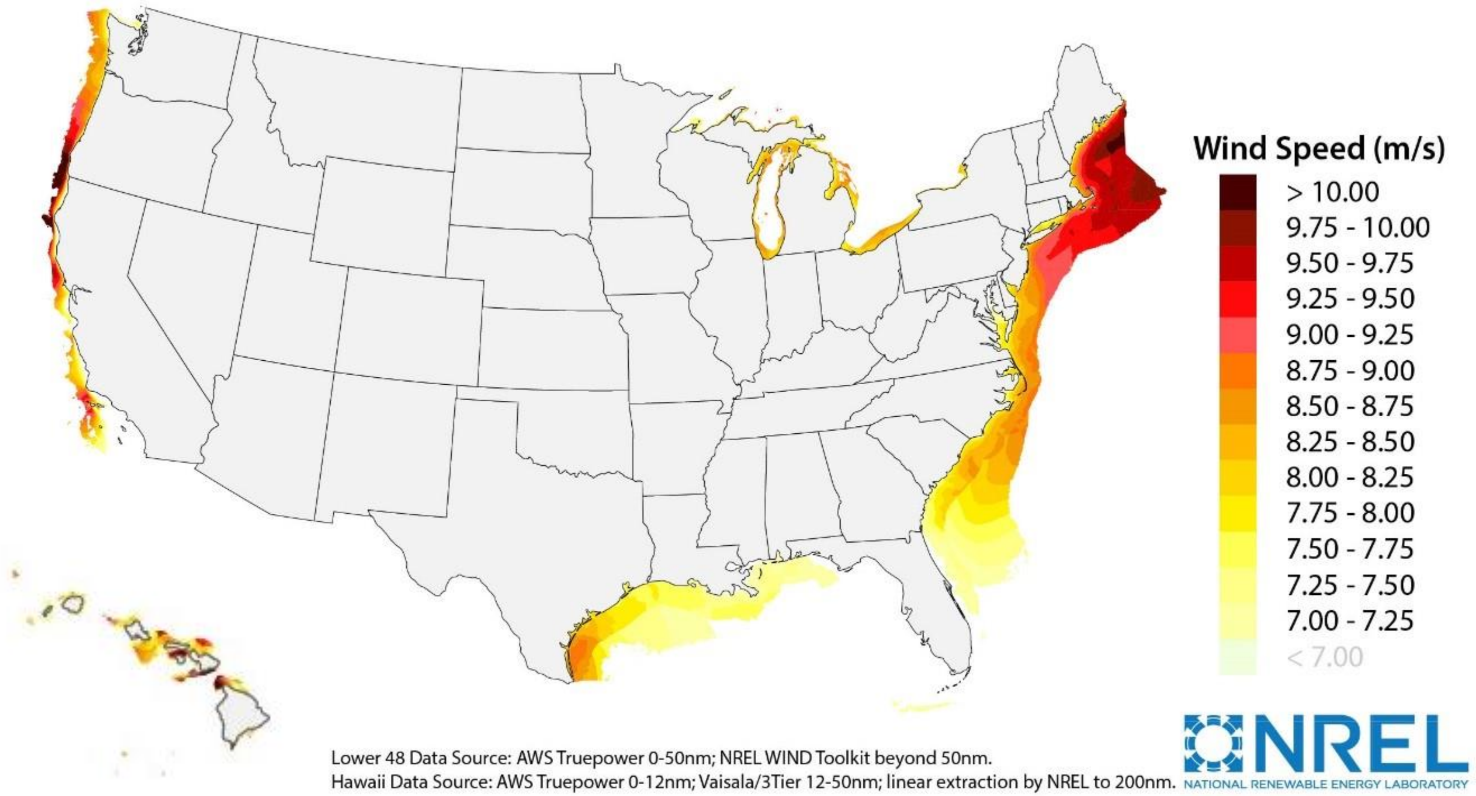

Previous administrations goals to produce electricity from offshore wind:

- 30GW by 2030 **(2.5K turbines)**

Introduction

Offshore wind resources map (~100 m height)

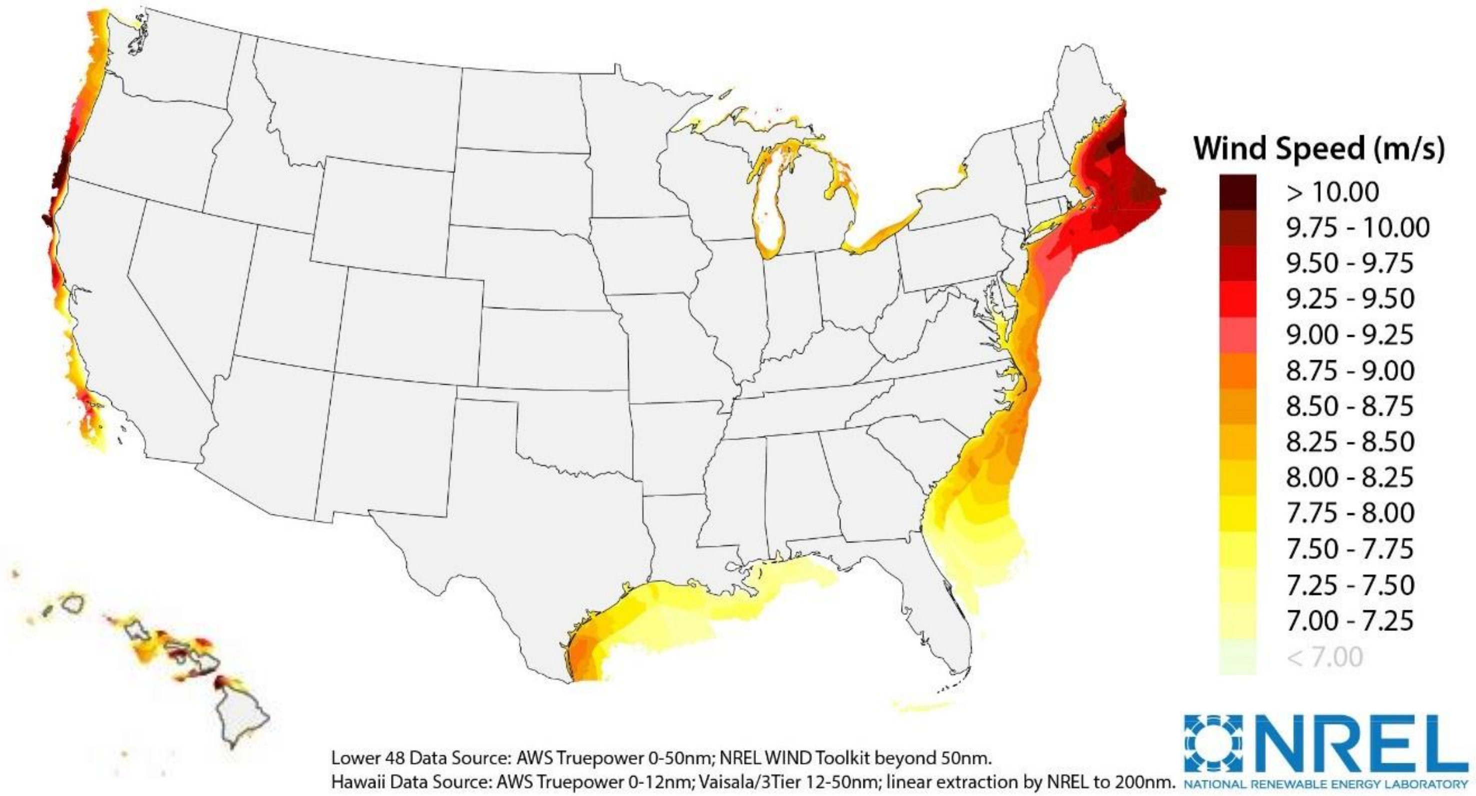

Previous administrations goals to produce electricity from offshore wind:

- 30GW by 2030 **(2.5K turbines)**
- 3000 GW by 2050..! **(250K turbines)**

Introduction

Offshore wind resources map (~100 m height)

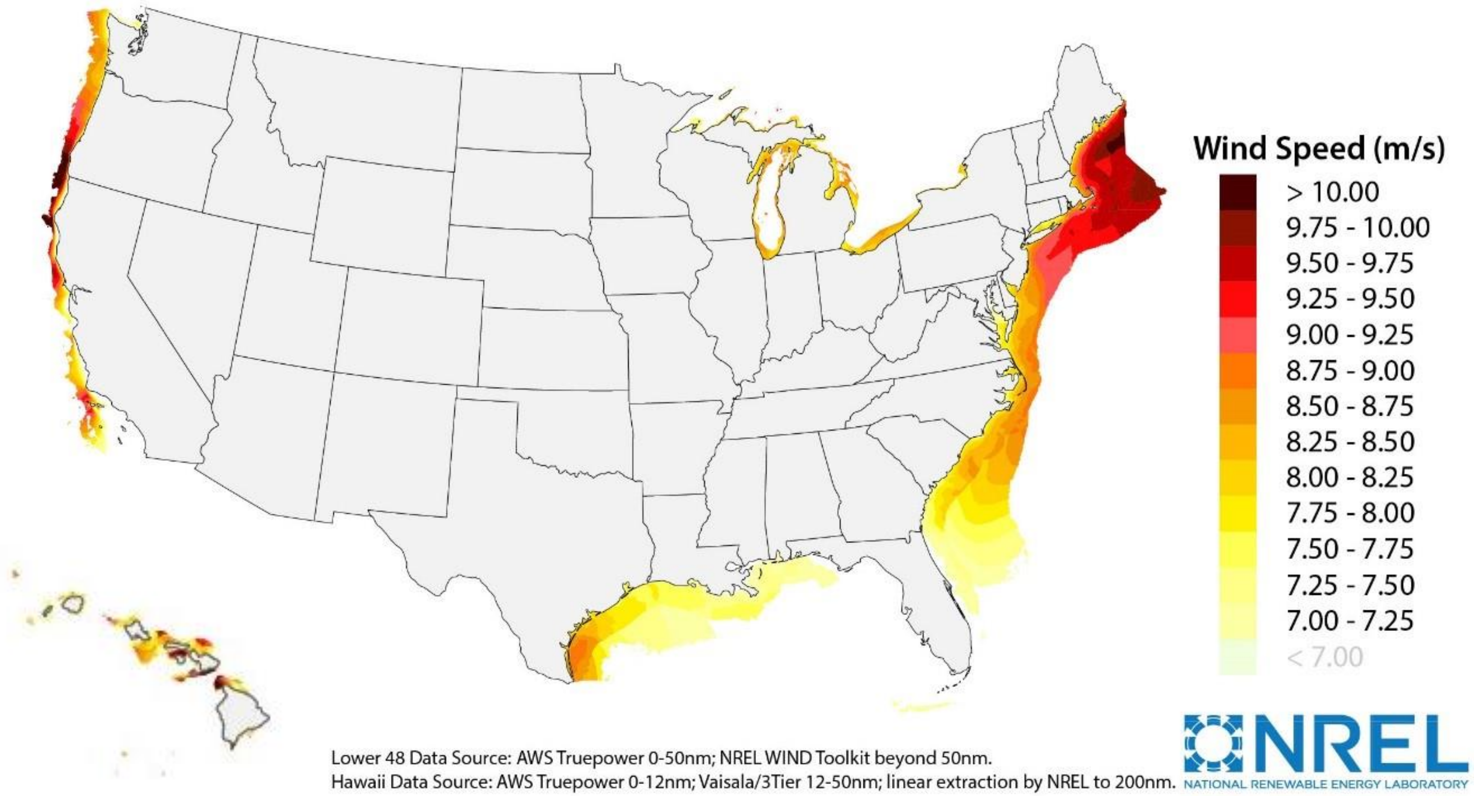

Previous administrations goals to produce electricity from offshore wind:

- 30GW by 2030 **(2.5K turbines)**
- 3000 GW by 2050..! **(250K turbines)**

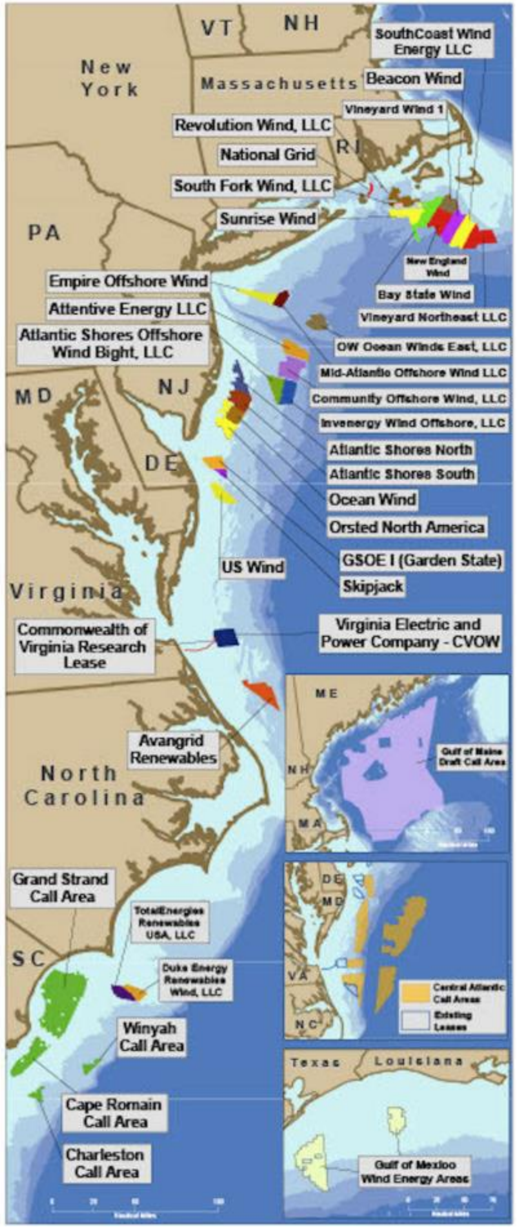

© BOEM

Introduction

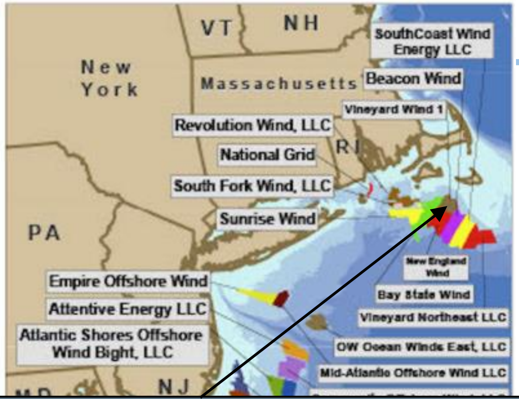

Offshore wind resources map (~100 m height)

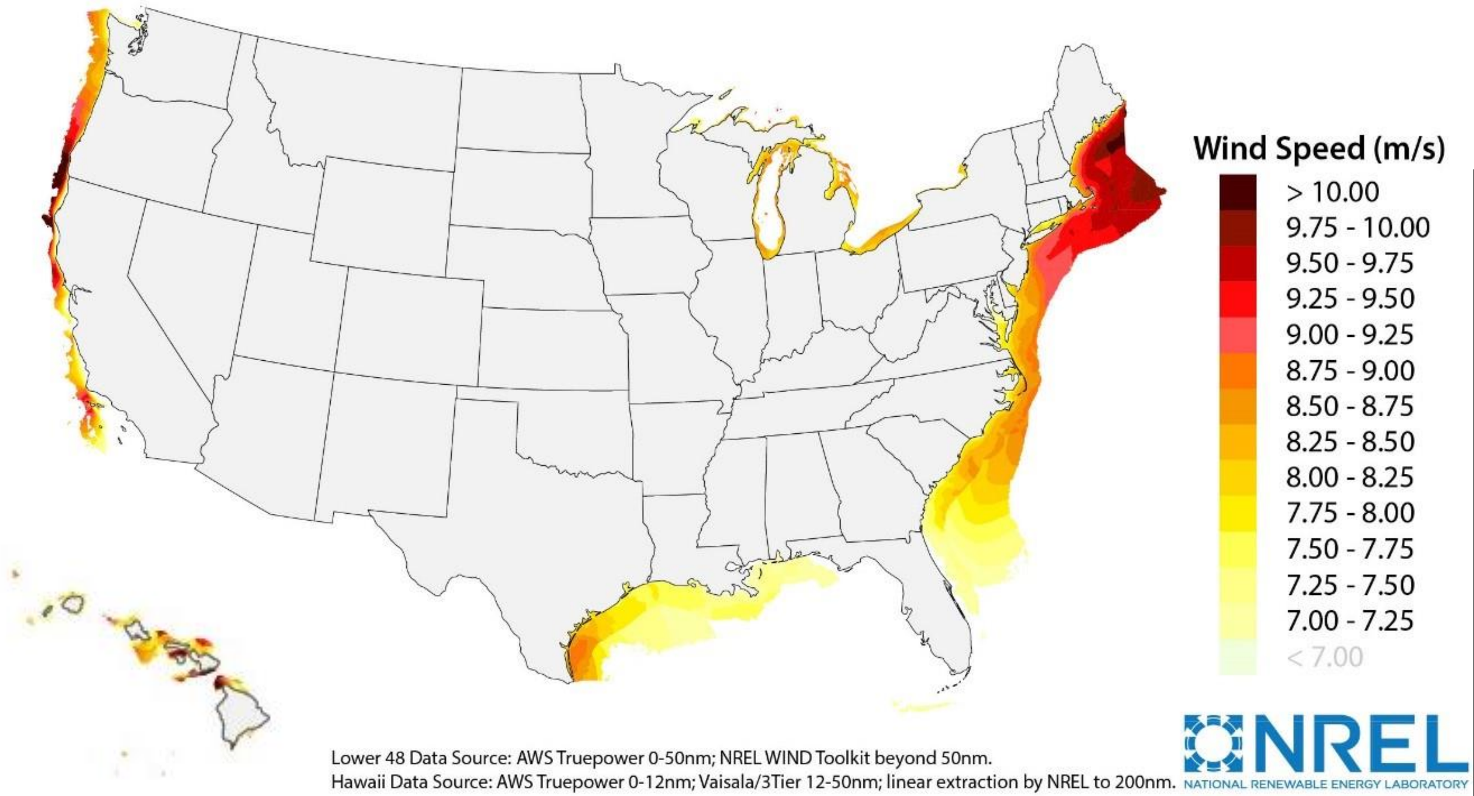


Wind turbines operate at Vineyard Wind 1 offshore wind farm off the coast of Massachusetts.

Previous administrations goals to produce electricity from offshore wind:

- 30GW by 2030 **(2.5K turbines)**
- 3000 GW by 2050..! **(250K turbines)**

As of now, it has 62 turbines that will generate a total of 800 megawatts. That is enough electricity to power about 400,000 homes.

WFIP3 DOE project: Observation component

The third Wind Forecast Improvement Project (WFIP3), November 2023-August 2025

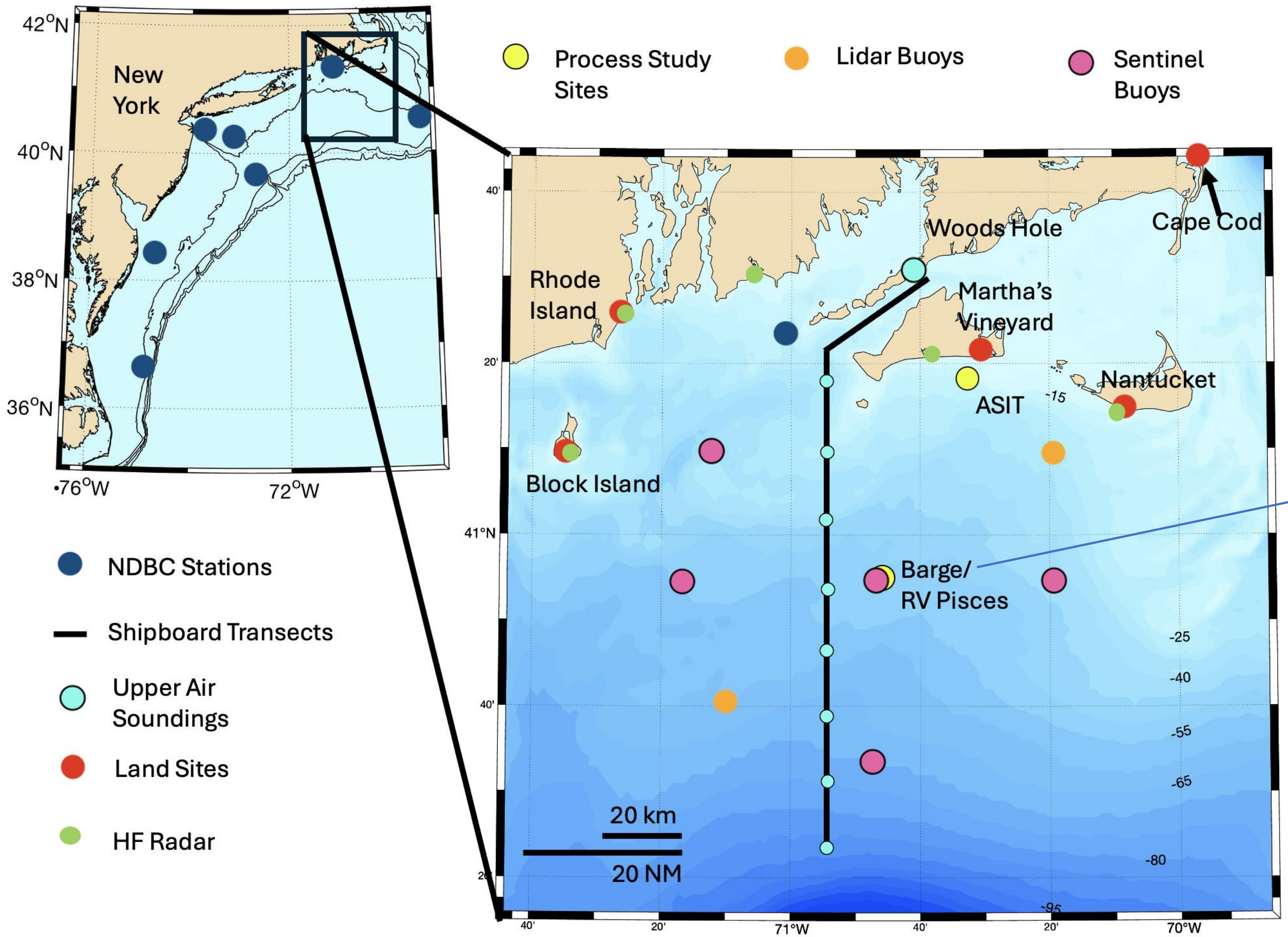

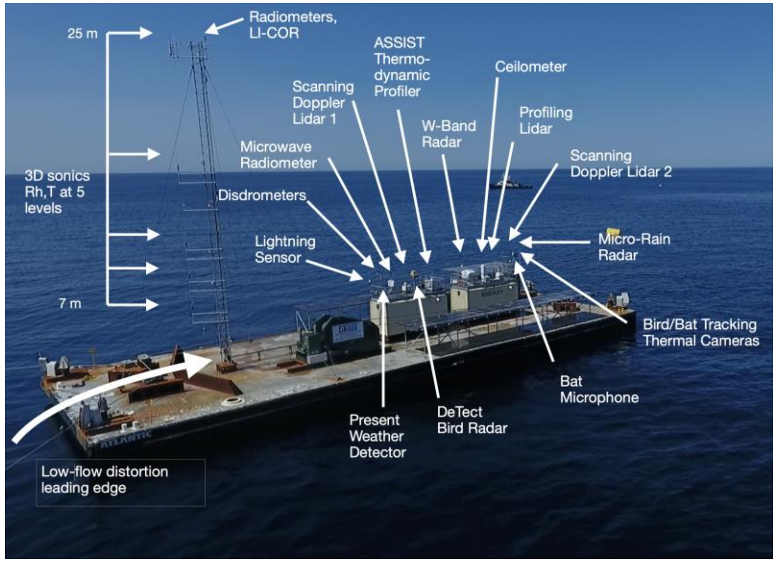

A 46-m barge was moored, completing 85 days of unattended sampling on-station.

WFIP3 DOE project: Modeling component

Studied Period: Summers 2017/2018/2019/2020/2021 (JJA)

A total of **1418** wind turbines.

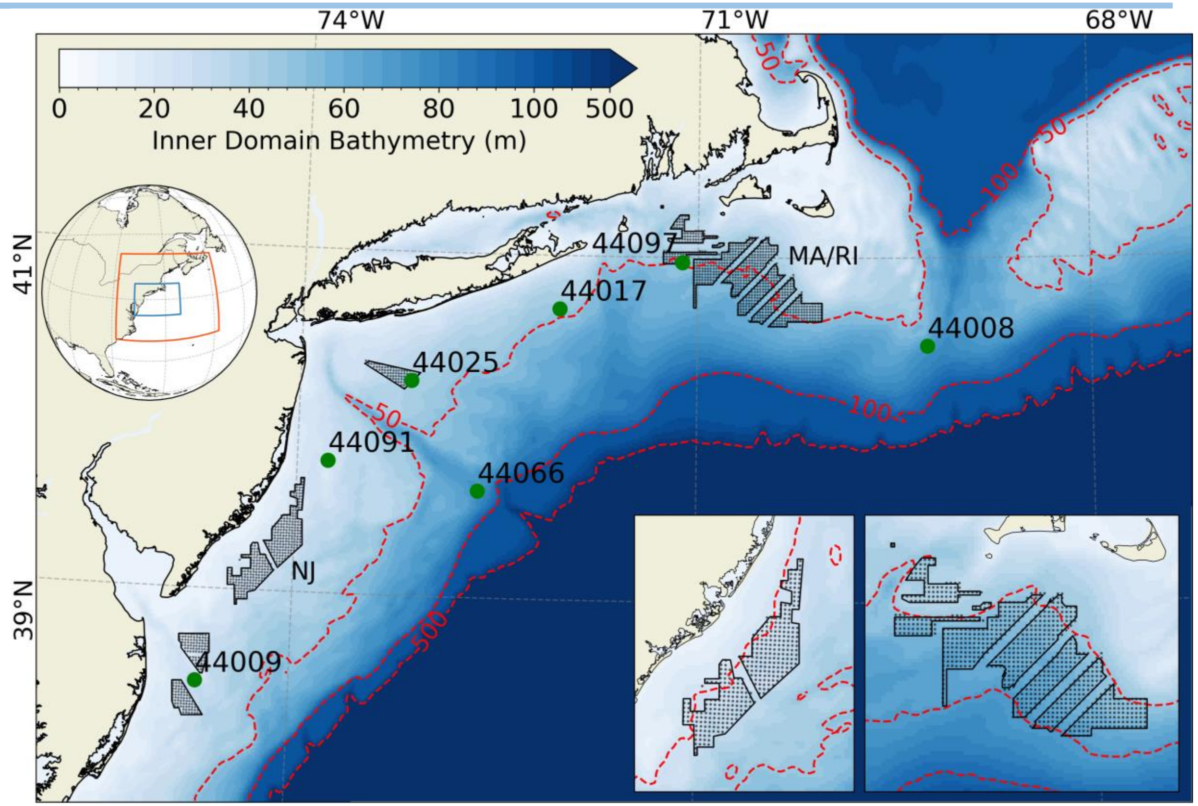

WFIP3 DOE project: Modeling component

Studied Period: Summers 2017/2018/2019/2020/2021 (JJA)

A total of **1418** wind turbines.

1.5 km high resolution WRF-ROMS-WW3 coupled modeling

The Fitch parameterization (Fitch et al. 2012) is used to represents wind turbines in the atmosphere.
-> wind turbines are not explicitly represented in the ocean

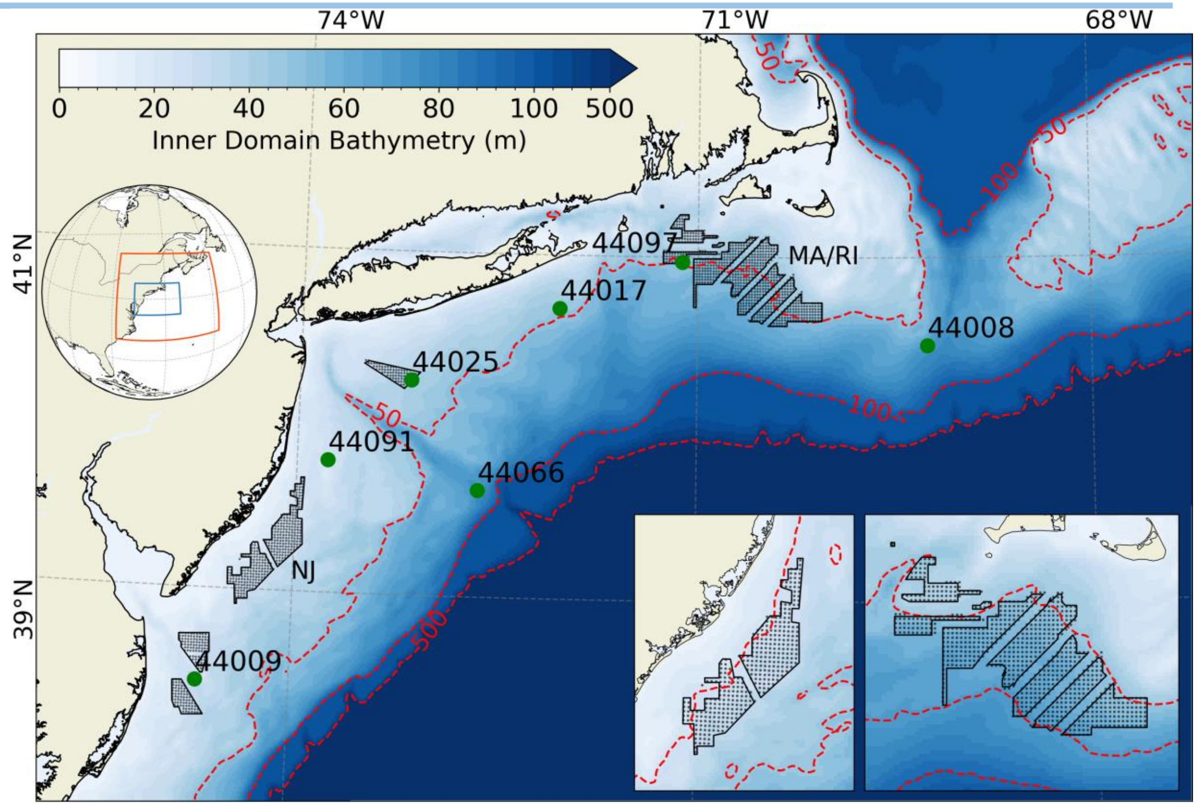

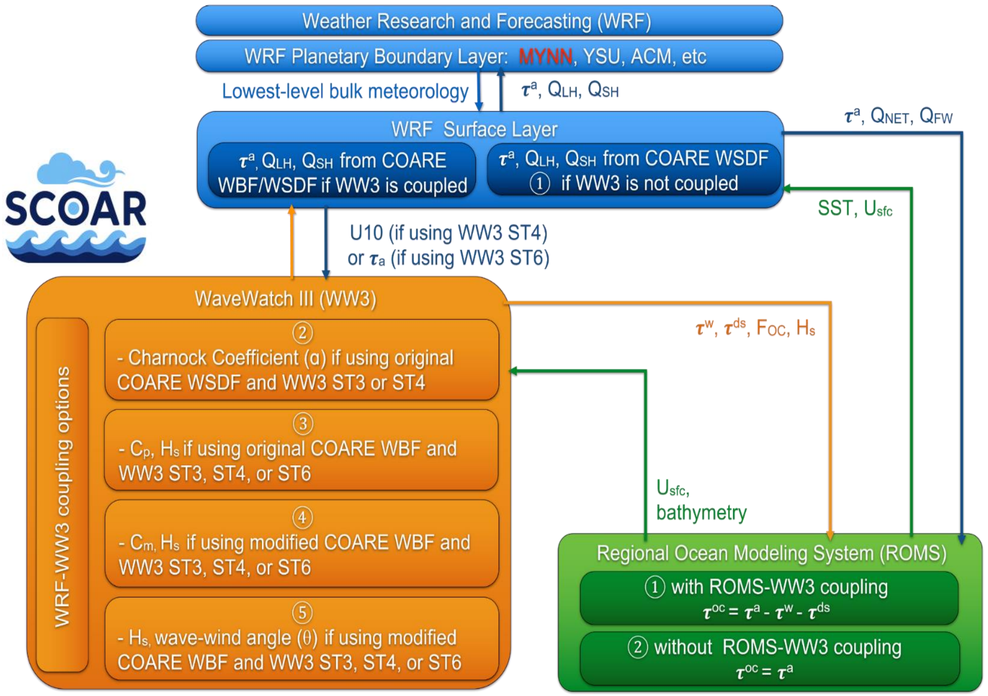

WFIP3 DOE project: Modeling component

Studied Period: Summers 2017/2018/2019/2020/2021 (JJA)

A total of **1418** wind turbines.

1.5 km high resolution WRF-ROMS-WW3 coupled modeling

The Fitch parameterization (Fitch et al. 2012) is used to represents wind turbines in the atmosphere.
-> wind turbines are not explicitly represented in the ocean

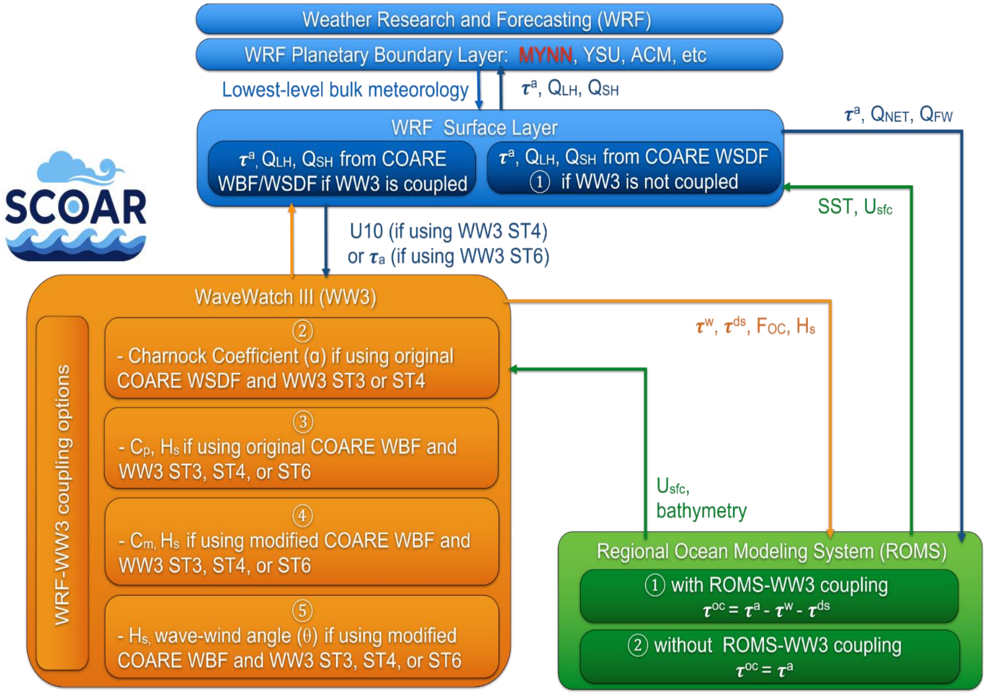

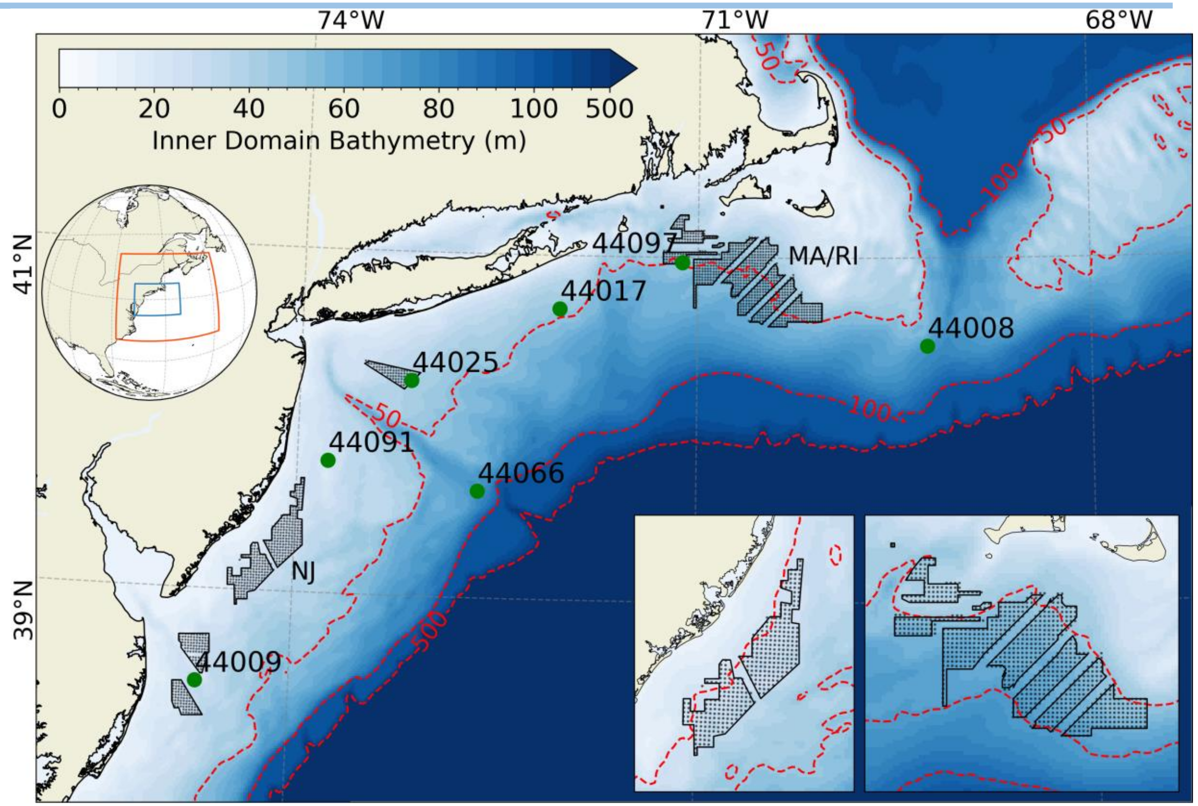

-> Fully coupled including wind farms (WF)

-> Fully coupled without wind farms (NOWF)

Wind Wake

Wind turbines extract kinetic energy from the atmosphere to generate electricity. This reduces wind speed and increases turbulence downstream. **—>Wind wake effect**

This reduces wind speed and increases turbulence, modifying the kinematic/thermodynamic profiles in the atmospheric boundary layer and air-sea heat and momentum exchanges.

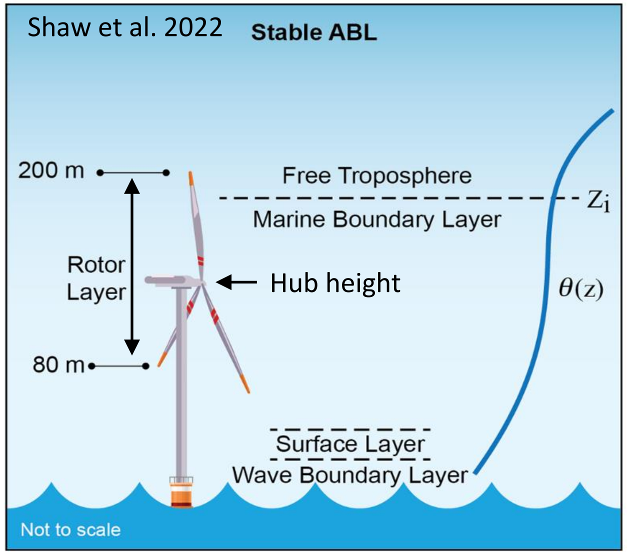

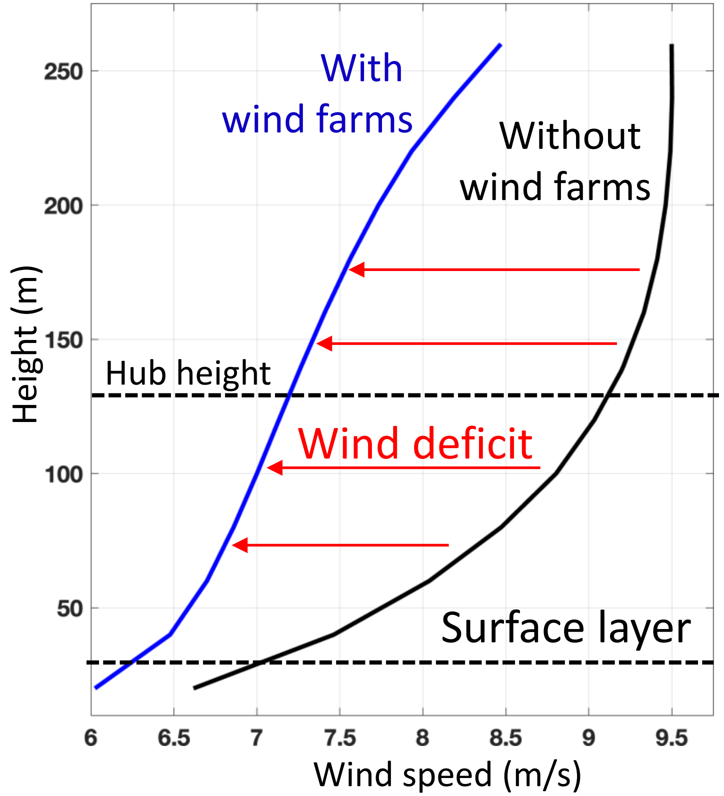

The Fitch parameterization

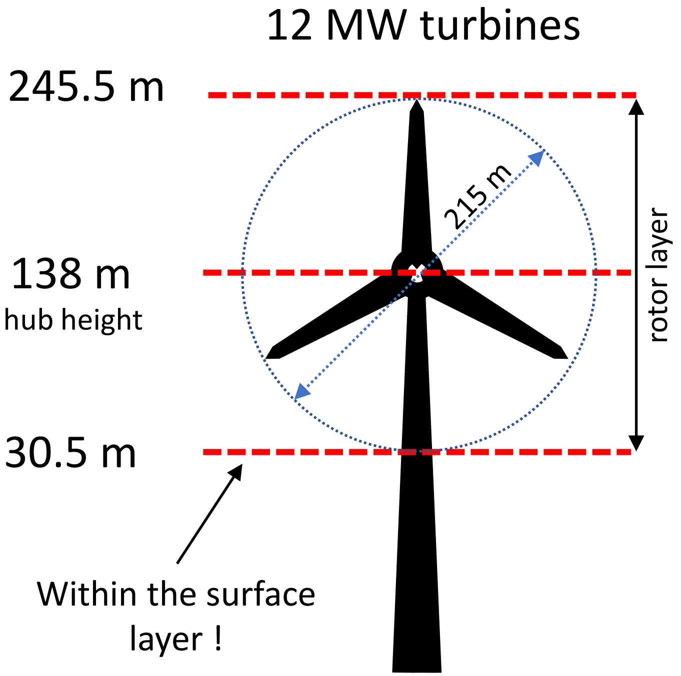

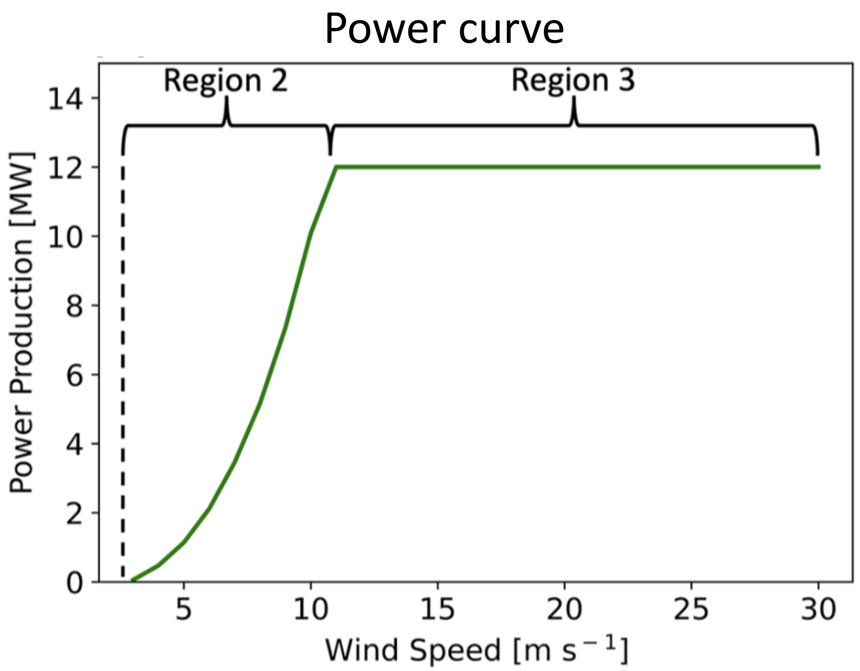

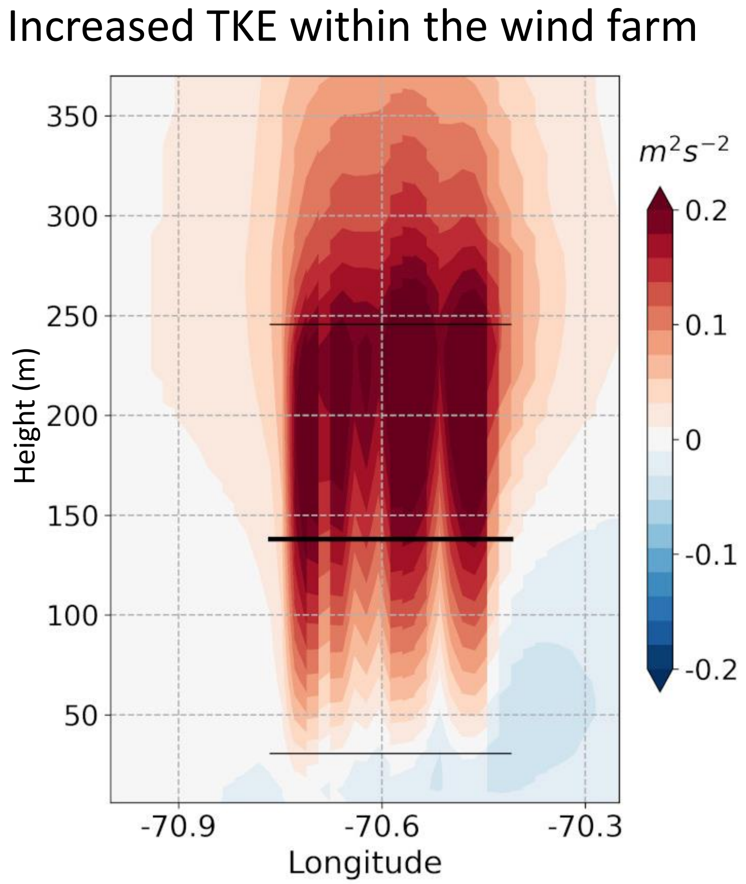

The turbulence coefficient C_{TKE} is calculated as the difference between the thrust coefficient (C_T) and the power coefficient (C_P): $\alpha\, C_{TKE} = (C_T - C_P)$

α determines the fraction of turbine-generated TKE added to the model.

The default value α = 0.25 assumes that 25% of the turbine-produced TKE is injected into the atmosphere.

The Fitch parameterization

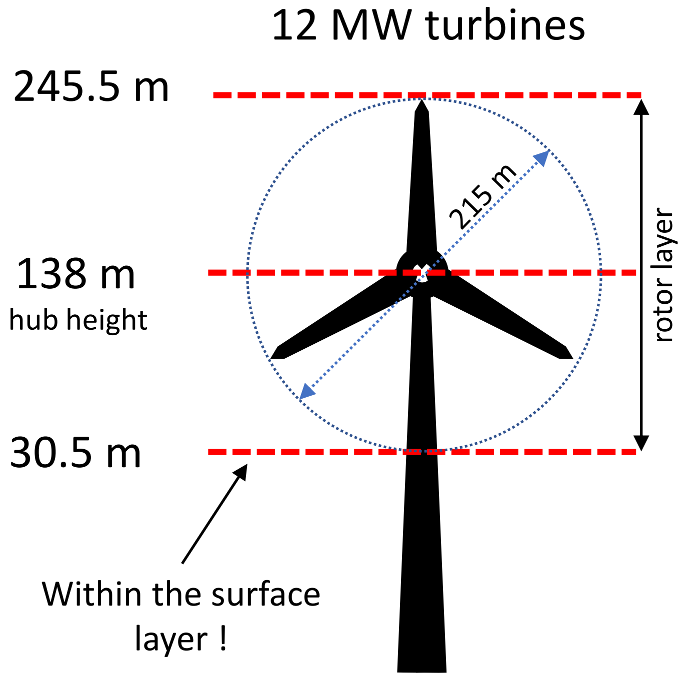

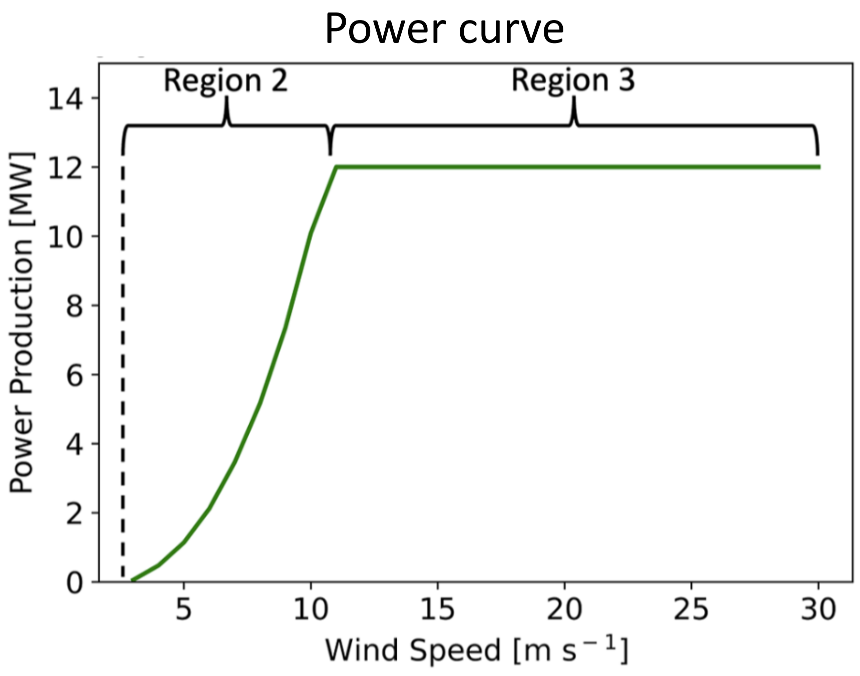

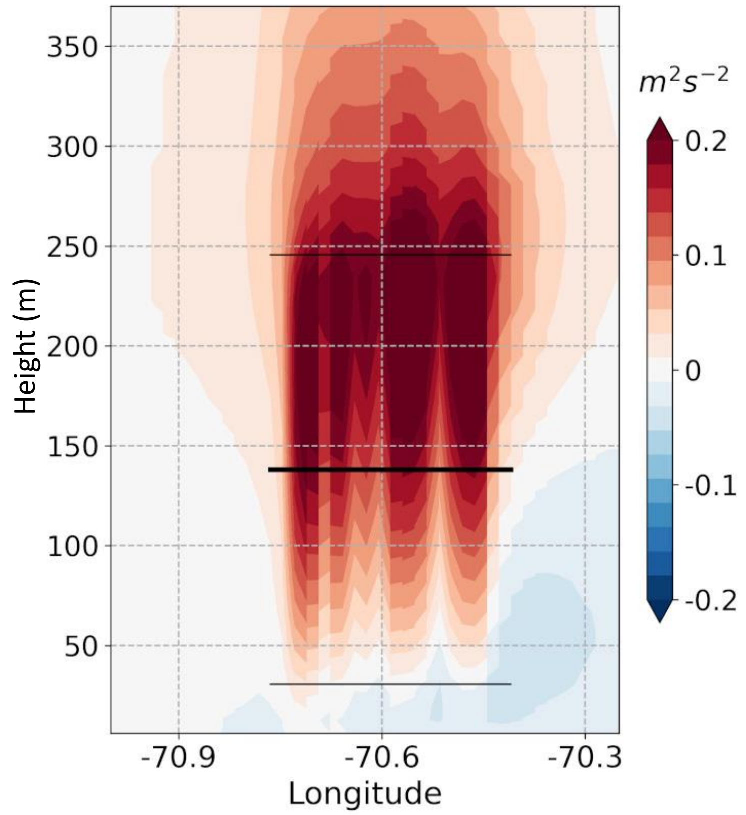

The turbulence coefficient C_{TKE} is calculated as the difference between the thrust coefficient (C_T) and the power coefficient (C_P): $\alpha\, C_{TKE} = (C_T - C_P)$

α determines the fraction of turbine-generated TKE added to the model.

-> Additional WF run using α = 1.0

The default value α = 0.25 assumes that 25% of the turbine-produced TKE is injected into the atmosphere.

Hub height wind response to wind farm

Hub height (138) m wind response to offshore wind farms

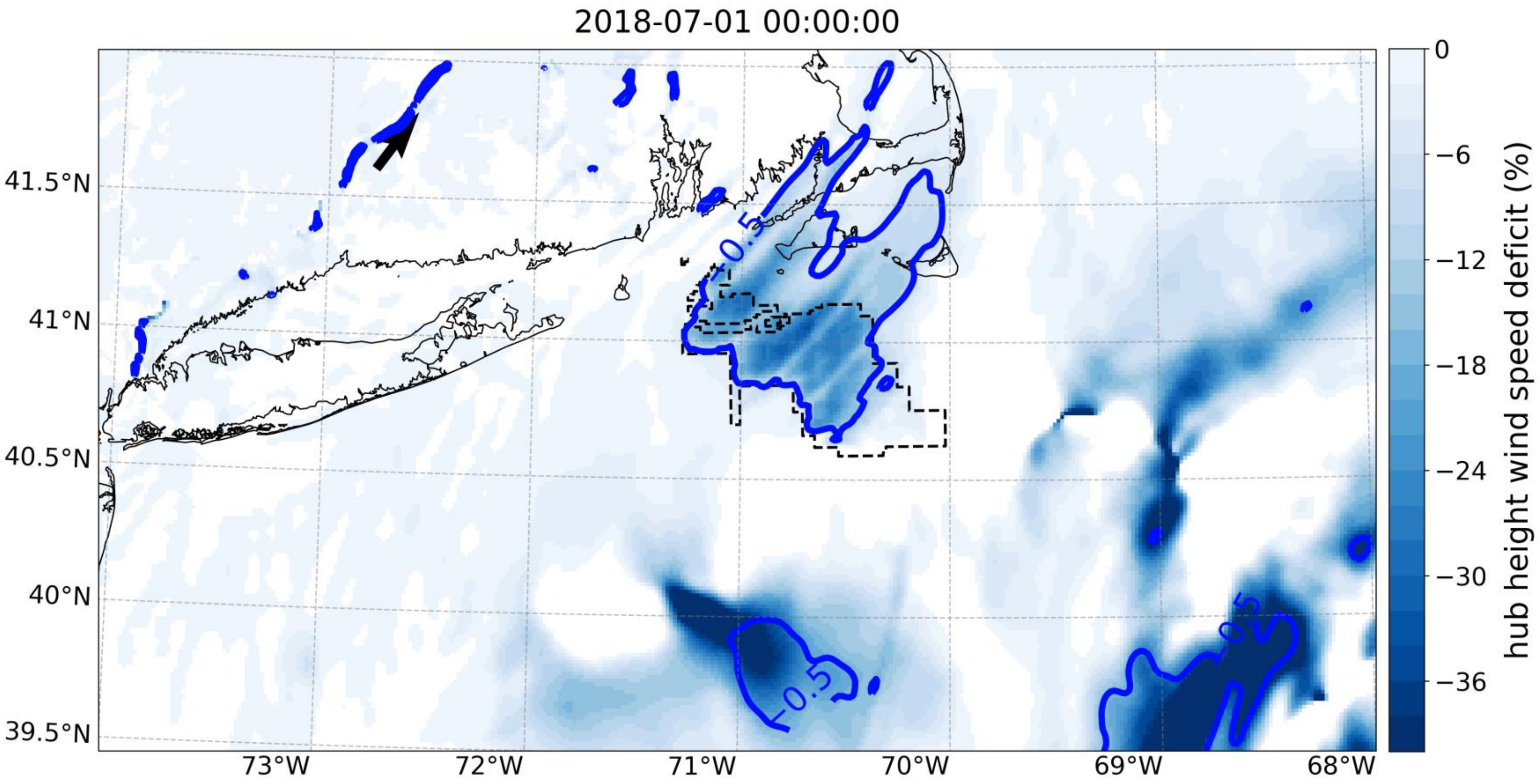

Wind and waves summer climatology in the region

- Predominantly southwesterly winds, with moderate near-surface wind speeds.
- Long southerly fetch in favor of predominant south to southeasterly waves.
- In contrast, waves from the north-northwest are almost nonexistent due to the limited fetch in that direction.

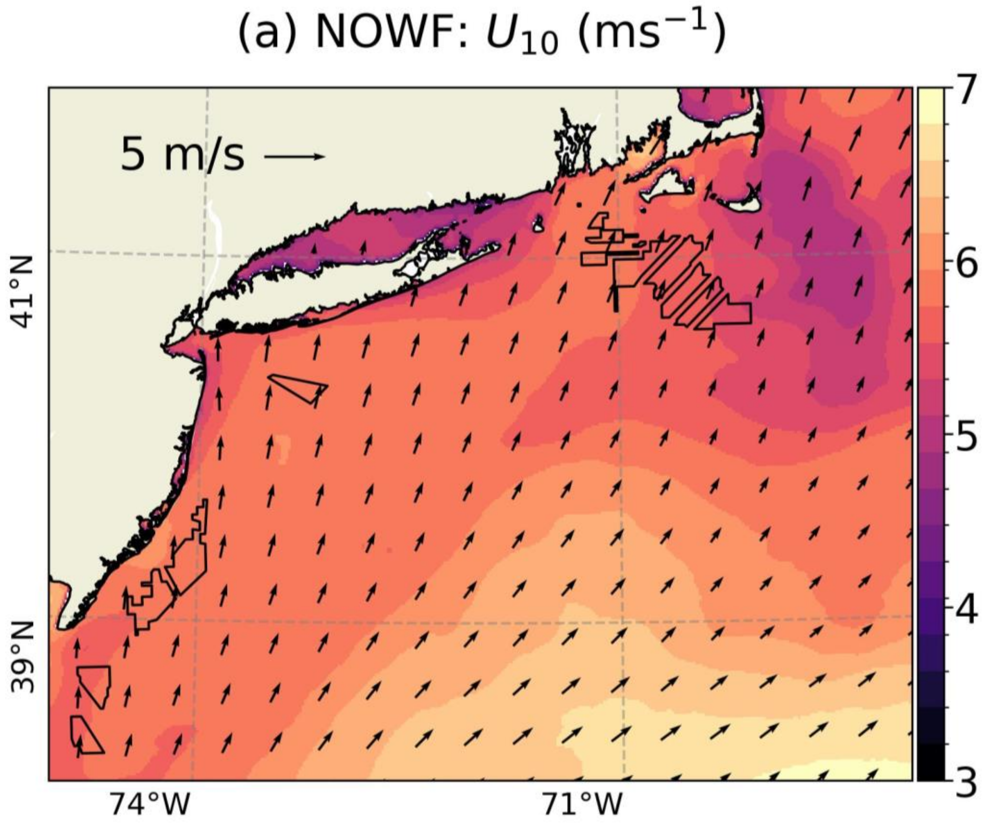

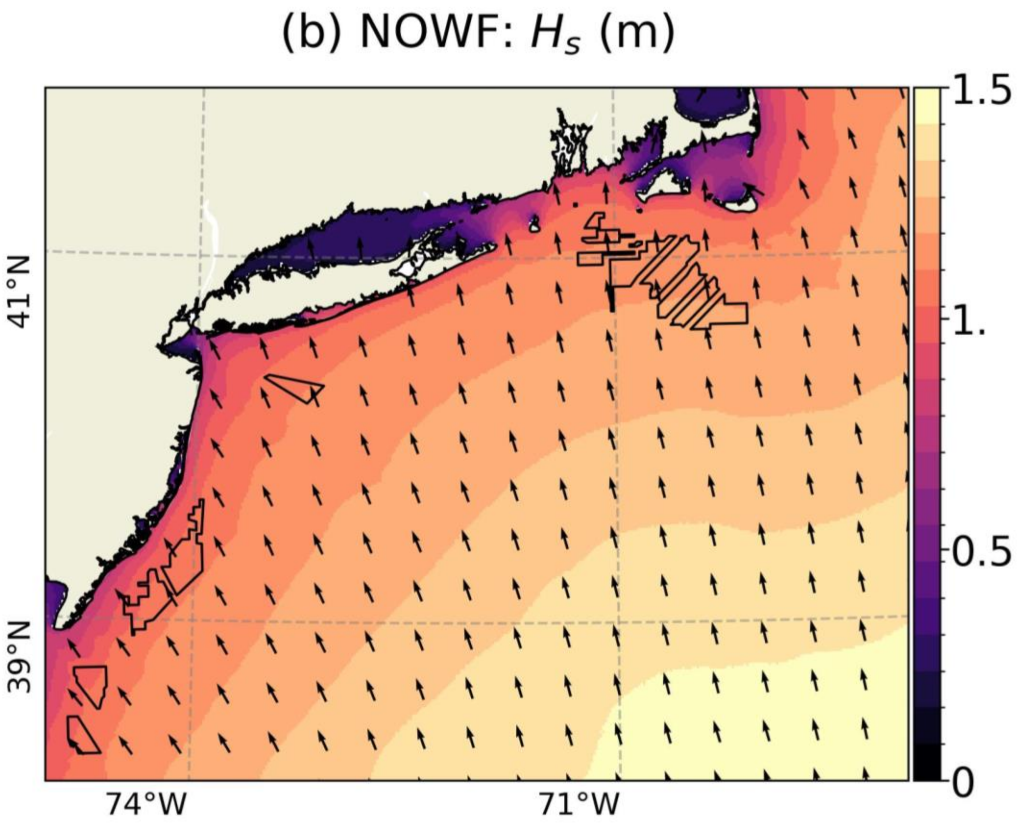

Comparison to observations

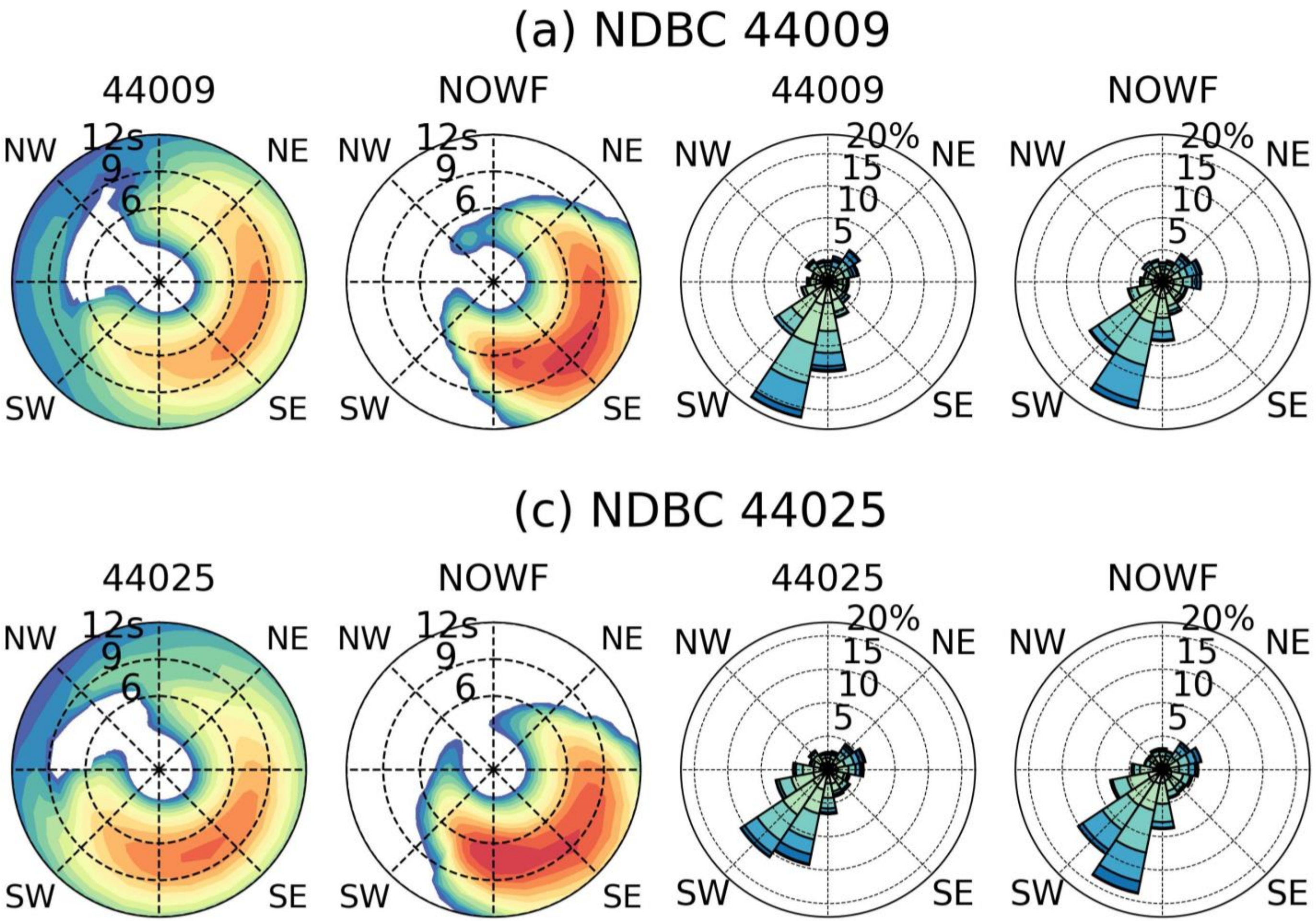

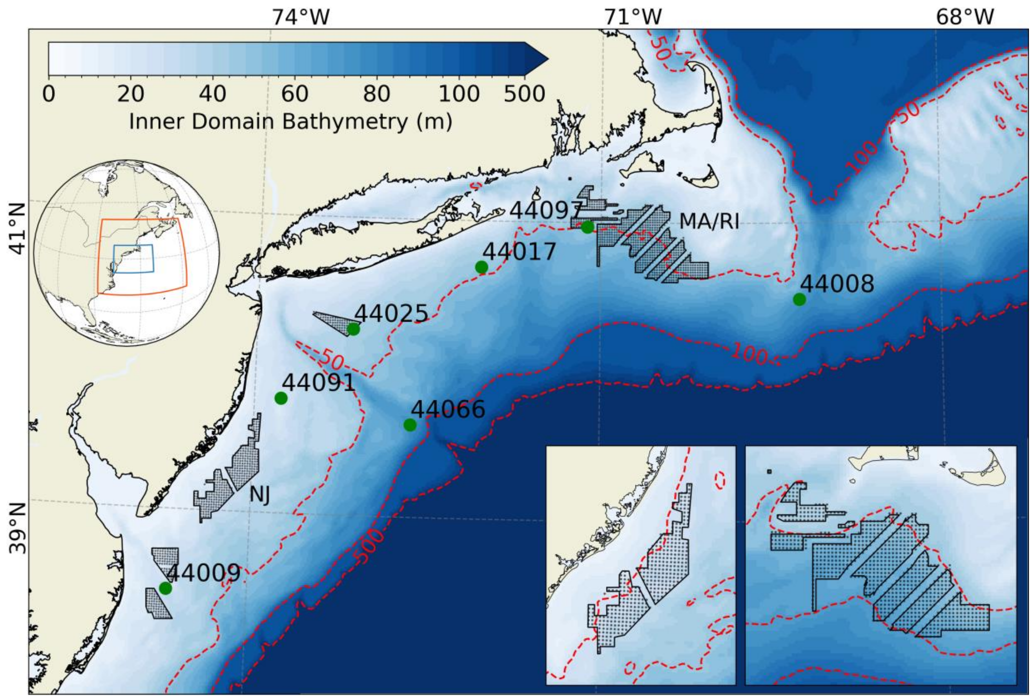

Mean differences: WF – NOWF

Coupled with wind farms (WF)
Coupled without wind farms (NOWF)

Dots: Significant at 99% confidence level

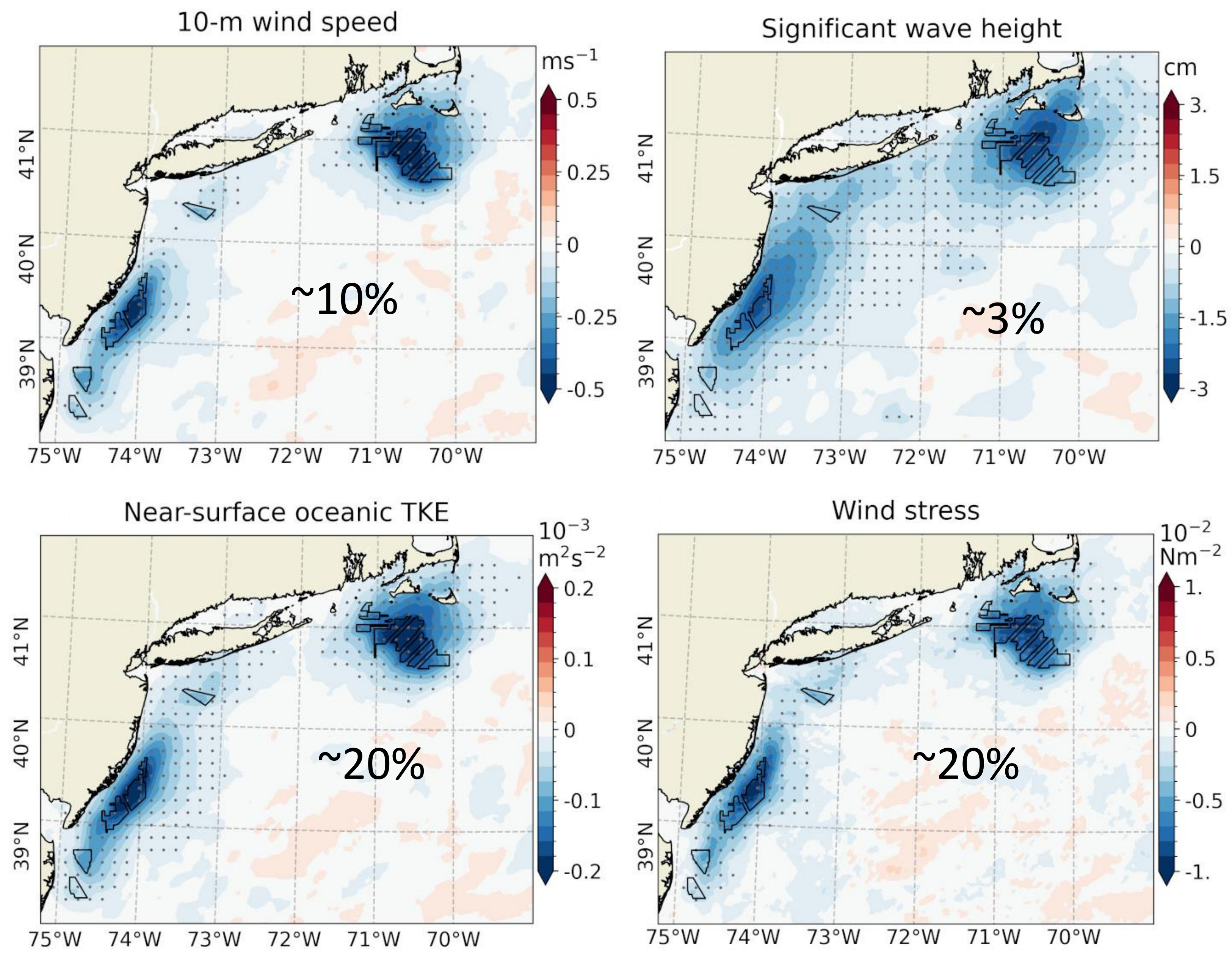

Atmospheric stability dependence

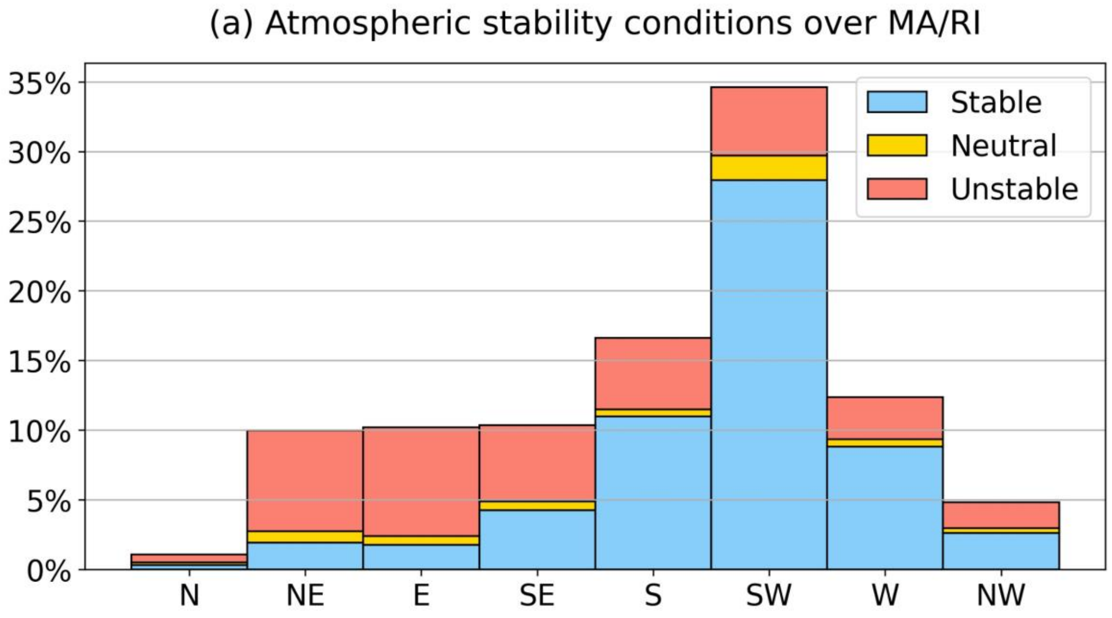

Atmospheric stability classifications using the Obukhov kength (L)

$$L = -\frac{u_*^3 \overline{\theta_v}}{\kappa g (\overline{w' \theta_v'})}.$$

Stable: 60%
Unstable: 35%

Atmospheric stability dependence

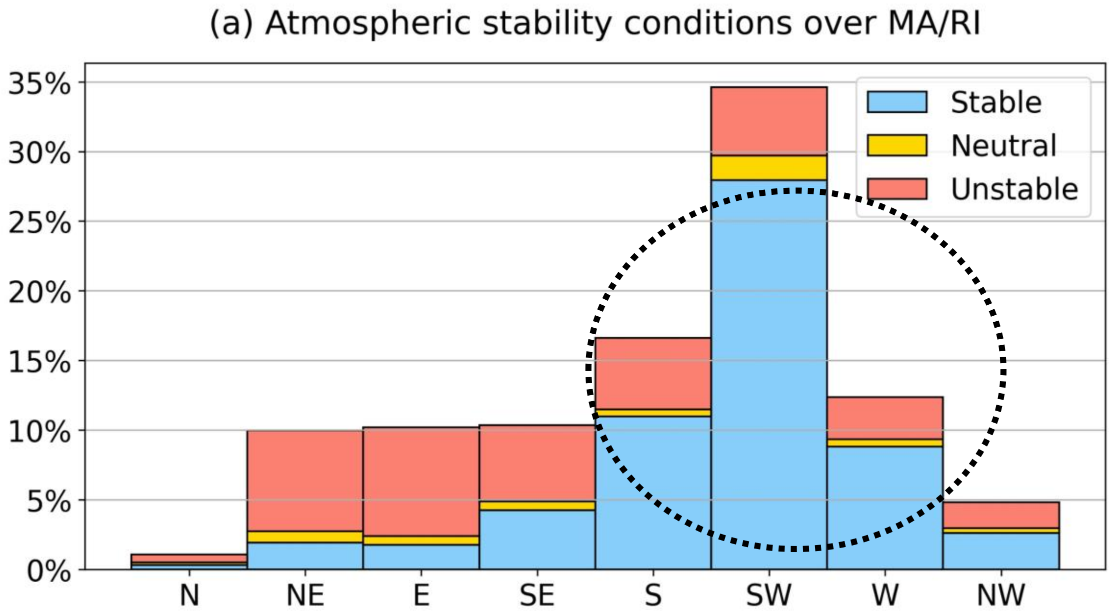

Averaged over stable conditions

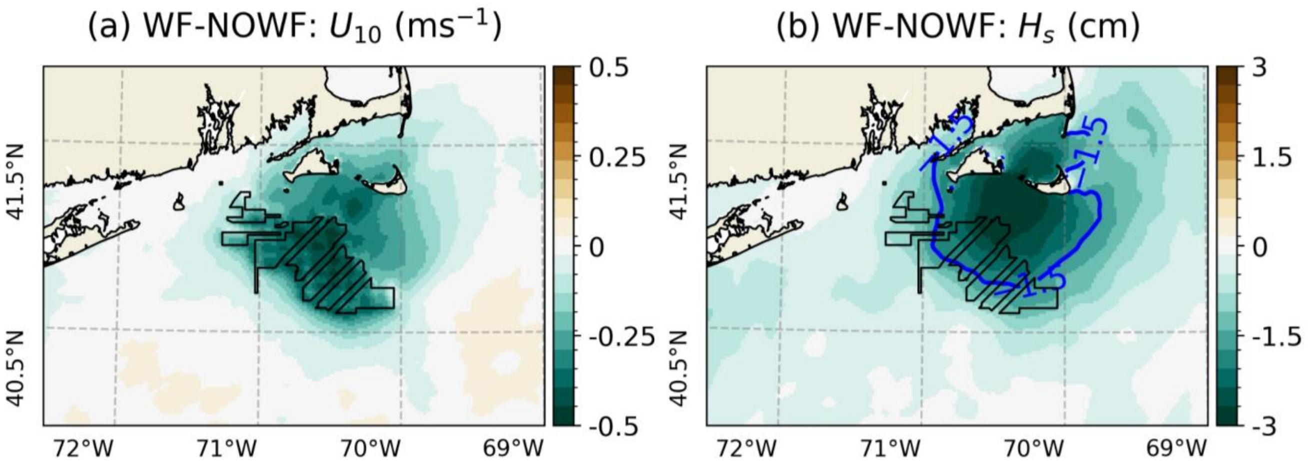

Atmospheric stability classifications using the Obukhov kength (L)

$$L = -\frac{u_*^3 \overline{\theta_v}}{\kappa g (\overline{w' \theta_v'})}.$$

Stable: 60%
Unstable: 35%

Atmospheric stability dependence

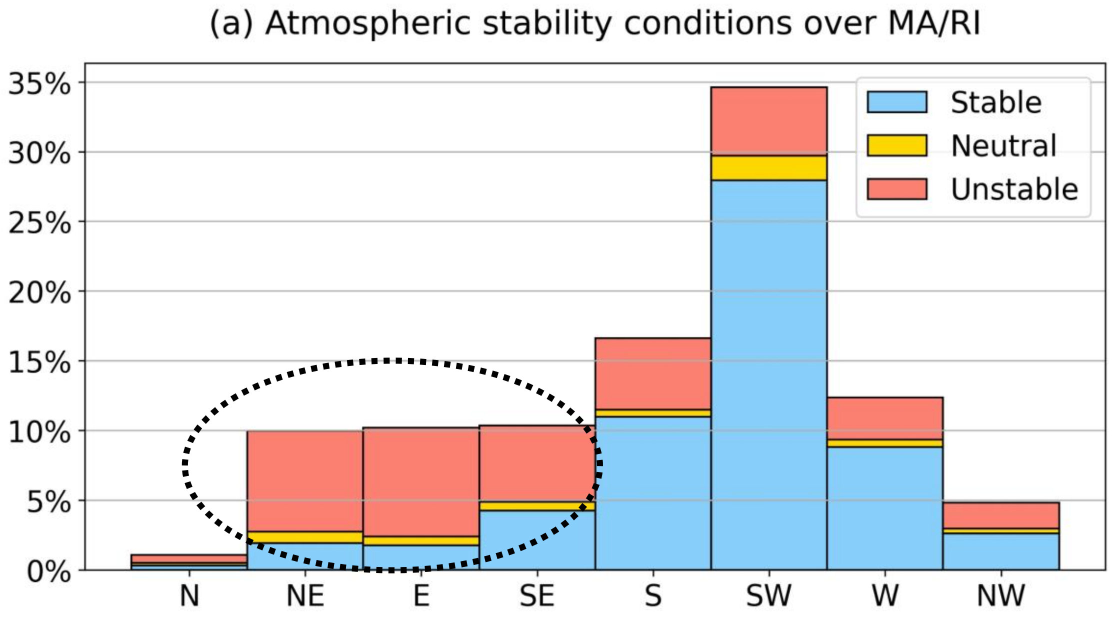

Atmospheric stability classifications using the Obukhov kength (L)

$$L = -\frac{u_*^3 \overline{\theta_v}}{\kappa g \left(\overline{w' \theta_v'}\right)}.$$

Stable: 60%
Unstable: 35%

Averaged over stable conditions

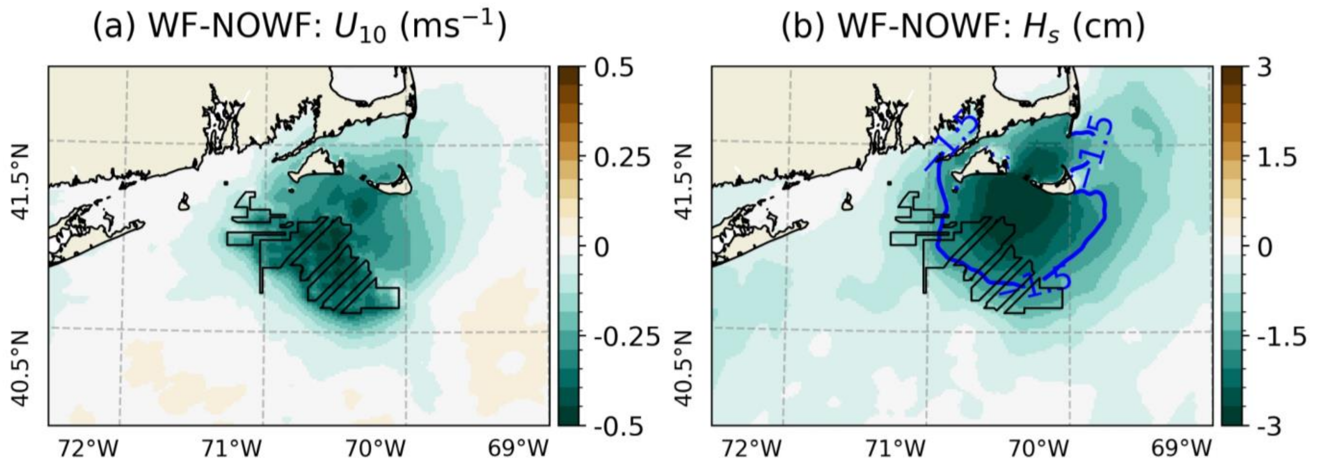

Averaged over unstable conditions

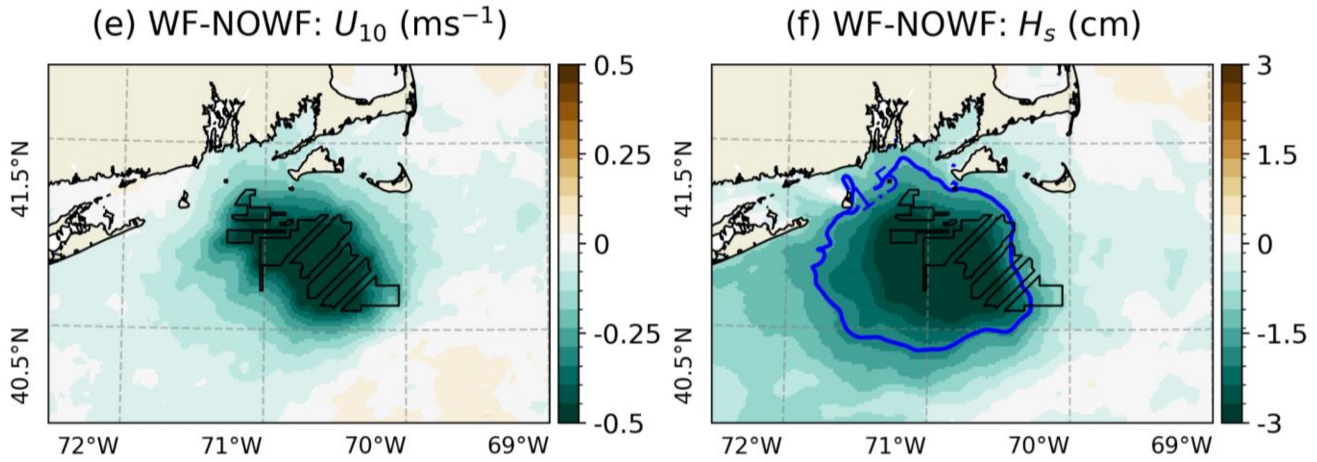

Wave spectrum differences

Composite of southwesterly wind conditions over the New Jersey wind farms

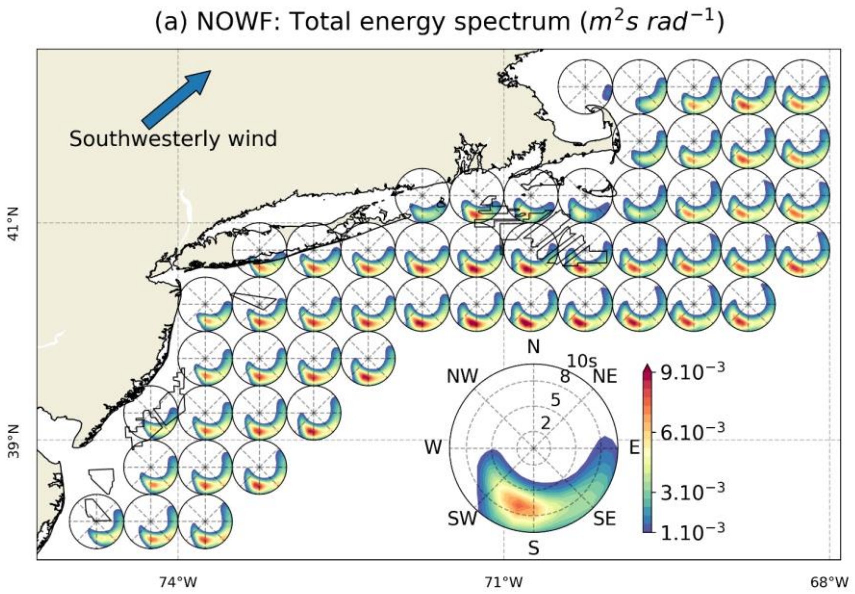

Wave spectrum differences

Composite of southwesterly wind conditions over the New Jersey wind farms

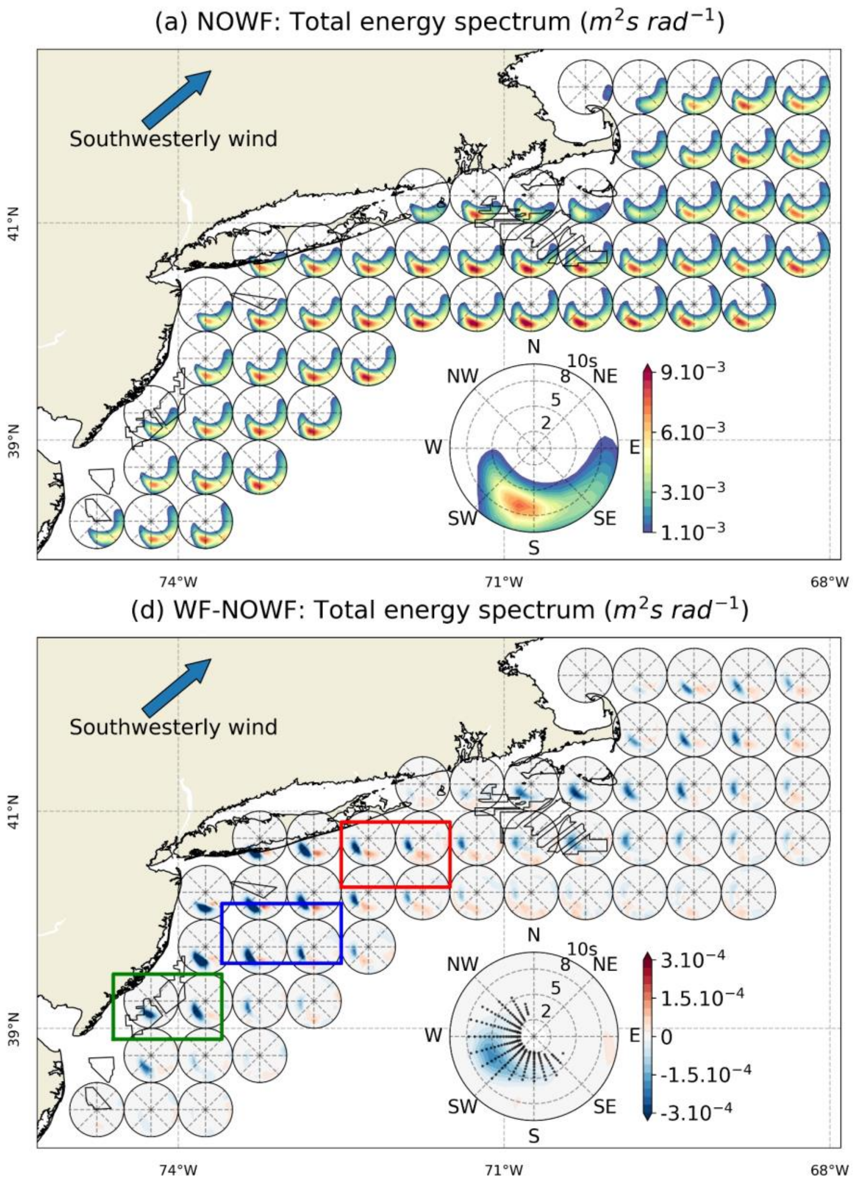

Wave spectrum differences

Composite of southwesterly wind conditions over the New Jersey wind farms

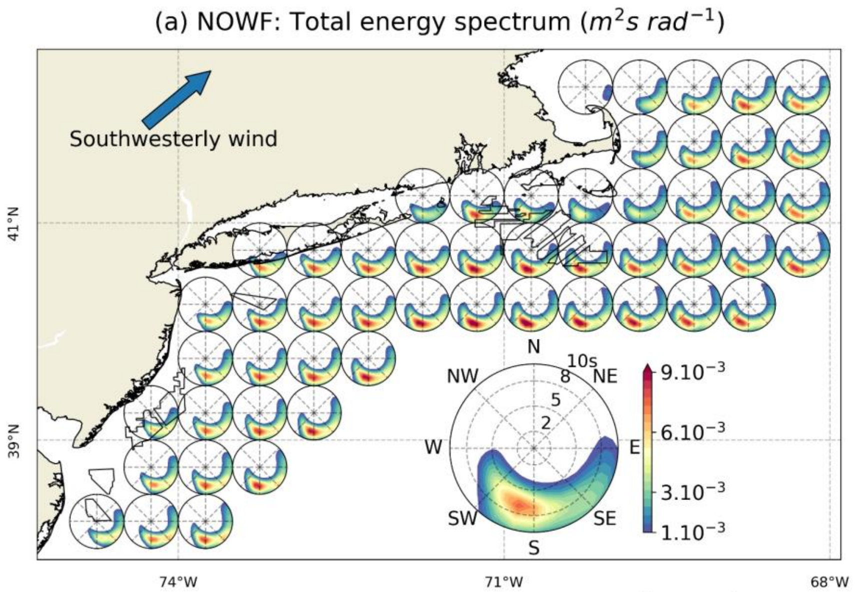

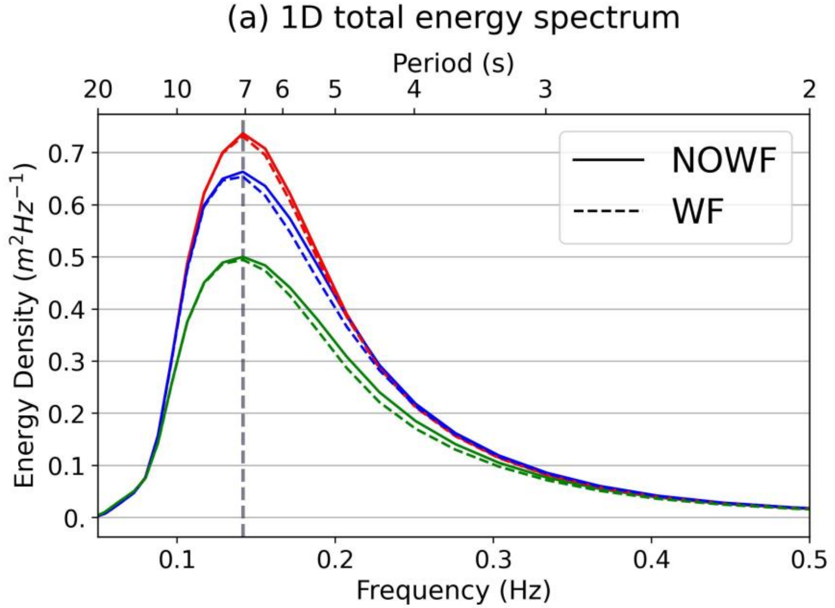

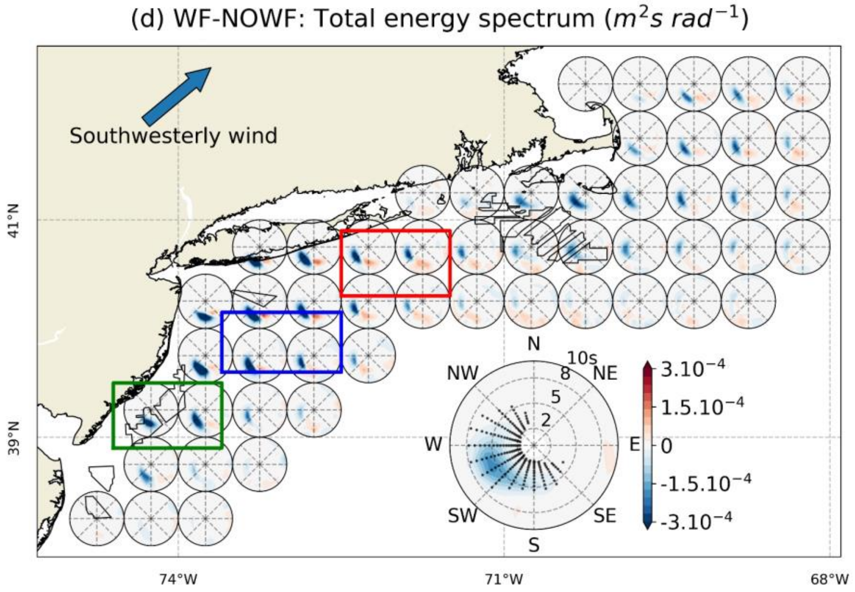

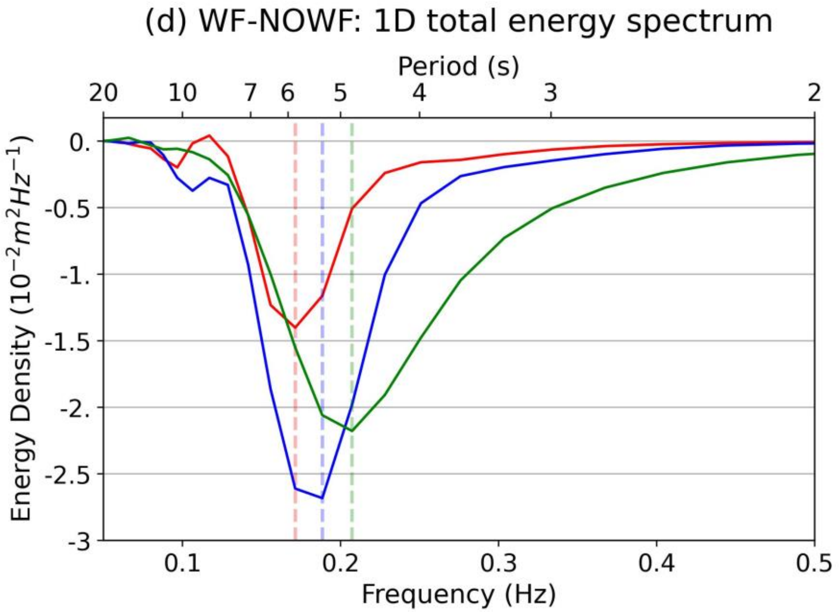

Wave spectrum differences

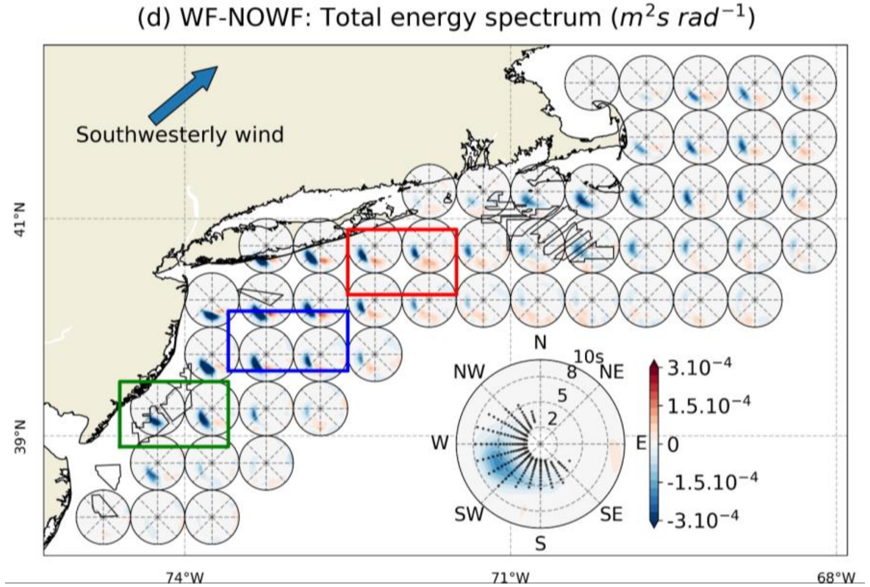

Averaged over New Jersey (NJ) wind farm during Southwesterly wind conditions

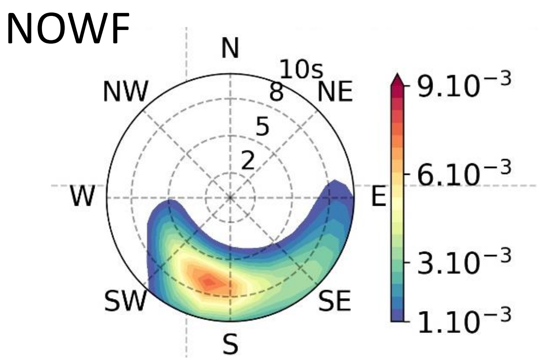

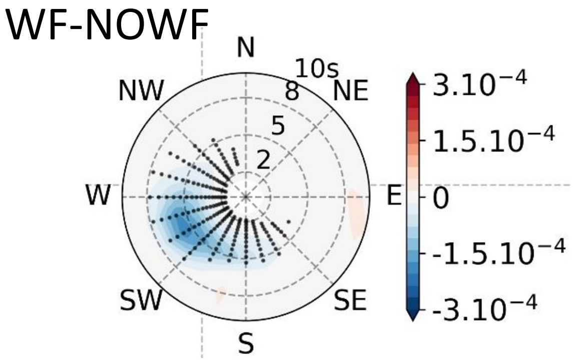

Wave spectrum differences

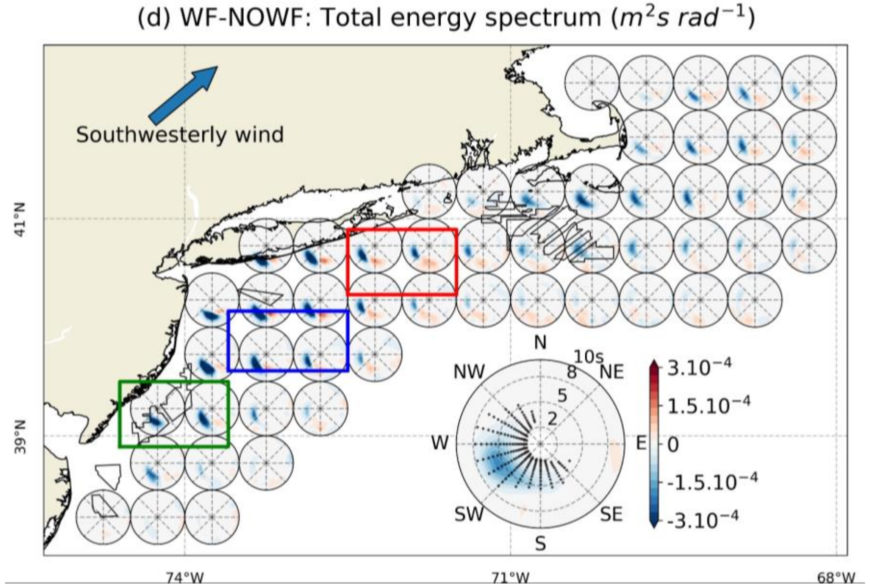

Averaged over New Jersey (NJ) wind farm during Southwesterly wind conditions

NOWF

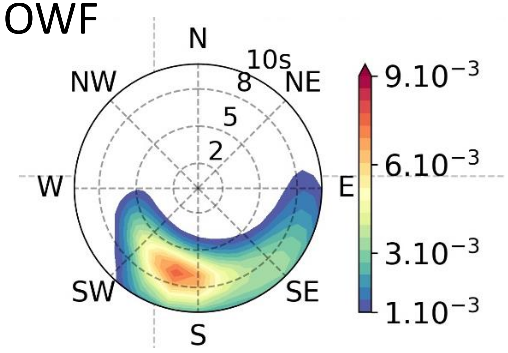

WF-NOWF

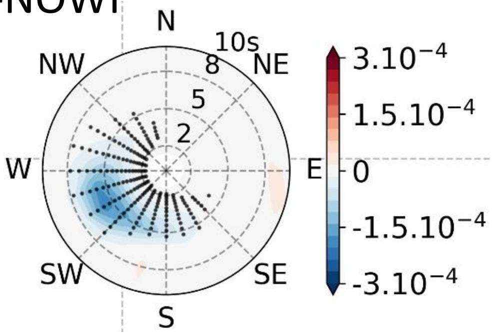

NOWF: wind-sea

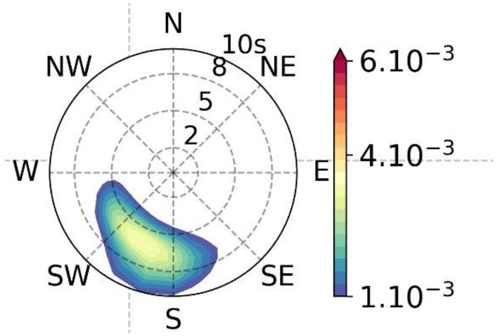

NOWF: swell

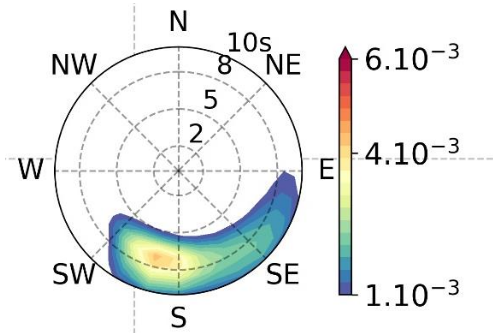

Wave spectrum differences

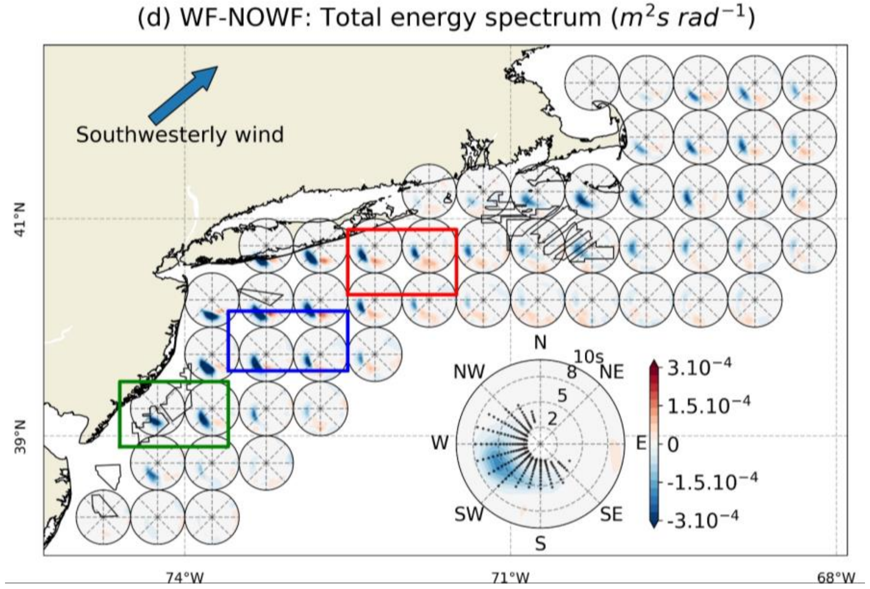

Averaged over New Jersey (NJ) wind farm during Southwesterly wind conditions

NOWF

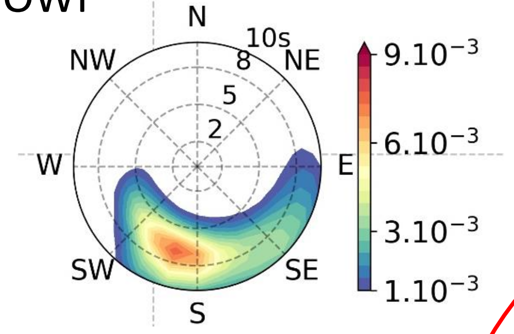

WF-NOWF

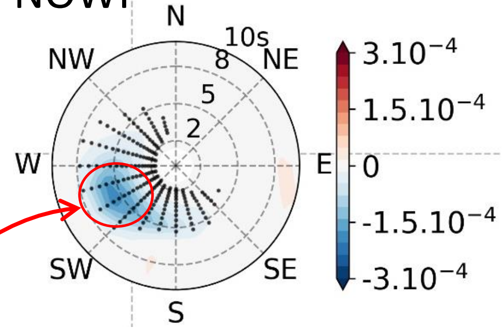

NOWF: wind-sea

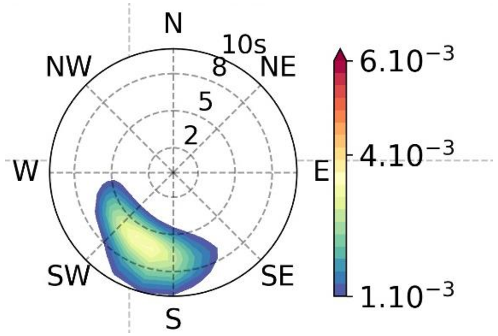

NOWF: swell

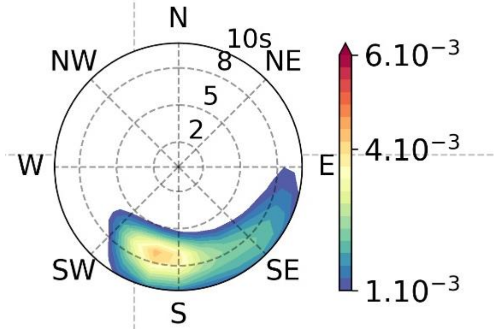

WF-NOWF: wind-sea

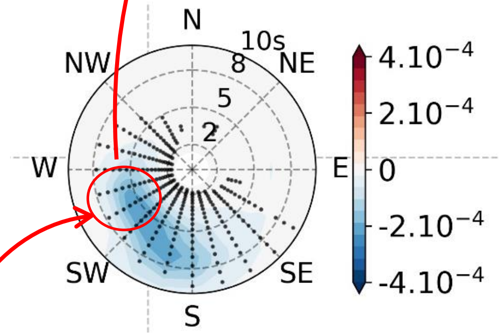

Wave growth is reduced as the wind speed is reduced

Wave spectrum differences

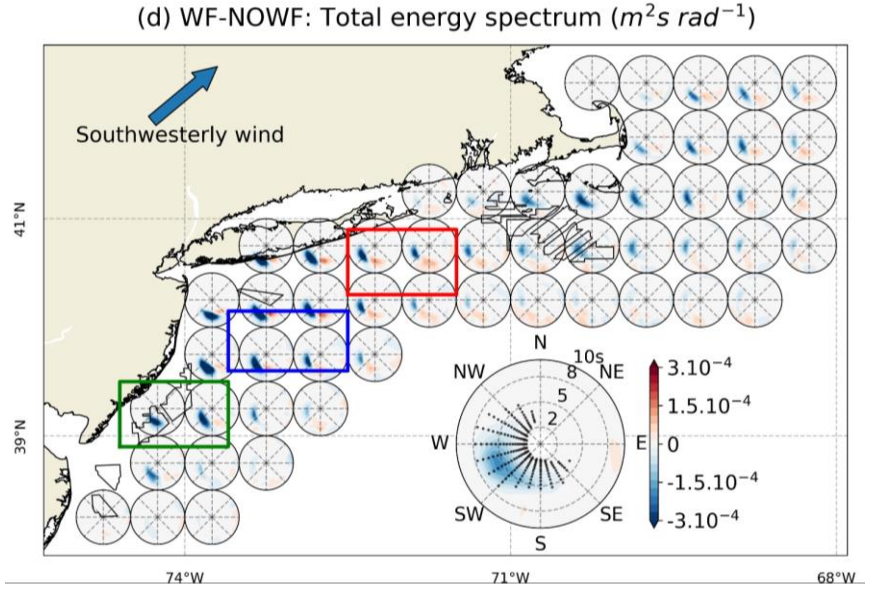

Averaged over New Jersey (NJ) wind farm during Southwesterly wind conditions

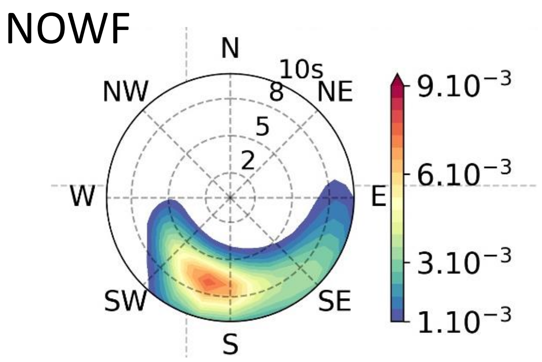

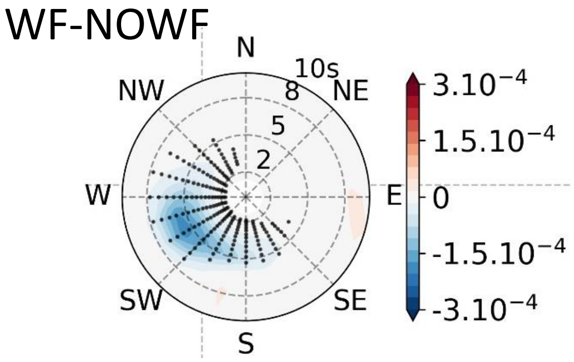

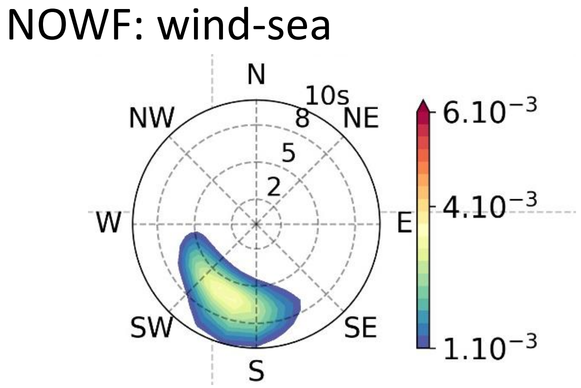

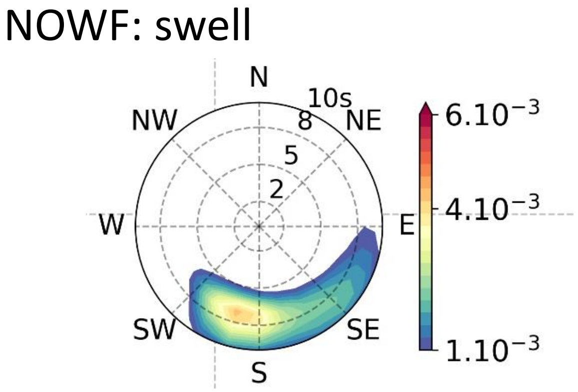

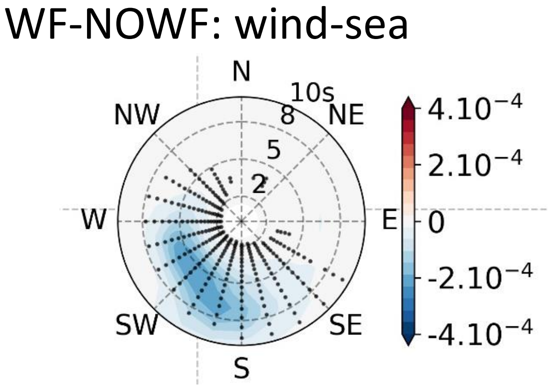

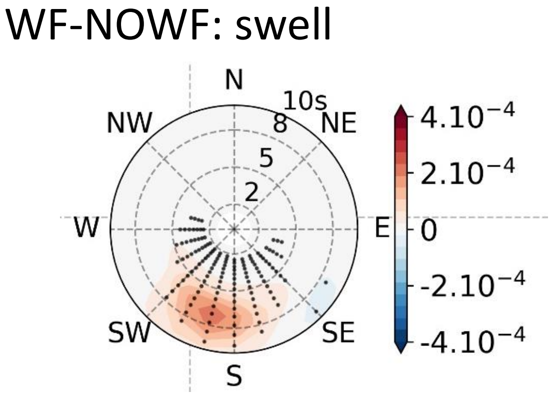

Wave spectrum differences

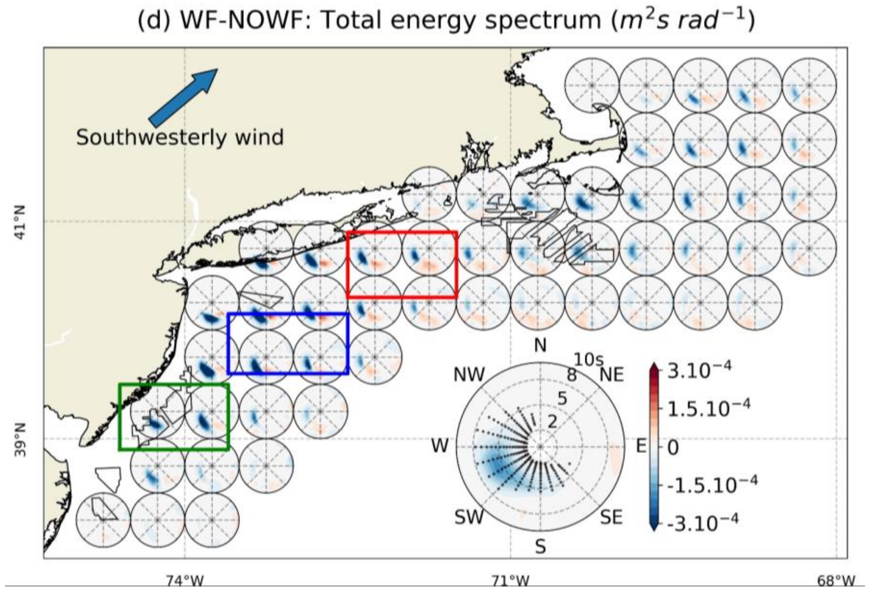

Averaged over New Jersey (NJ) wind farm during Southwesterly wind conditions

NOWF

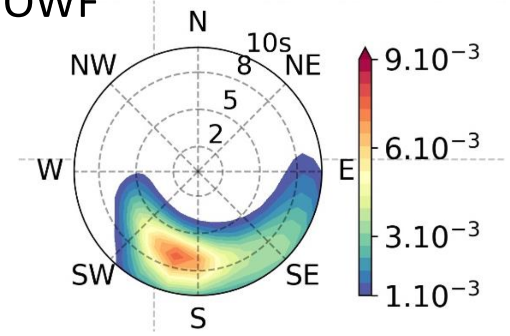

WF-NOWF

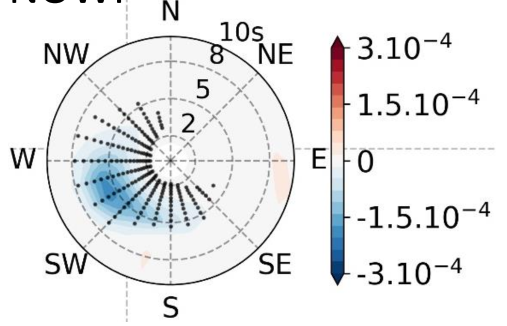

NOWF: wind-sea

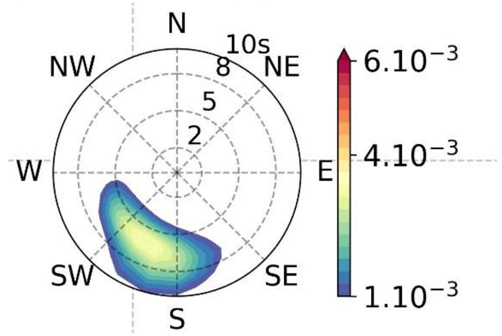

NOWF: swell

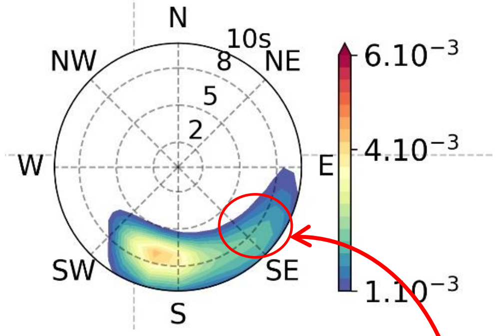

WF-NOWF: wind-sea

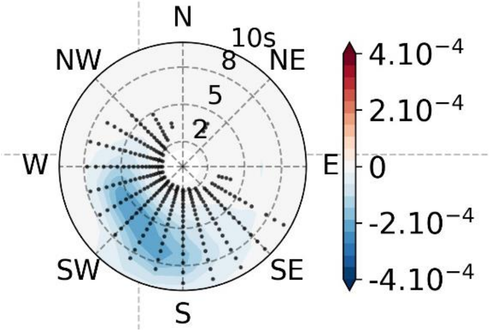

WF-NOWF: swell

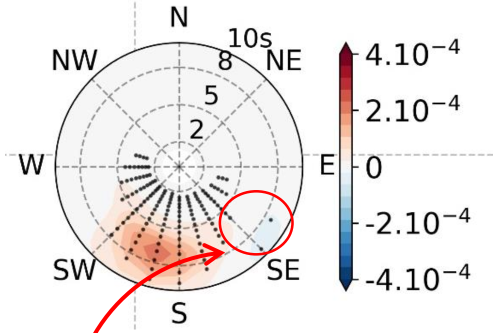

No impact on the remote southeasterly swell, disconnected from the local wind.

Wave spectrum differences

(d) WF-NOWF: Total energy spectrum ($m^2 s\ rad^{-1}$)

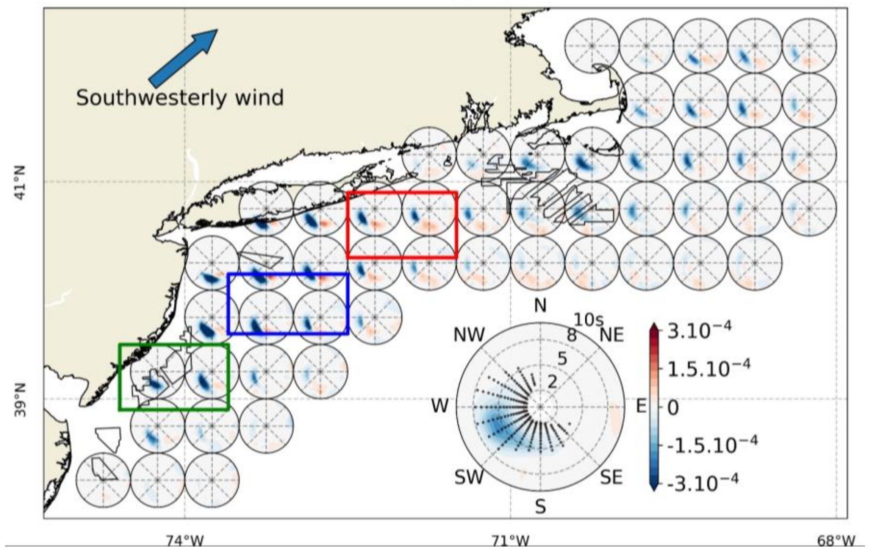

Averaged over New Jersey (NJ) wind farm during Southwesterly wind conditions

NOWF

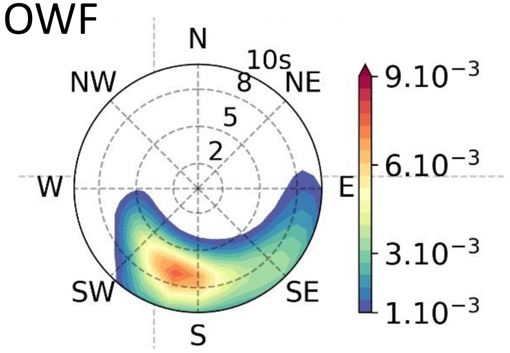

WF-NOWF

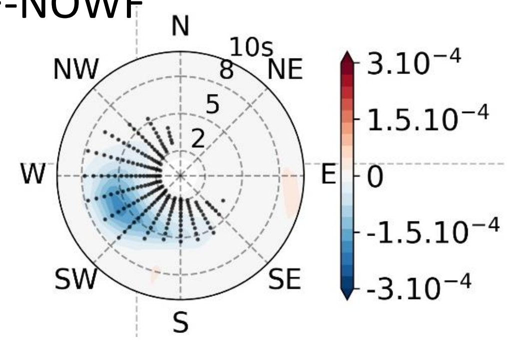

NOWF: wind-sea

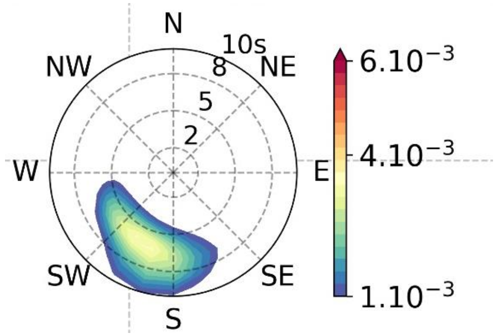

NOWF: swell

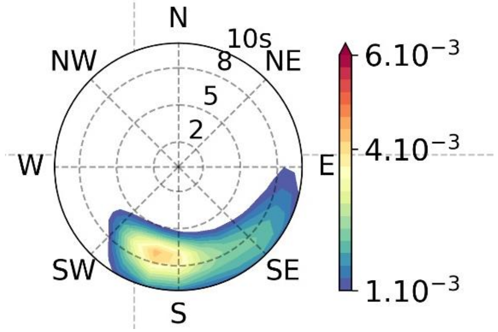

WF-NOWF: wind-sea

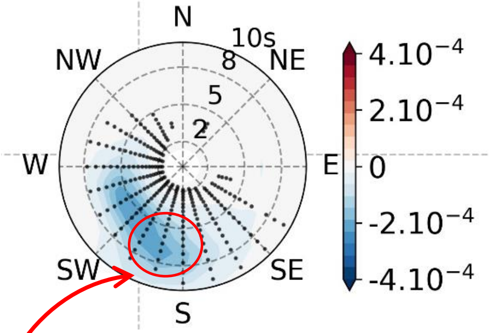

WF-NOWF: swell

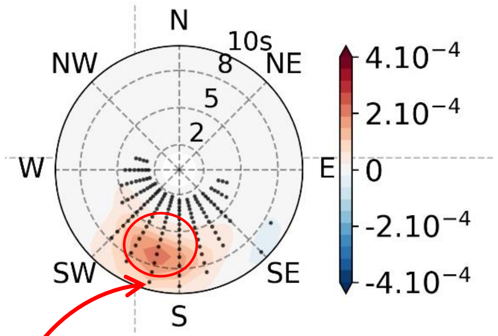

Wave regime shift from ‘wind-sea’ to ‘swell’ as the wind speed is reduced

Wave spectrum differences

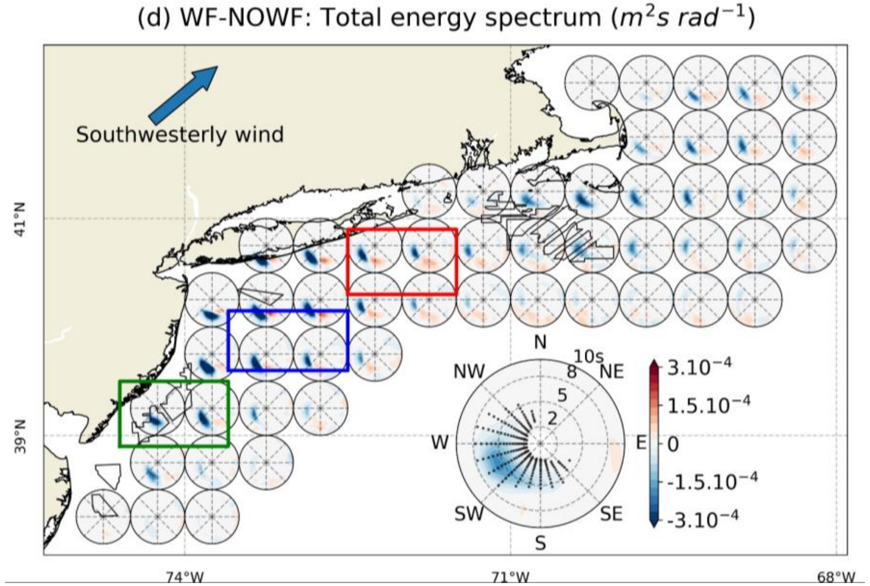

Averaged over New Jersey (NJ) wind farm during Southwesterly wind conditions

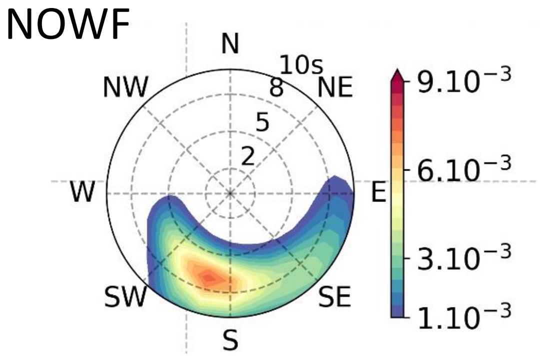

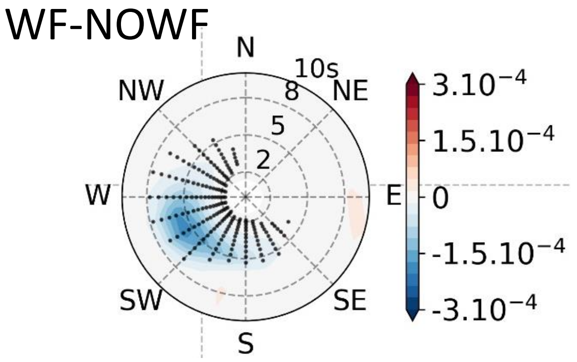

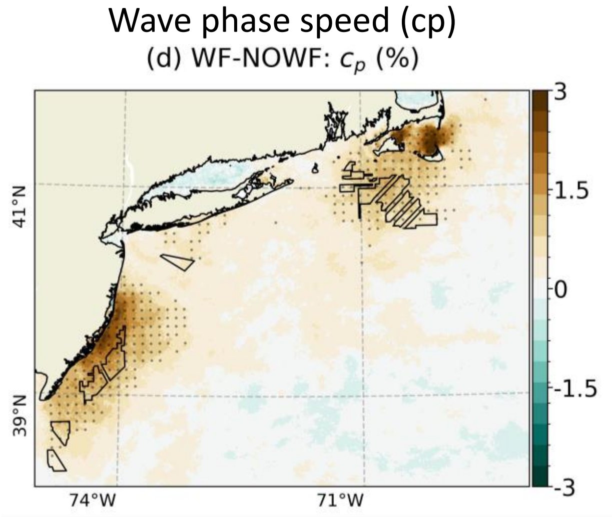

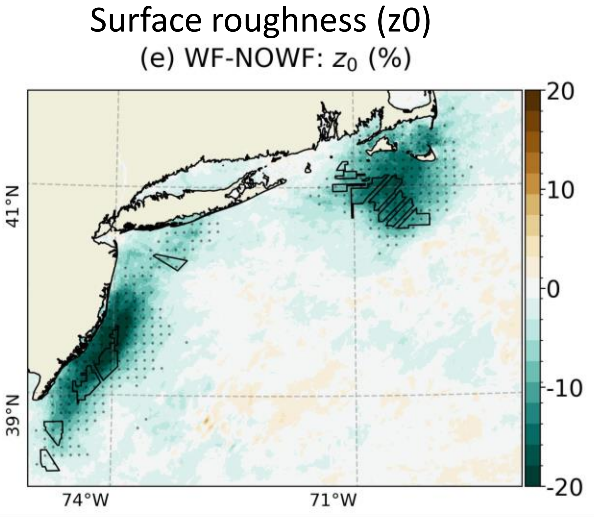

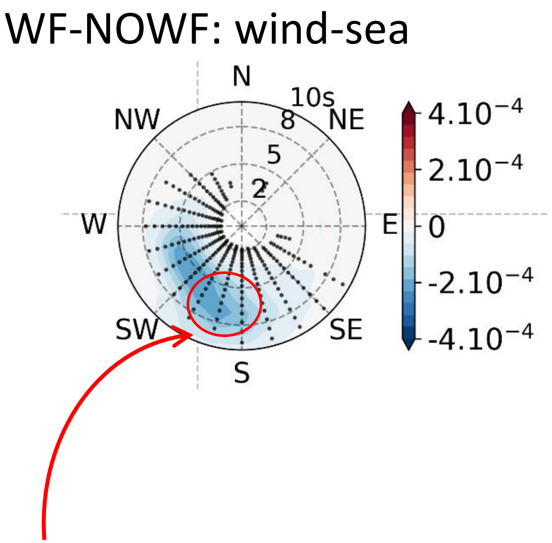

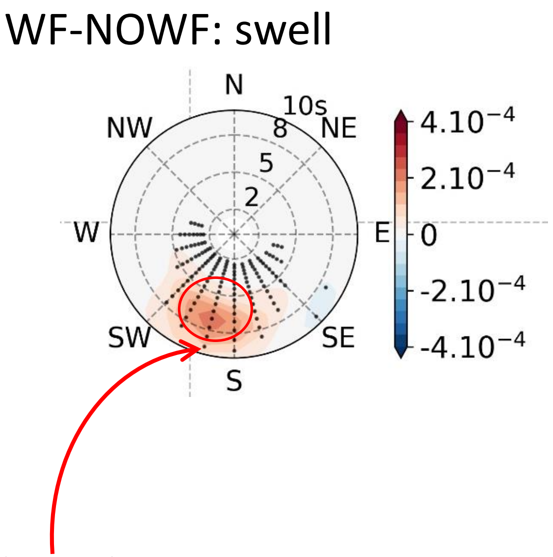

Wave regime shift from ‘wind-sea’ to ‘swell’ as the wind speed is reduced

SST and Mixed Layer Depth impact

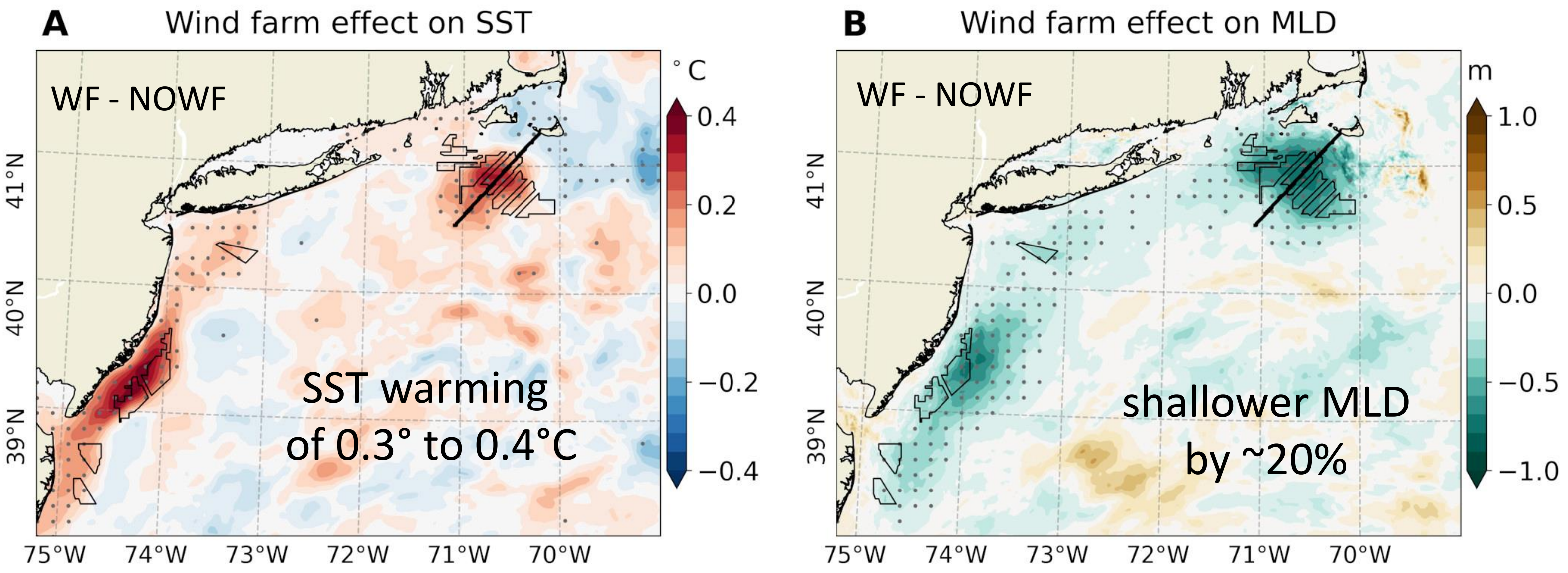

MLD estimated using 0.03 $kg.m^{-3}$ density threshold

SST and Mixed Layer Depth impact

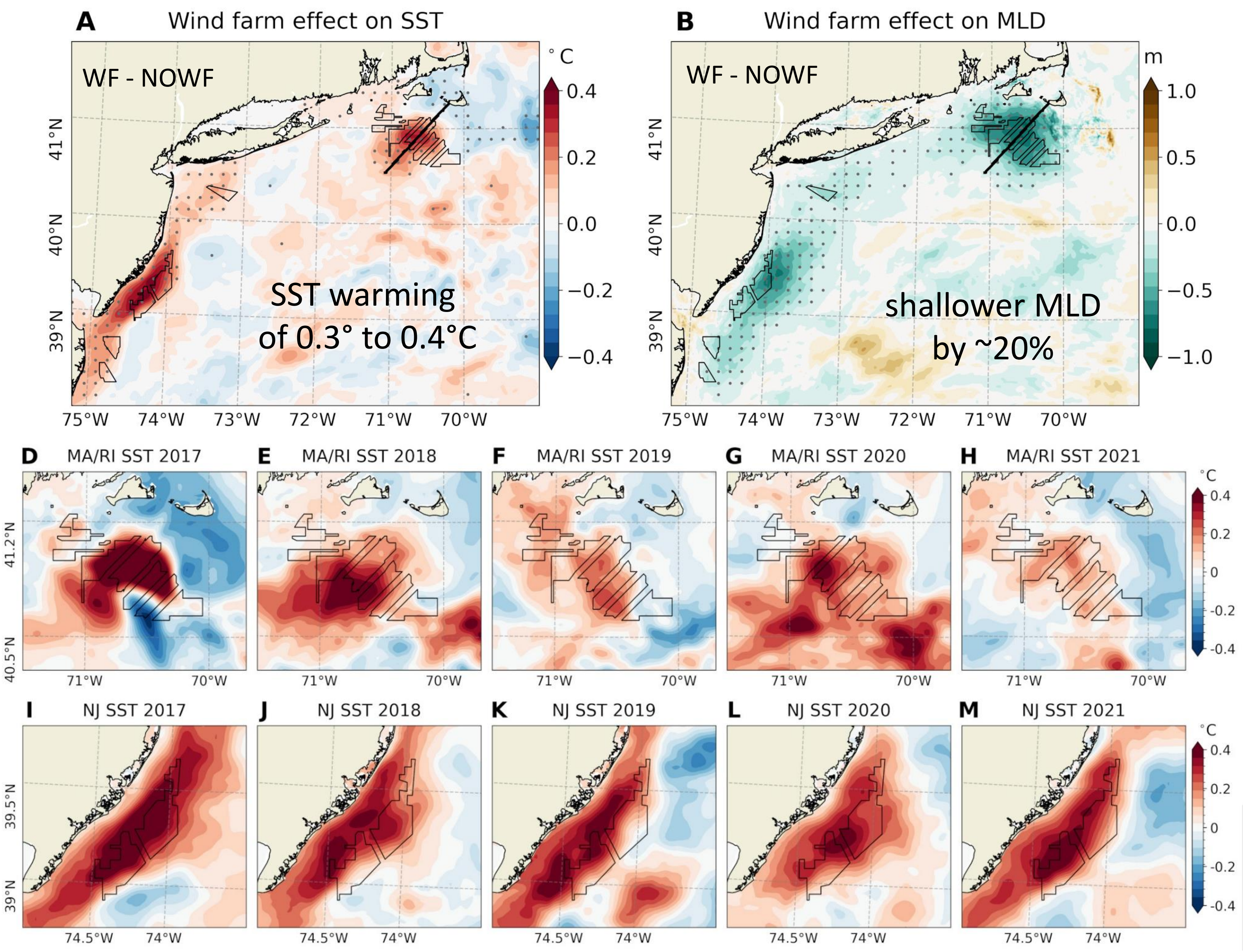

MLD estimated using 0.03 kg.m^{-3} density threshold

Strong interannual variability !

Robustness of the SST response

SST responses under different atmospheric stability conditions and α.

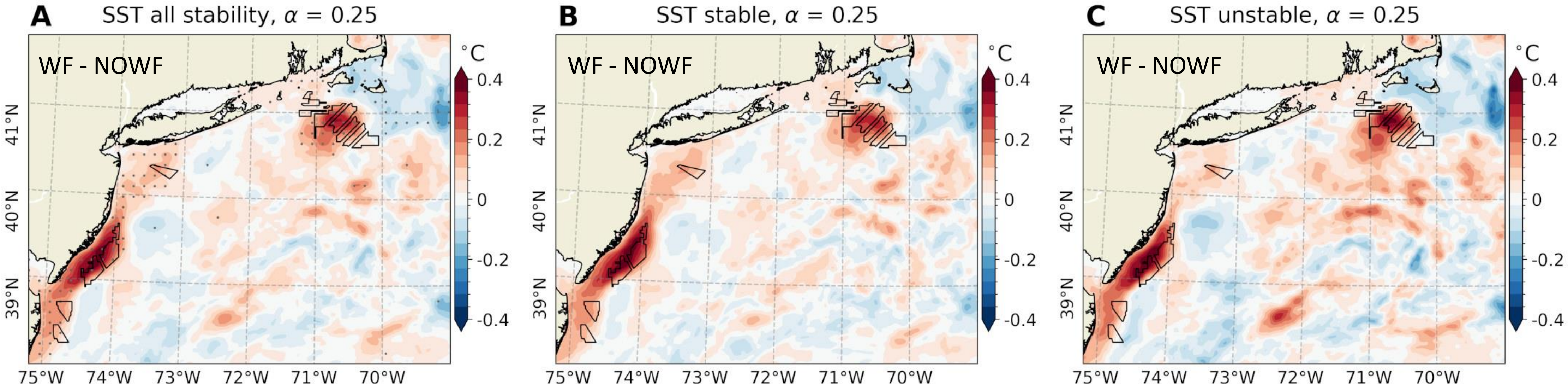

Robustness of the SST response

SST responses under different atmospheric stability conditions and α.

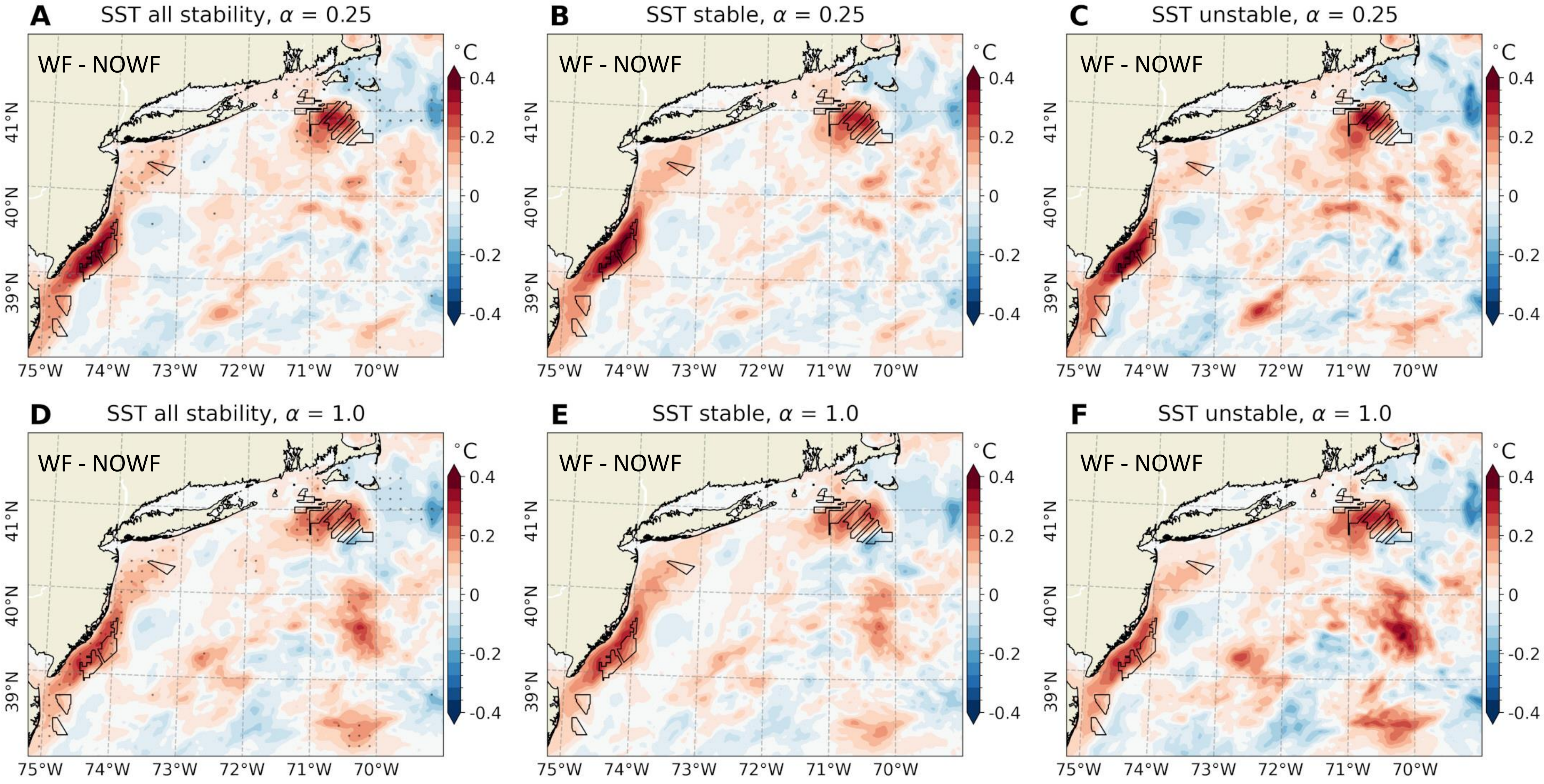

Vertical ocean- atmosphere structure: MA/RI focus.

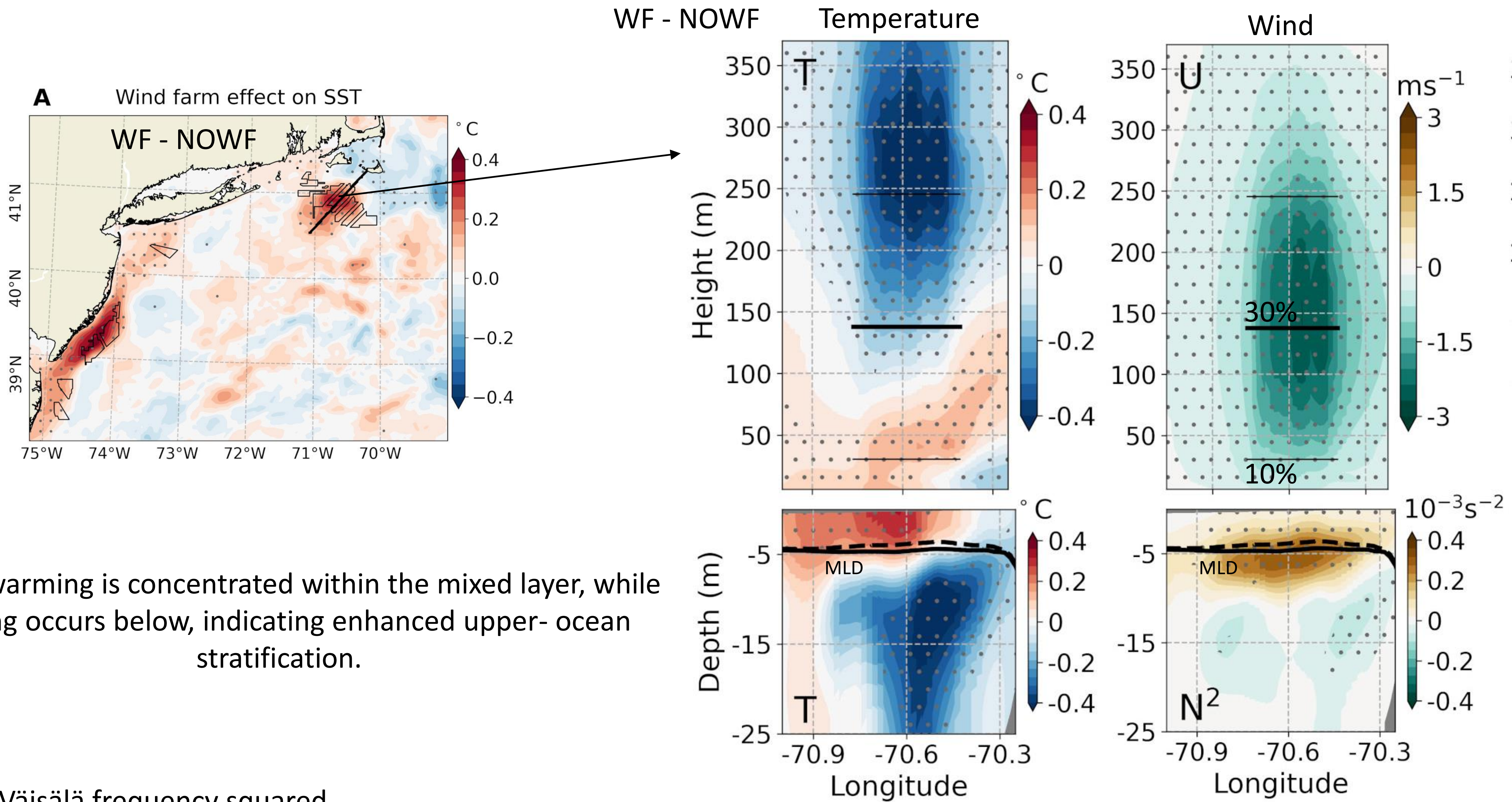

Ocean warming is concentrated within the mixed layer, while cooling occurs below, indicating enhanced upper- ocean stratification.

N^2:Brunt- Väisälä frequency squared

Ocean mixed layer heat budget

$$\underbrace{\frac{\partial\langle T\rangle}{\partial t}}_{\text{TEND}} = \underbrace{-\langle\nabla\cdot(\mathbf{u}T)\rangle}_{\text{HADV}} + \underbrace{\frac{1}{H}(wT)_{z=-h}}_{\text{VADV}} + \underbrace{\left\langle\nabla\cdot\left(\kappa_h\nabla T\right)\right\rangle}_{\text{HMIX}} \underbrace{- \frac{1}{H}\left(\kappa_v\frac{\partial T}{\partial z}\right)_{z=-h}}_{\text{VMIX}} + \underbrace{\frac{Q_{net} - Q_{sw}\,|_{z=-h}}{\rho c_p H}}_{\text{QFLX}} \underbrace{- \frac{\Delta T}{H}\frac{\partial h}{\partial t}}_{\text{ENT}}$$

Ocean mixed layer heat budget

$$\underbrace{\frac{\partial \langle T\rangle}{\partial t}}_{\text{TEND}} = \underbrace{-\langle \nabla\cdot(\mathrm{u}T)\rangle}_{\text{HADV}} + \underbrace{\frac{1}{H}(wT)_{z=-h}}_{\text{VADV}} + \underbrace{\left\langle \nabla\cdot\left(\kappa_h \nabla T\right)\right\rangle}_{\text{HMIX}} - \underbrace{\frac{1}{H}\left(\kappa_v \frac{\partial T}{\partial z}\right)_{z=-h}}_{\text{VMIX}} + \underbrace{\frac{Q_{net}-Q_{sw}|_{z=-h}}{\rho c_p H}}_{\text{QFLX}} - \underbrace{\frac{\Delta T}{H}\frac{\partial h}{\partial t}}_{\text{ENT}}$$

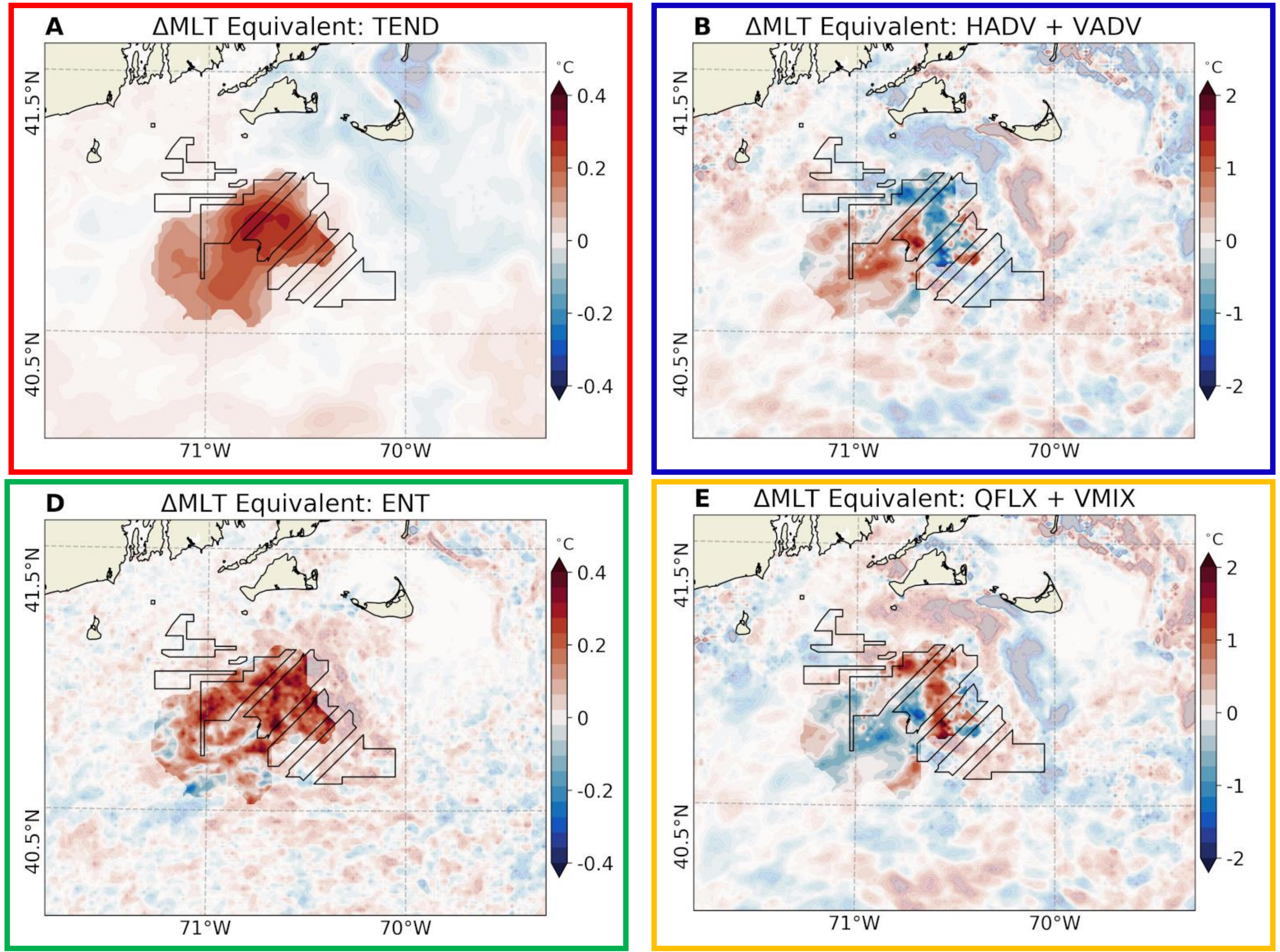

Reduced entrainment cooling due to shallow MLD plays dominant role

In the MA/RI region, the MLT increases by ~0.18°C, primarily due to reduced ENT cooling (0.17°C)

Ocean mixed layer heat budget

$$\underbrace{\frac{\partial \langle T \rangle}{\partial t}}_{\text{TEND}} = \underbrace{-\langle \nabla \cdot (\mathrm{u}T) \rangle}_{\text{HADV}} + \underbrace{\frac{1}{H}(wT)_{z=-h}}_{\text{VADV}} + \underbrace{\left\langle \nabla \cdot \left(\kappa_h \nabla T \right) \right\rangle}_{\text{HMIX}} \underbrace{- \frac{1}{H}\left(\kappa_v \frac{\partial T}{\partial z} \right)_{z=-h}}_{\text{VMIX}} + \underbrace{\frac{Q_{net} - Q_{sw}|_{z=-h}}{\rho c_p H}}_{\text{QFLX}} \underbrace{- \frac{\Delta T}{H} \frac{\partial h}{\partial t}}_{\text{ENT}}$$

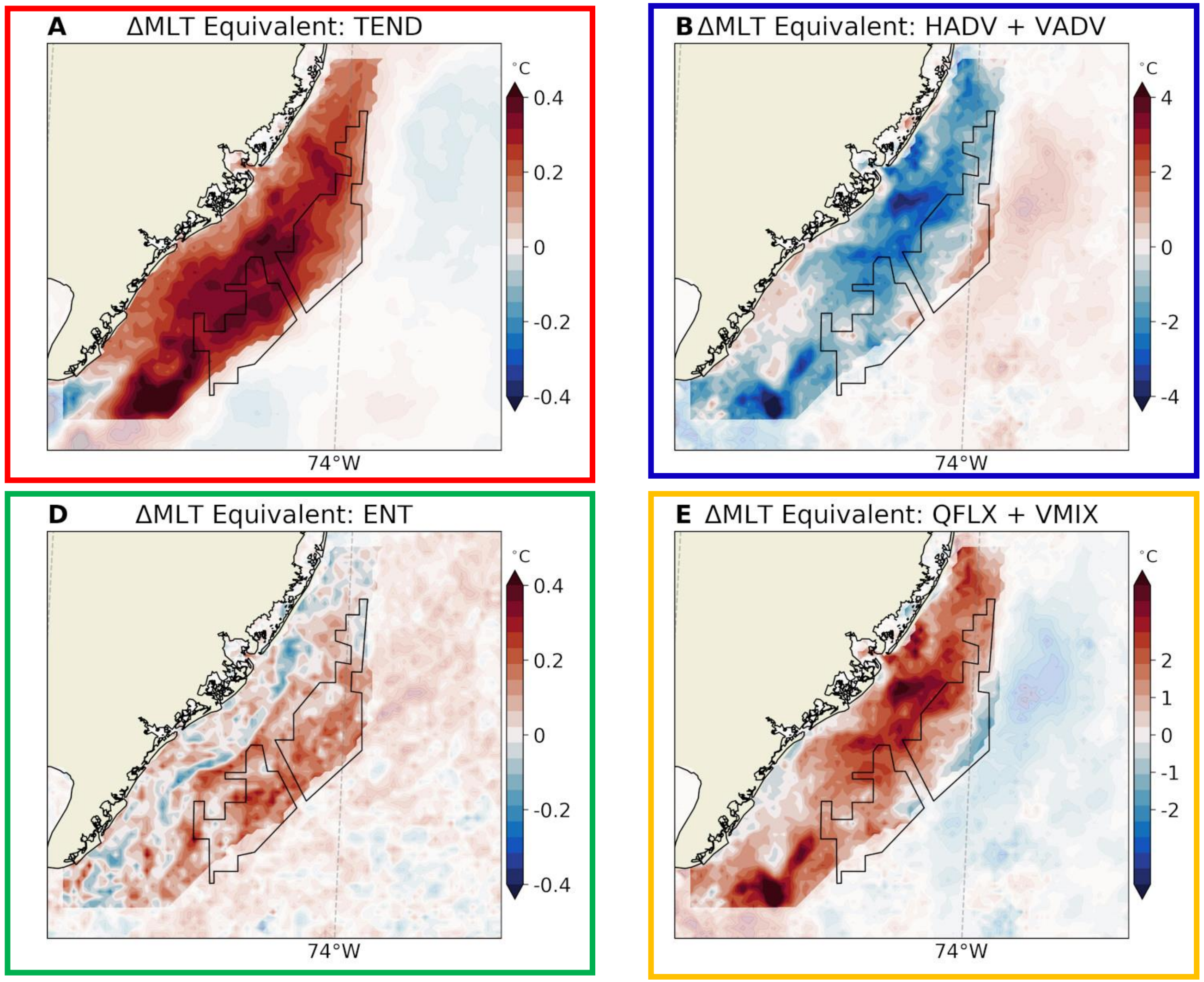

Ocean mixed layer heat budget

$$\underbrace{\frac{\partial\langle T\rangle}{\partial t}}_{\text{TEND}} = \underbrace{-\langle\nabla\cdot(\mathbf{u}T)\rangle}_{\text{HADV}} + \underbrace{\frac{1}{H}(wT)_{z=-h}}_{\text{VADV}} + \underbrace{\left\langle\nabla\cdot\left(\kappa_h\nabla T\right)\right\rangle}_{\text{HMIX}} \underbrace{- \frac{1}{H}\left(\kappa_v\frac{\partial T}{\partial z}\right)_{z=-h}}_{\text{VMIX}} + \underbrace{\frac{Q_{net}-Q_{sw}|_{z=-h}}{\rho c_p H}}_{\text{QFLX}} \underbrace{- \frac{\Delta T}{H}\frac{\partial h}{\partial t}}_{\text{ENT}}$$

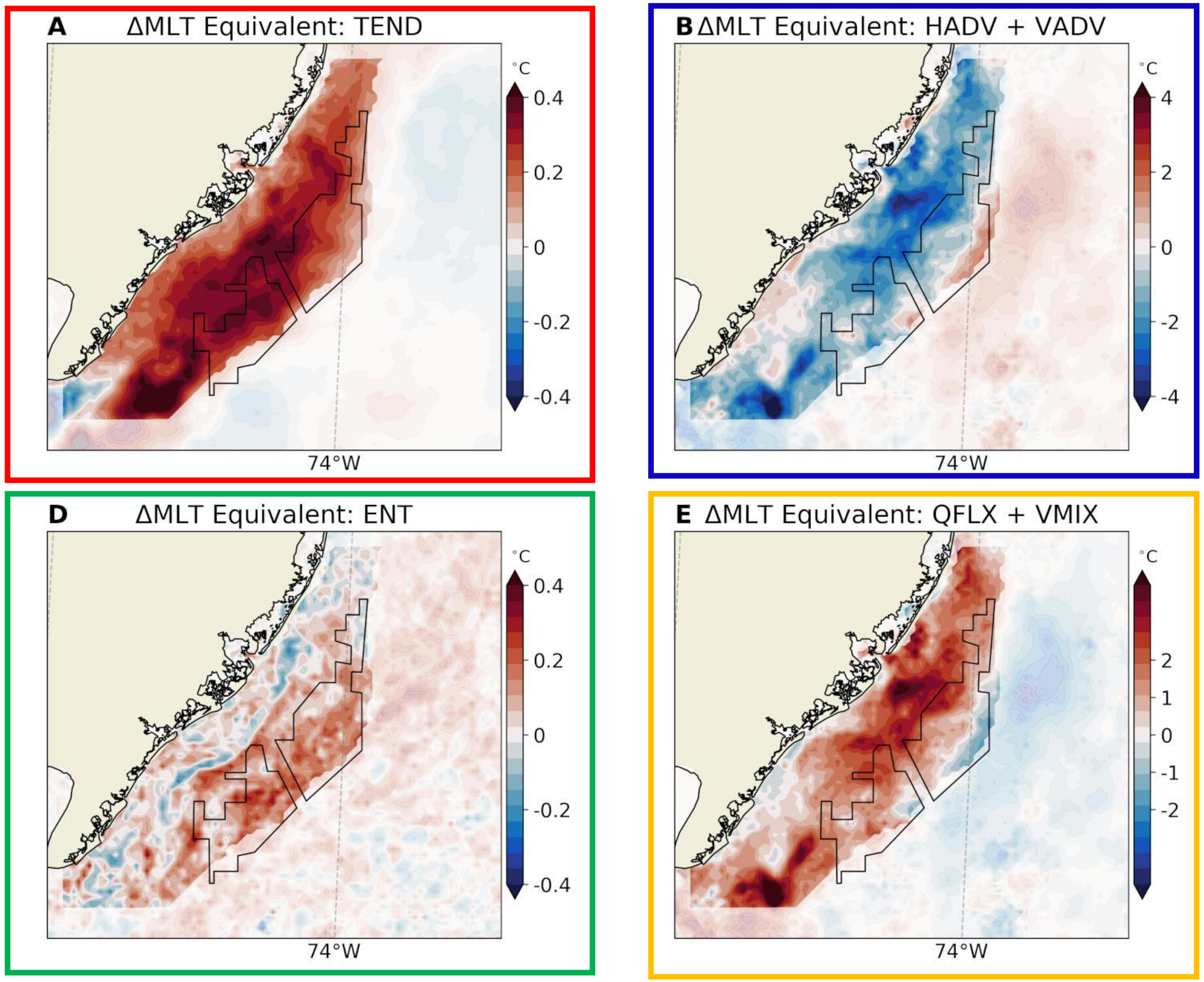

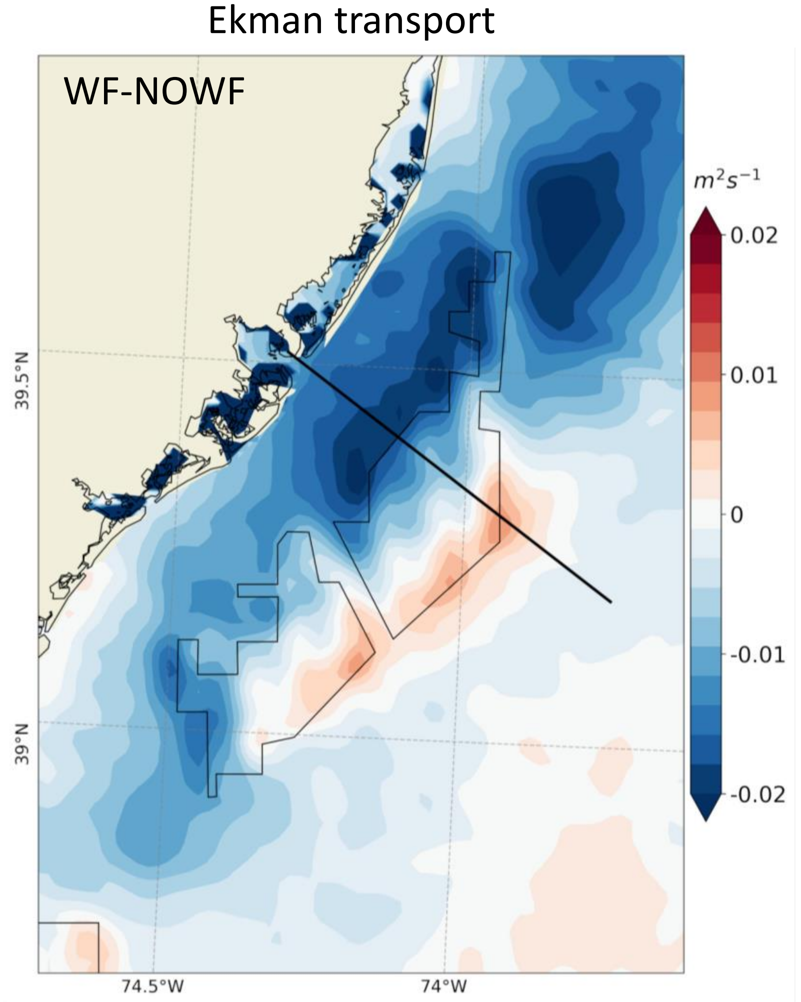

Ocean- to- atmosphere feedback

SST response to wind farms: WF - NOC_WF

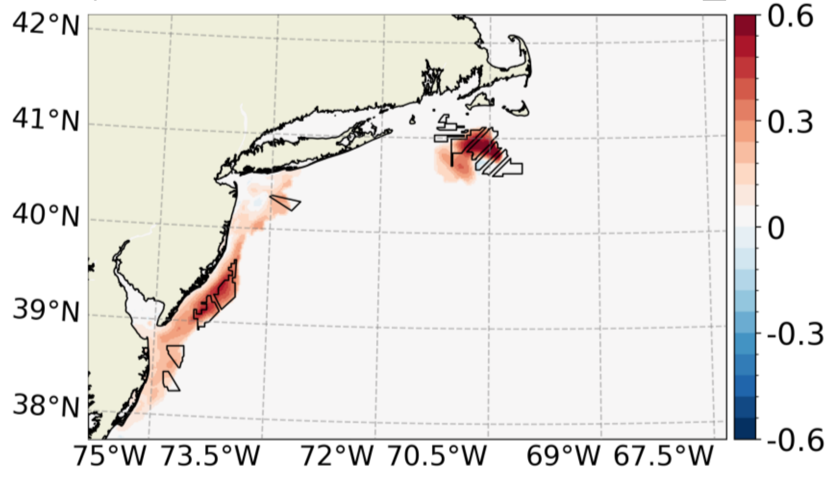

Isolating SST feedback and coupling effect.

How does this anomalous SST warming affect the marine boundary layer ?

Ocean- to- atmosphere feedback

SST response to wind farms: WF - NOC_WF

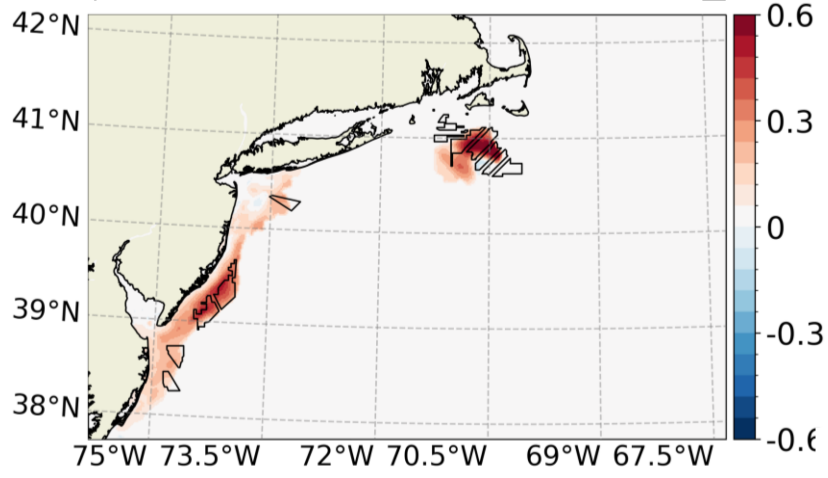

Isolating SST feedback and coupling effect.

How does this anomalous SST warming affect the marine boundary layer ?

boundary layer height

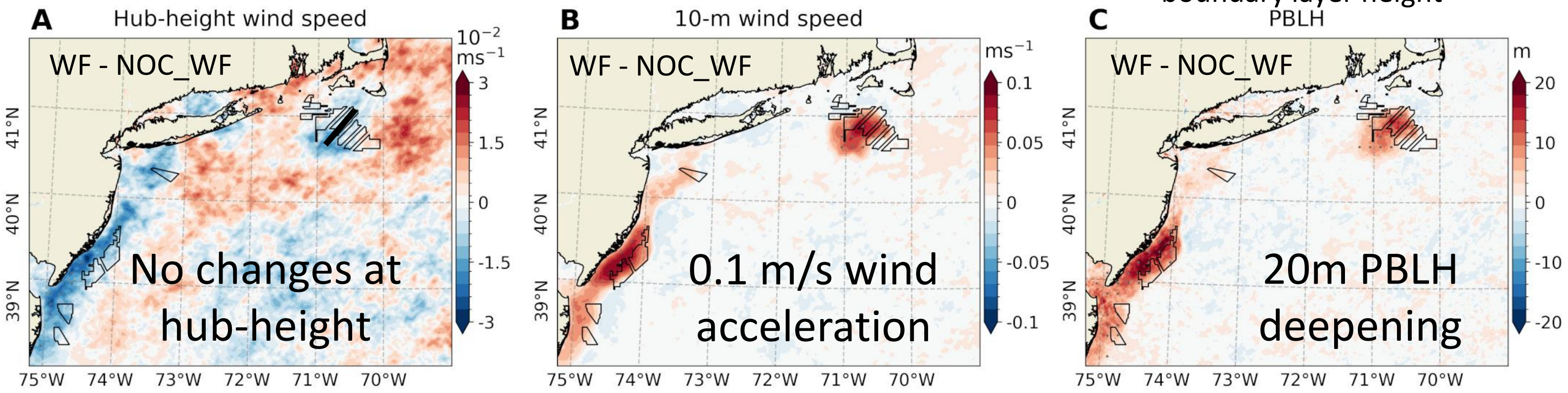

Ocean- to- atmosphere feedback

SST response to wind farms: WF - NOC_WF

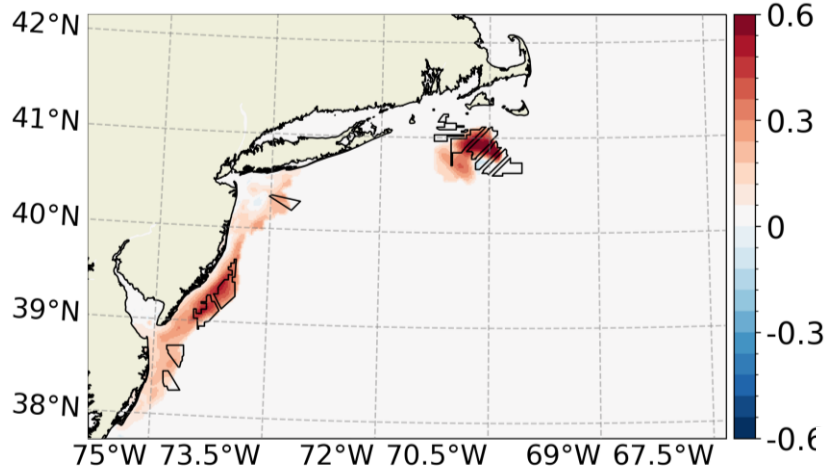

Isolating SST feedback and coupling effect.

How does this anomalous SST warming affect the marine boundary layer ?

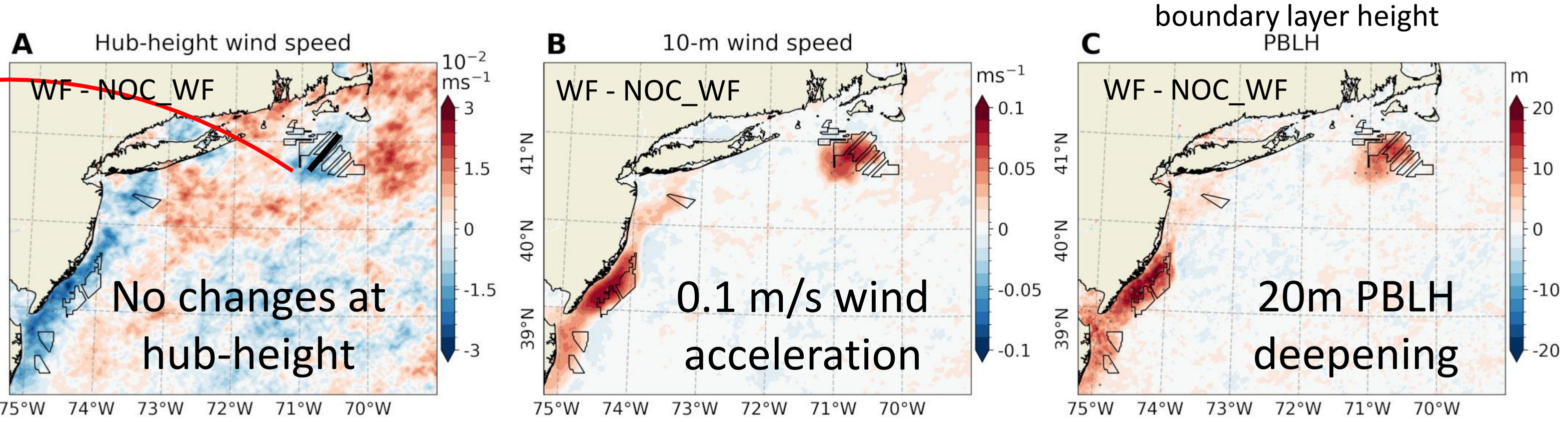

Impacts on wind appear to be limited to the surface layer (<50 m)

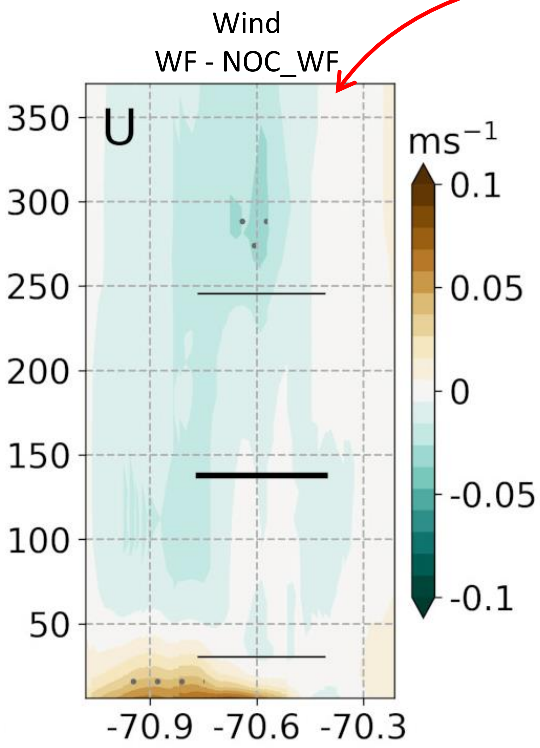

Ocean- to- atmosphere feedback

SST response to wind farms: WF - NOC_WF

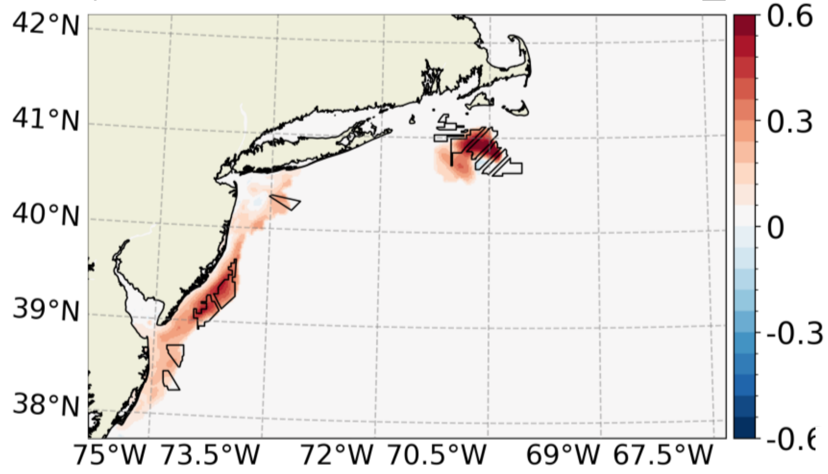

Isolating SST feedback and coupling effect.

How does this anomalous SST warming affect the marine boundary layer ?

Wind
WF - NOC_WF

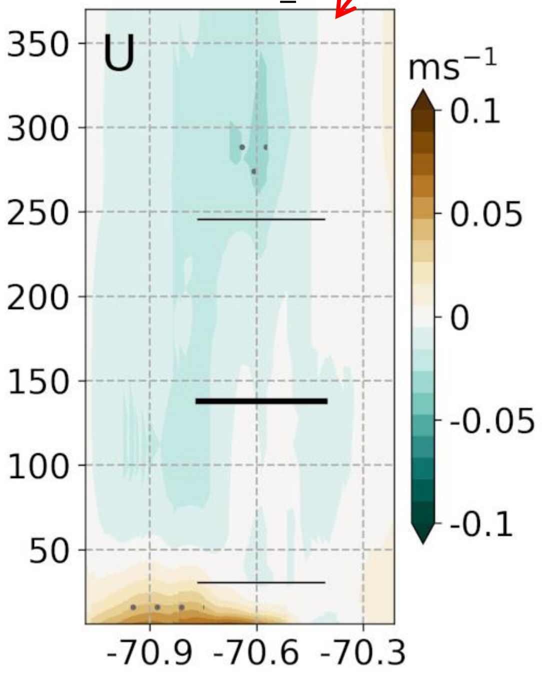

Impacts on wind appear to be limited to the surface layer (<50 m)

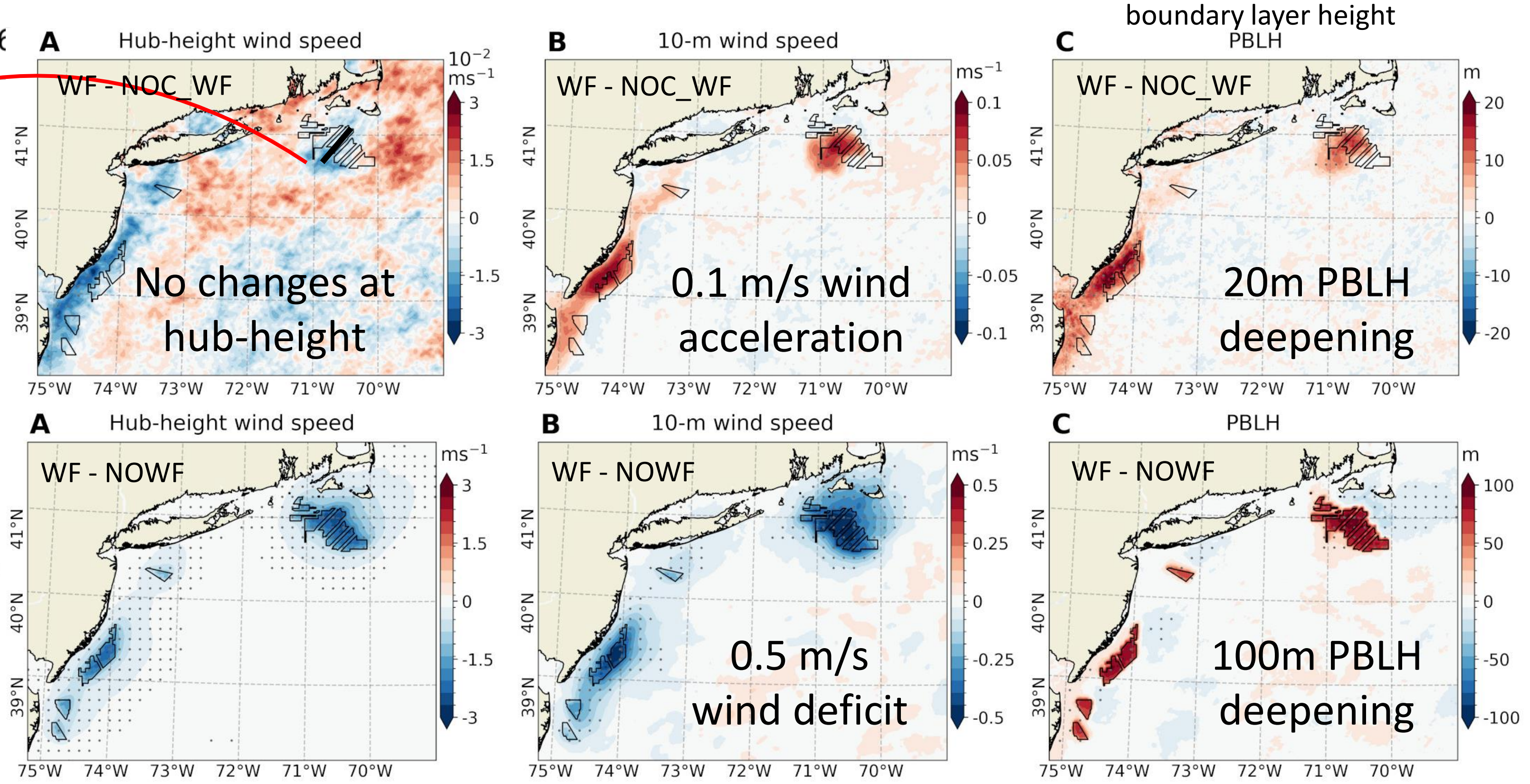

Conclusion

- The lower wind-sea energy suggests reduced wave growth in the vicinity of the wind farms while weaker winds favor the presence of longer-period waves.

- Wake-driven wind stress reduction may lead to anomalously warm SST of 0.3-0.4°C and shallow MLD.

- Ocean coupling accounts for ~10 to 20% of the wind speed deficit and PBL deepening at the wind farms.

- However, this coupling impact is limited to the surface layer with no significant changes at hub height.

- Perspectives:
  - Are changes similar during other seasons? Would the results changes with different wind farms size, layout and/or turbines specifications?

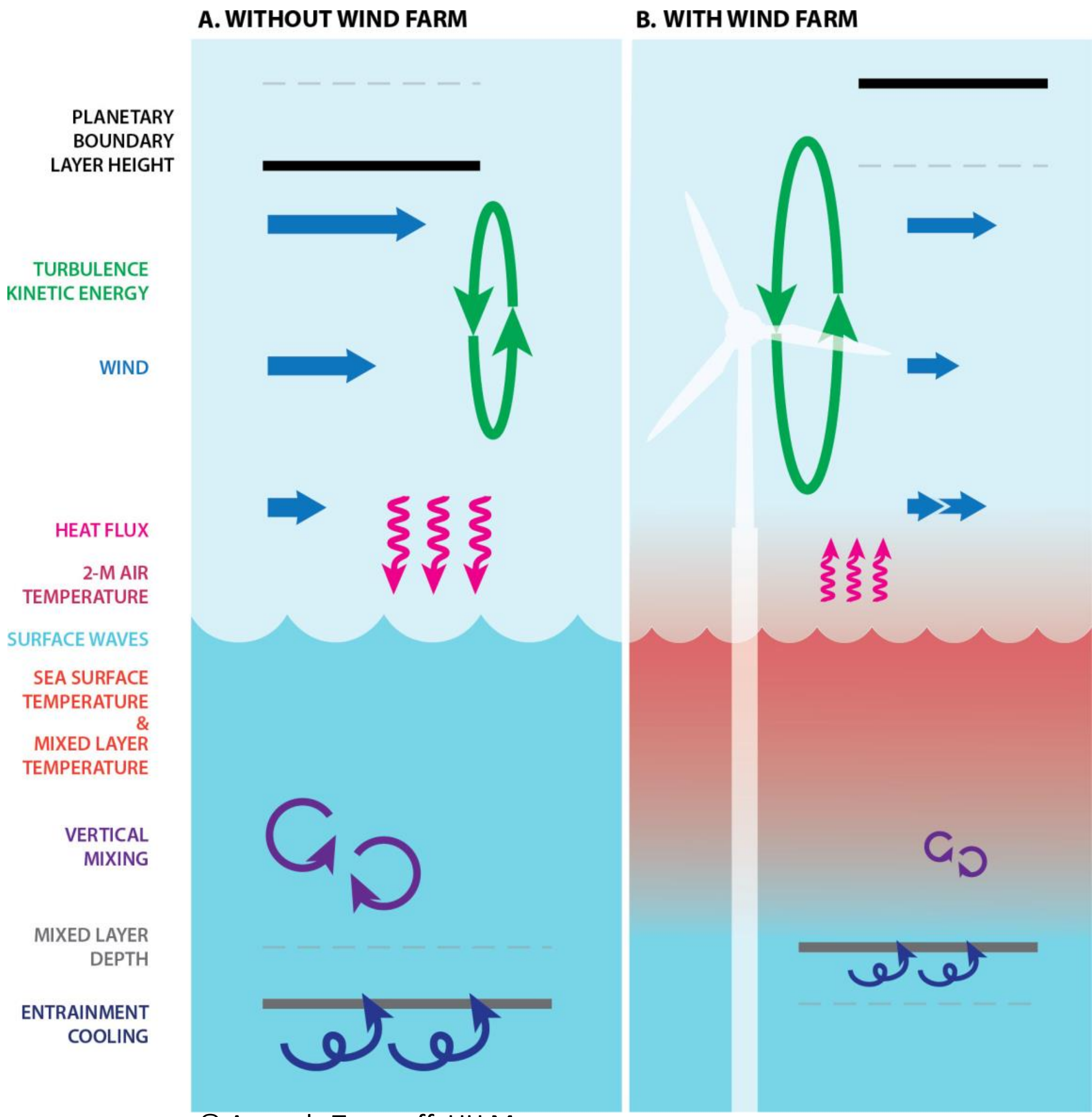

© Amanda Toperoff, UH Manoa

Ocean response to offshore wind farms off the Coast of New England

César Sauvage & Co-Authors

University of Hawai’i at Manoa, HI,USA

- **Sauvage, C.**, Seo, H., Zippel, S., Clayson, C-A., Edson, J. (2025). Fetch-dependent Surface Wave Responses To Offshore Wind Farms in the Northeast U.S. Coast. In JGR: Oceans.
- Seo, H., **Sauvage, C.**, Renkl, C., Lundquist, J., Kirincich, A. (2025). Sea Surface Warming and Ocean-to-Atmosphere Feedback Driven by Large-Scale Offshore Wind Farms under Seasonally Stratified Conditions. In Science Advances.

UNIVERSITY of HAWAI‘I MĀNOA

Oceanography Seminar
May 7, 2026
Contact: csauvage@hawaii.edu

U.S. DEPARTMENT OF ENERGY | Energy Efficiency & Renewable Energy

Supplementary Figures


sediment wakes
Boat wake
1 km
earthobservatory.nasa.gov

Supplementary Figures

Coupling frequency 1h
Horizontal resolution : 1.5 km
(7.5 km for OUTER domain)

Boundary forcing:

Atmospheric forcing:
hourly ERA5

Ocean forcing:
Daily Mercator Ocean Inter.

Wave forcing:
3-hourly spectral points
(Ifremer global runs)

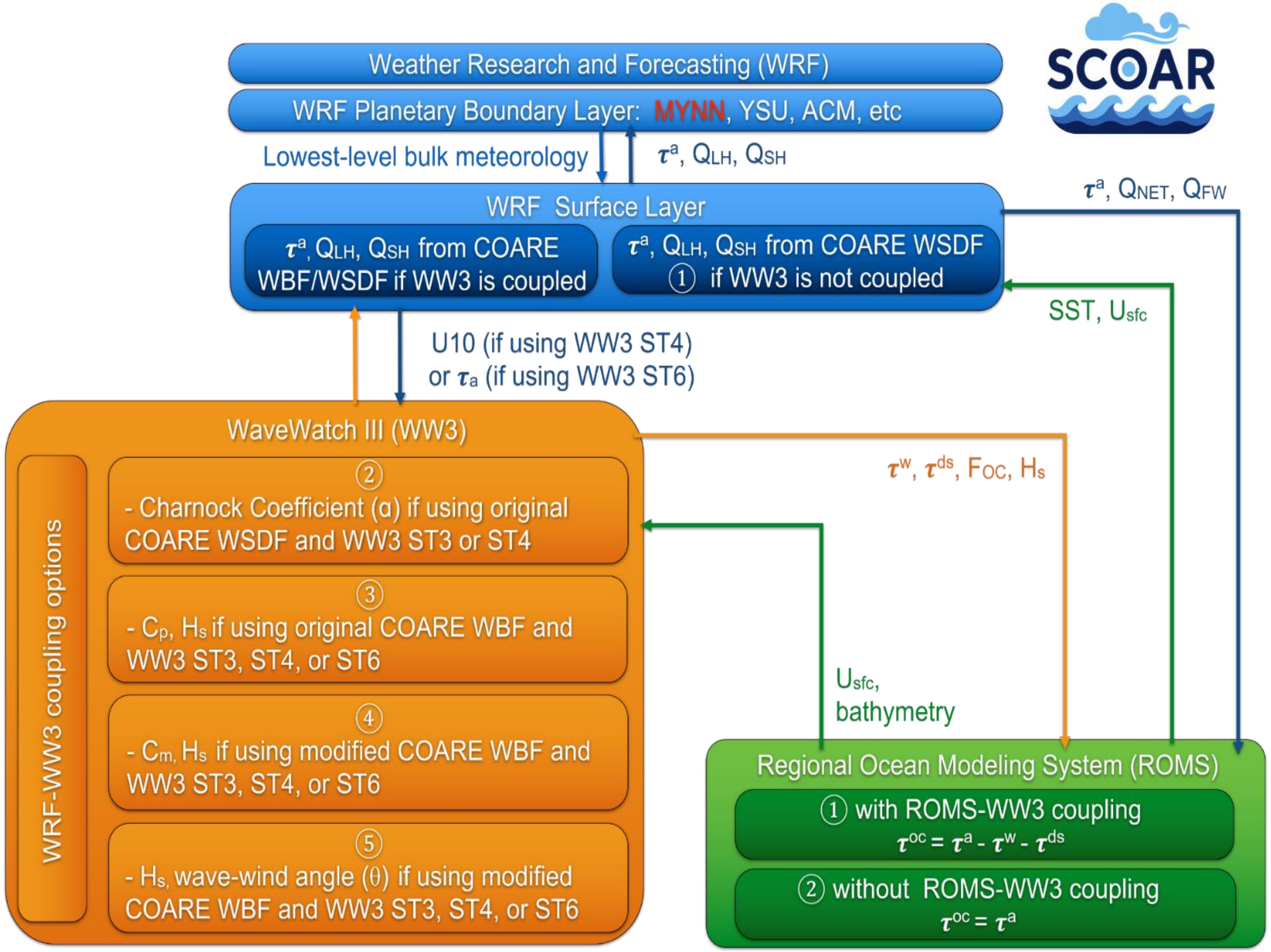

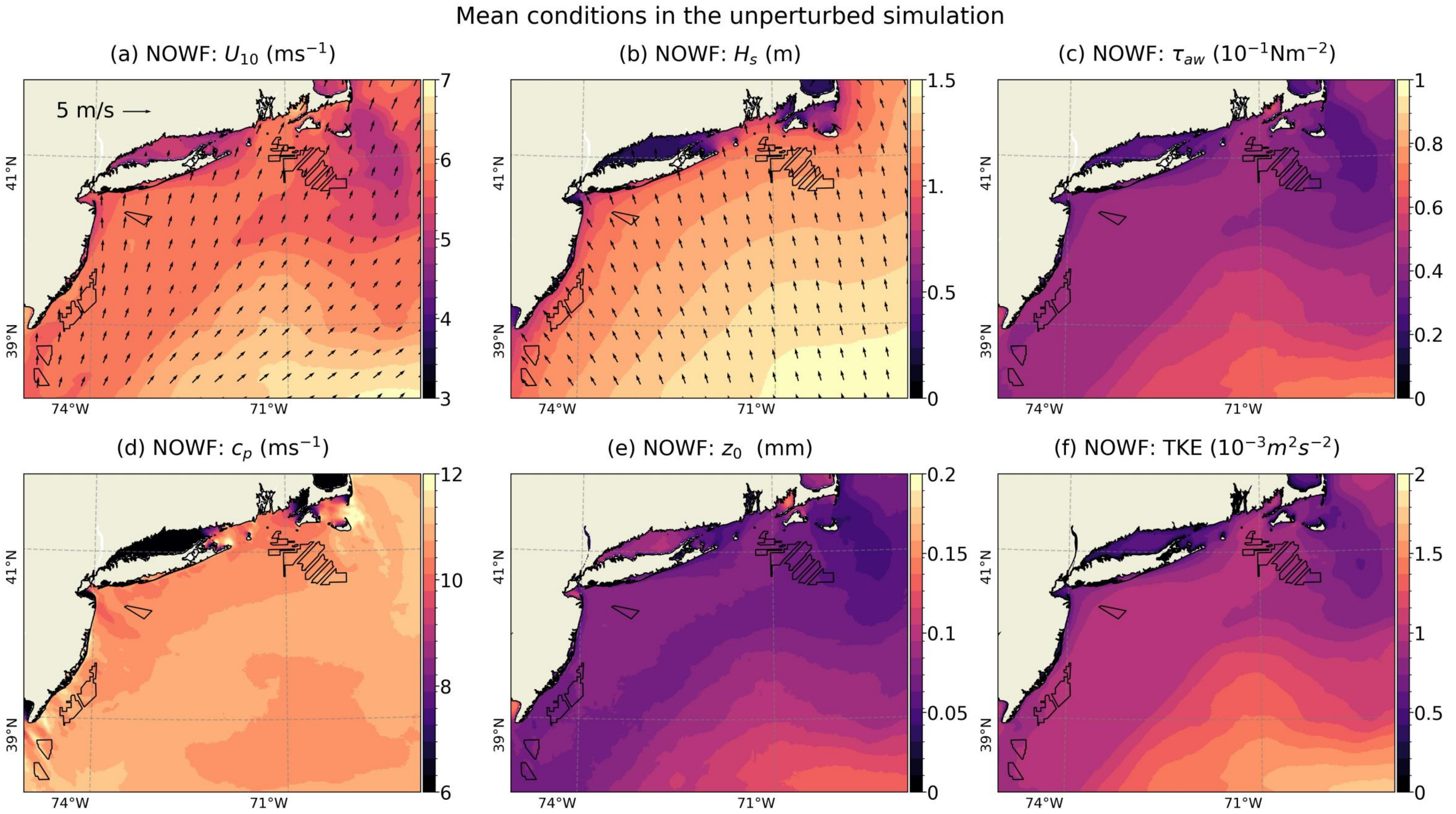
Mean conditions in the unperturbed simulation
(a) NOWF: U_{10} (ms^{-1})
5 m/s
(b) NOWF: H_s (m)
(c) NOWF: τ_{aw} ($10^{-1}Nm^{-2}$)
(d) NOWF: c_p (ms^{-1})
(e) NOWF: z_0 (mm)
(f) NOWF: TKE ($10^{-3}m^2s^{-2}$)
41°N
39°N
74°W
71°W

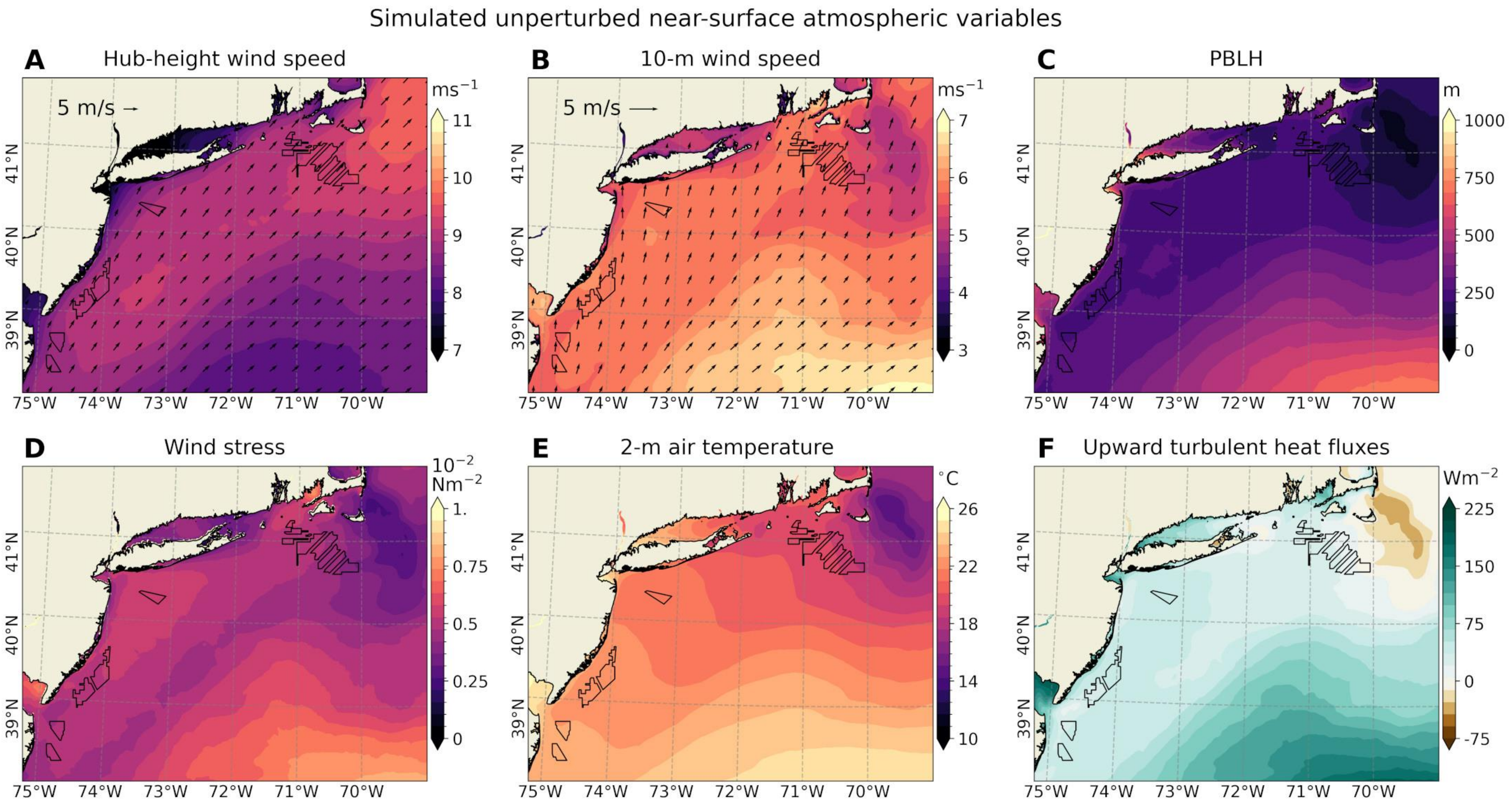

Simulated unperturbed near-surface atmospheric variables
A
Hub-height wind speed
5 m/s
ms^{-1}
11
10
9
8
7
B
10-m wind speed
5 m/s
ms^{-1}
7
6
5
4
3
C
PBLH
m
1000
750
500
250
0
D
Wind stress
10^{-2} Nm^{-2}
1.
0.75
0.5
0.25
0
E
2-m air temperature
°C
26
22
18
14
10
F
Upward turbulent heat fluxes
Wm^{-2}
225
150
75
0
-75
41°N
40°N
39°N
75°W
74°W
73°W
72°W
71°W
70°W

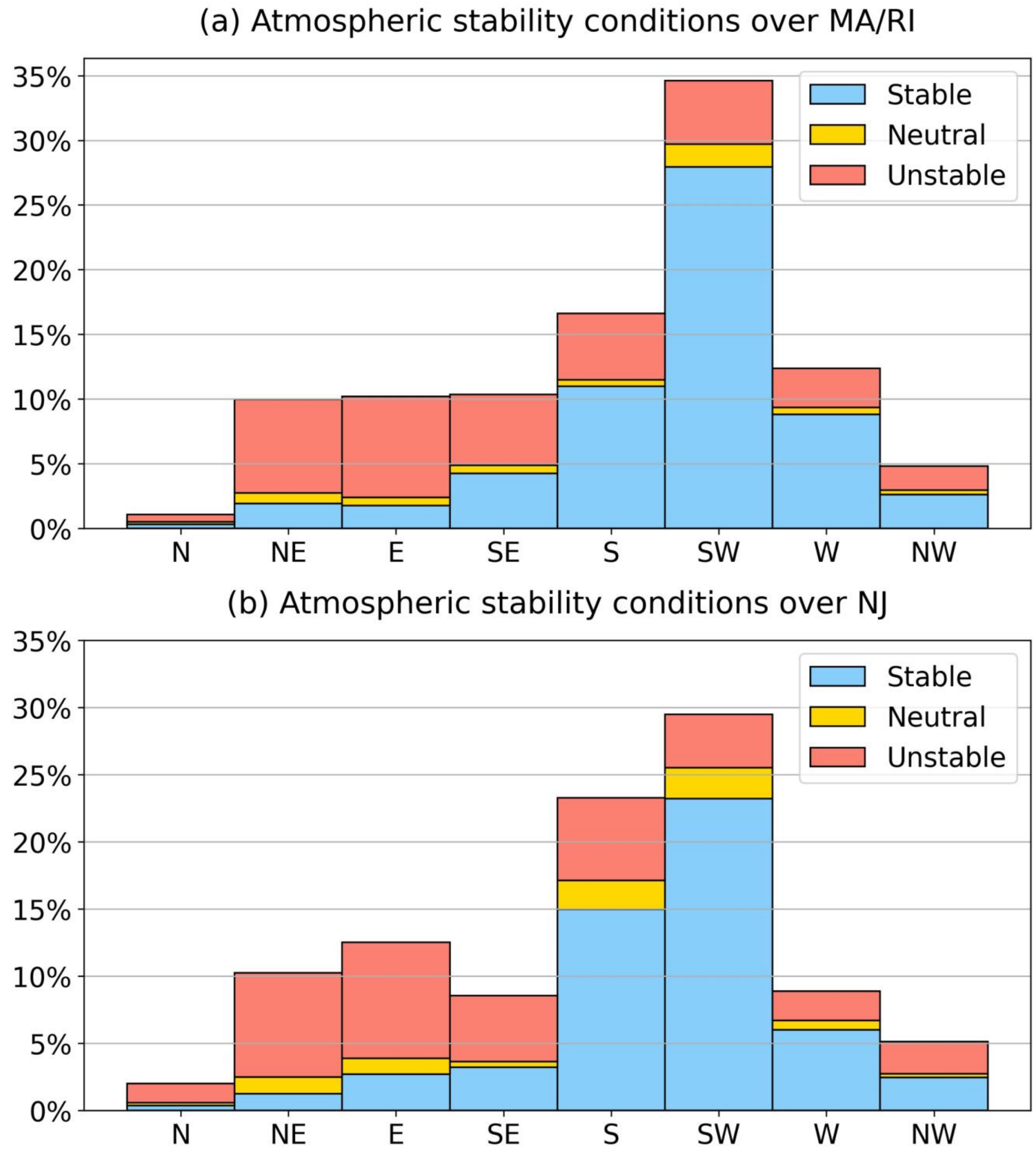
(a) Atmospheric stability conditions over MA/RI
35%
30%
25%
20%
15%
10%
5%
0%
Stable
Neutral
Unstable
N
NE
E
SE
S
SW
W
NW
(b) Atmospheric stability conditions over NJ
35%
30%
25%
20%
15%
10%
5%
0%
Stable
Neutral
Unstable
N
NE
E
SE
S
SW
W
NW

Comparison to observations

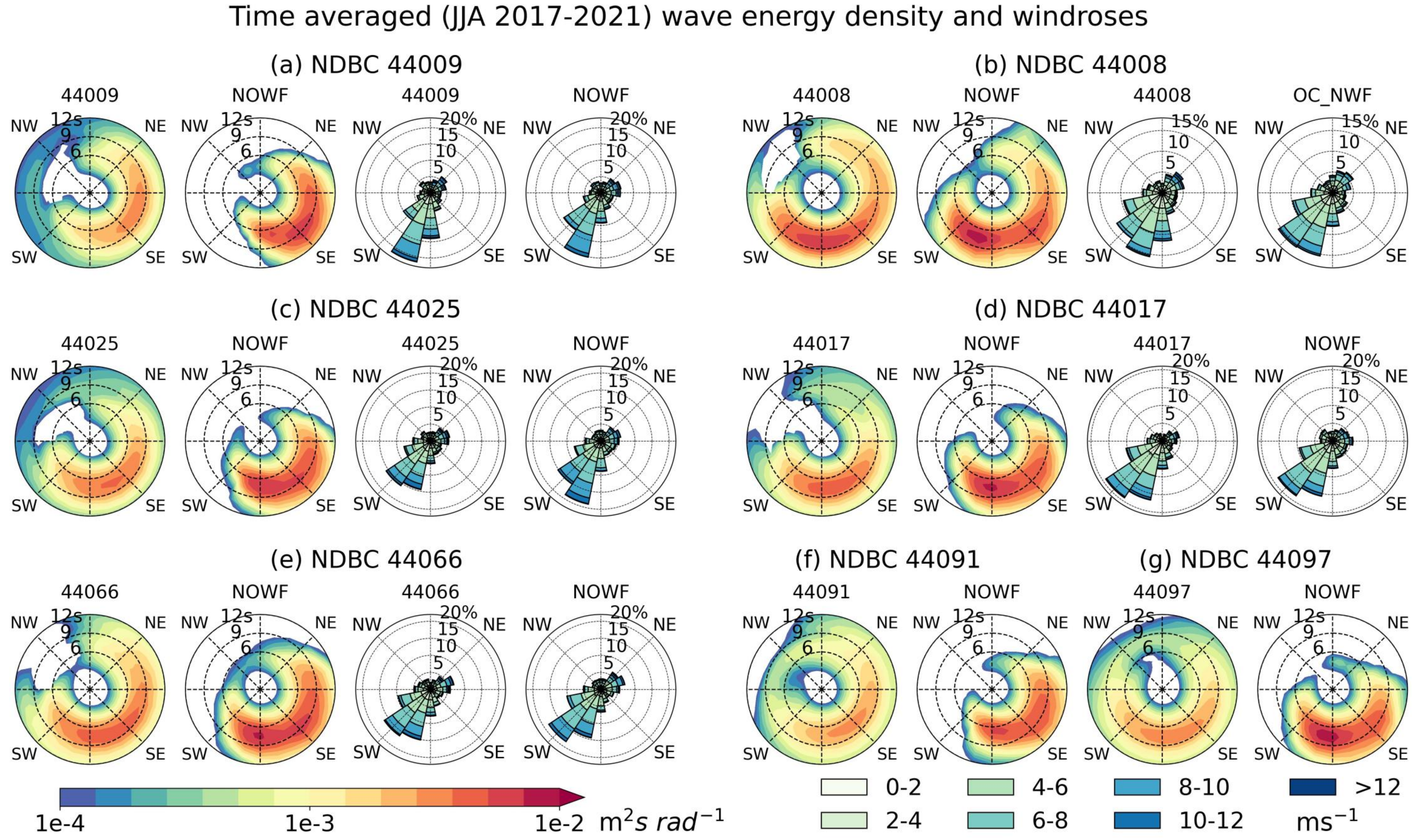

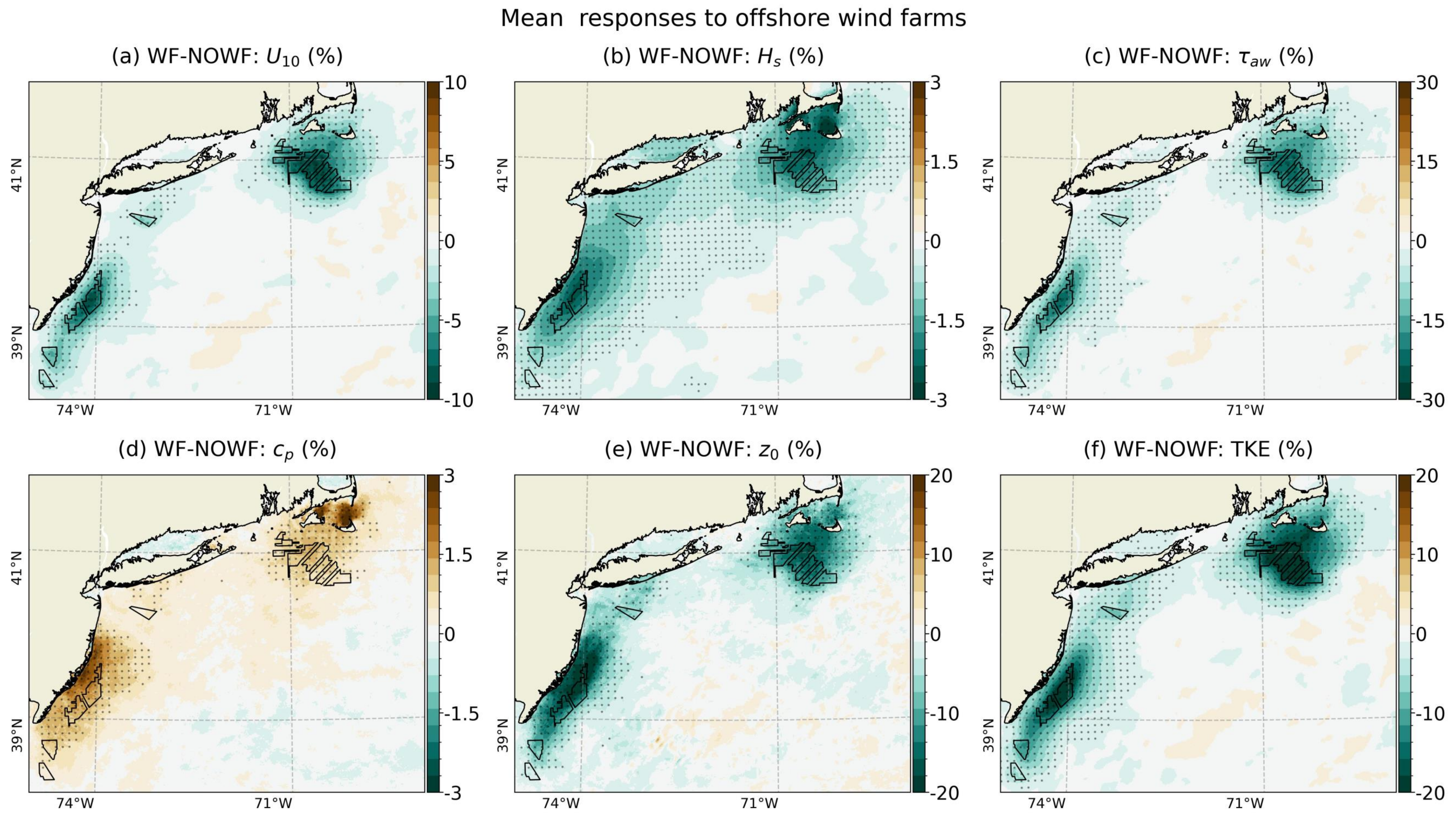

Mean responses to offshore wind farms
(a) WF-NOWF: U_{10} (%)
(b) WF-NOWF: H_s (%)
(c) WF-NOWF: τ_{aw} (%)
(d) WF-NOWF: c_p (%)
(e) WF-NOWF: z_0 (%)
(f) WF-NOWF: TKE (%)
41°N
39°N
74°W
71°W
10
5
0
-5
-10
3
1.5
-1.5
-3
30
15
-15
-30
20
10
-10
-20

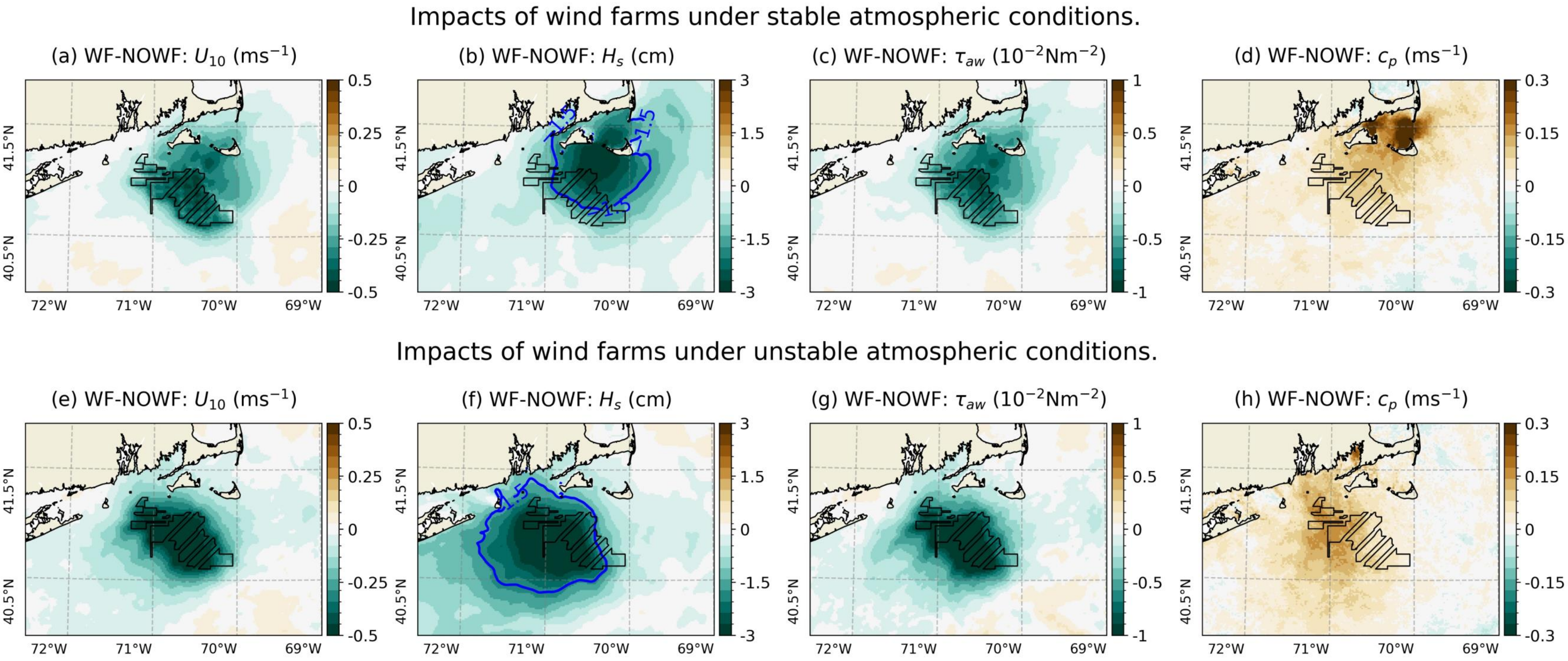

Impacts of wind farms under stable atmospheric conditions.
(a) WF-NOWF: U_{10} (ms^{-1})
(b) WF-NOWF: H_s (cm)
(c) WF-NOWF: τ_{aw} ($10^{-2}Nm^{-2}$)
(d) WF-NOWF: c_p (ms^{-1})
Impacts of wind farms under unstable atmospheric conditions.
(e) WF-NOWF: U_{10} (ms^{-1})
(f) WF-NOWF: H_s (cm)
(g) WF-NOWF: τ_{aw} ($10^{-2}Nm^{-2}$)
(h) WF-NOWF: c_p (ms^{-1})
72°W
71°W
70°W
69°W
41.5°N
40.5°N
-1.5

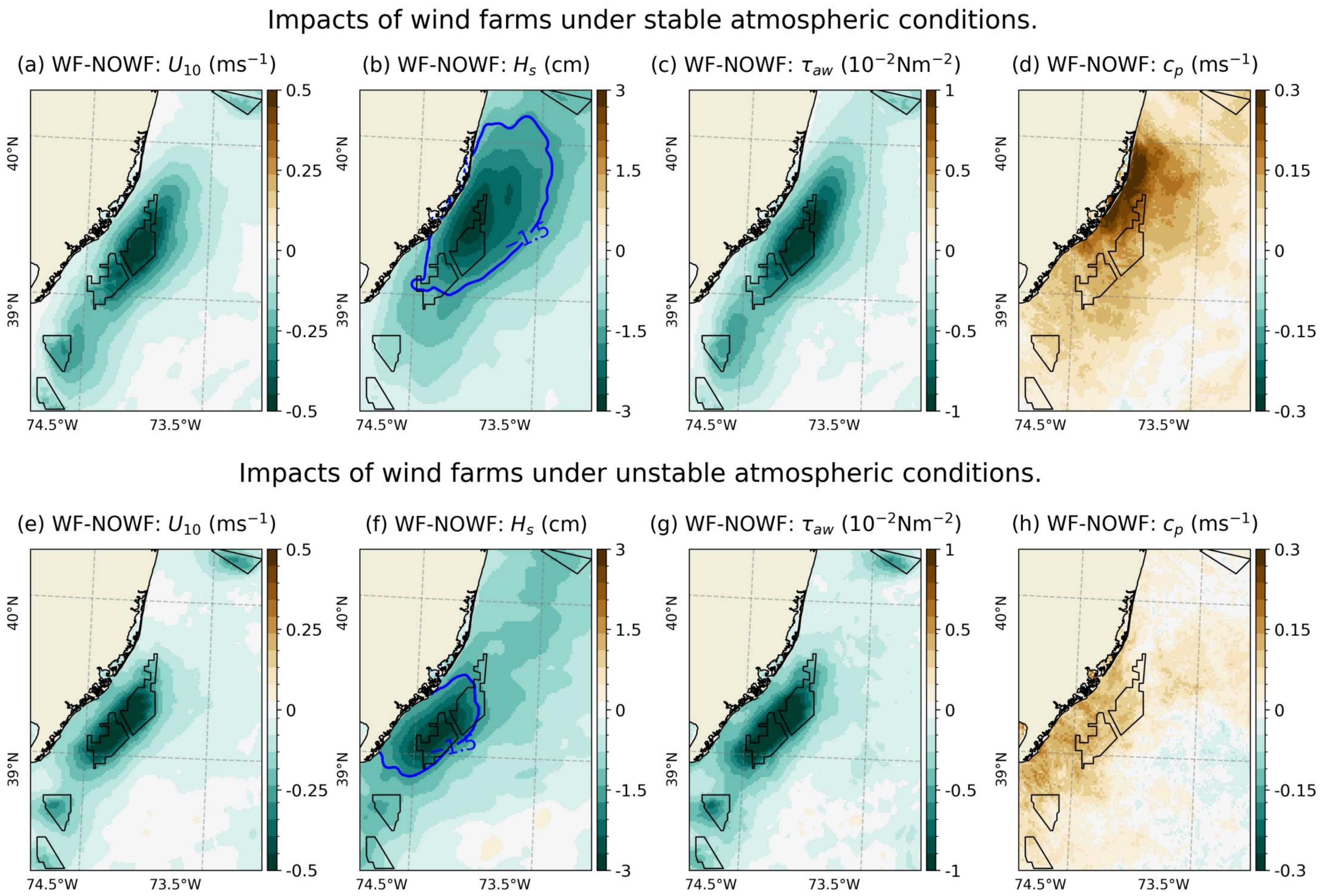

Impacts of wind farms under stable atmospheric conditions.
(a) WF-NOWF: U_{10} (ms^{-1})
(b) WF-NOWF: H_s (cm)
(c) WF-NOWF: τ_{aw} (10^{-2}Nm^{-2})
(d) WF-NOWF: c_p (ms^{-1})
Impacts of wind farms under unstable atmospheric conditions.
(e) WF-NOWF: U_{10} (ms^{-1})
(f) WF-NOWF: H_s (cm)
(g) WF-NOWF: τ_{aw} (10^{-2}Nm^{-2})
(h) WF-NOWF: c_p (ms^{-1})
40°N
39°N
74.5°W
73.5°W
−1.5

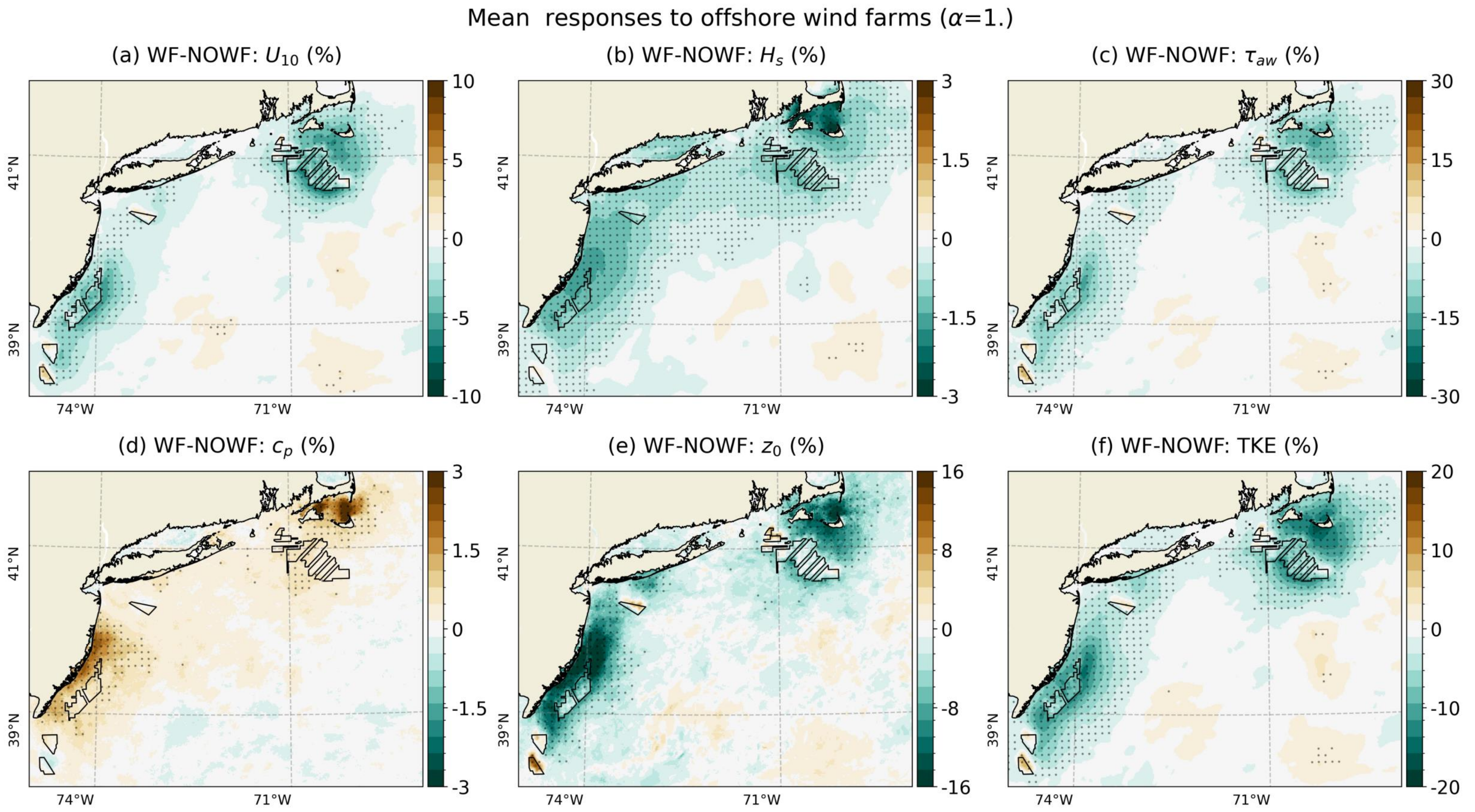

Mean responses to offshore wind farms (α=1.)
(a) WF-NOWF: U_{10} (%)
(b) WF-NOWF: H_s (%)
(c) WF-NOWF: τ_{aw} (%)
(d) WF-NOWF: c_p (%)
(e) WF-NOWF: z_0 (%)
(f) WF-NOWF: TKE (%)
10
5
0
-5
-10
3
1.5
0
-1.5
-3
30
15
0
-15
-30
16
8
0
-8
-16
20
10
0
-10
-20
41°N
39°N
74°W
71°W

Wave spectrum differences

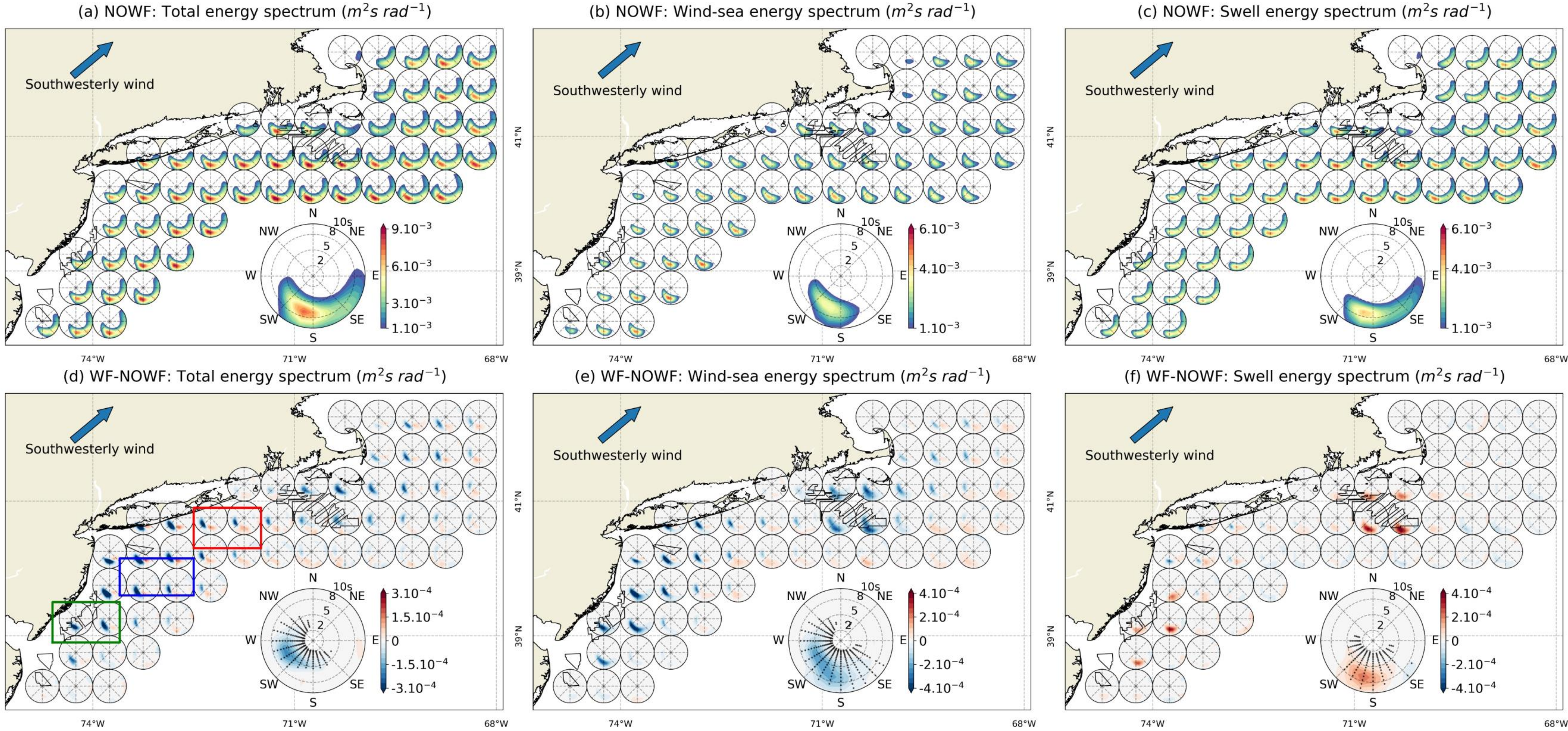

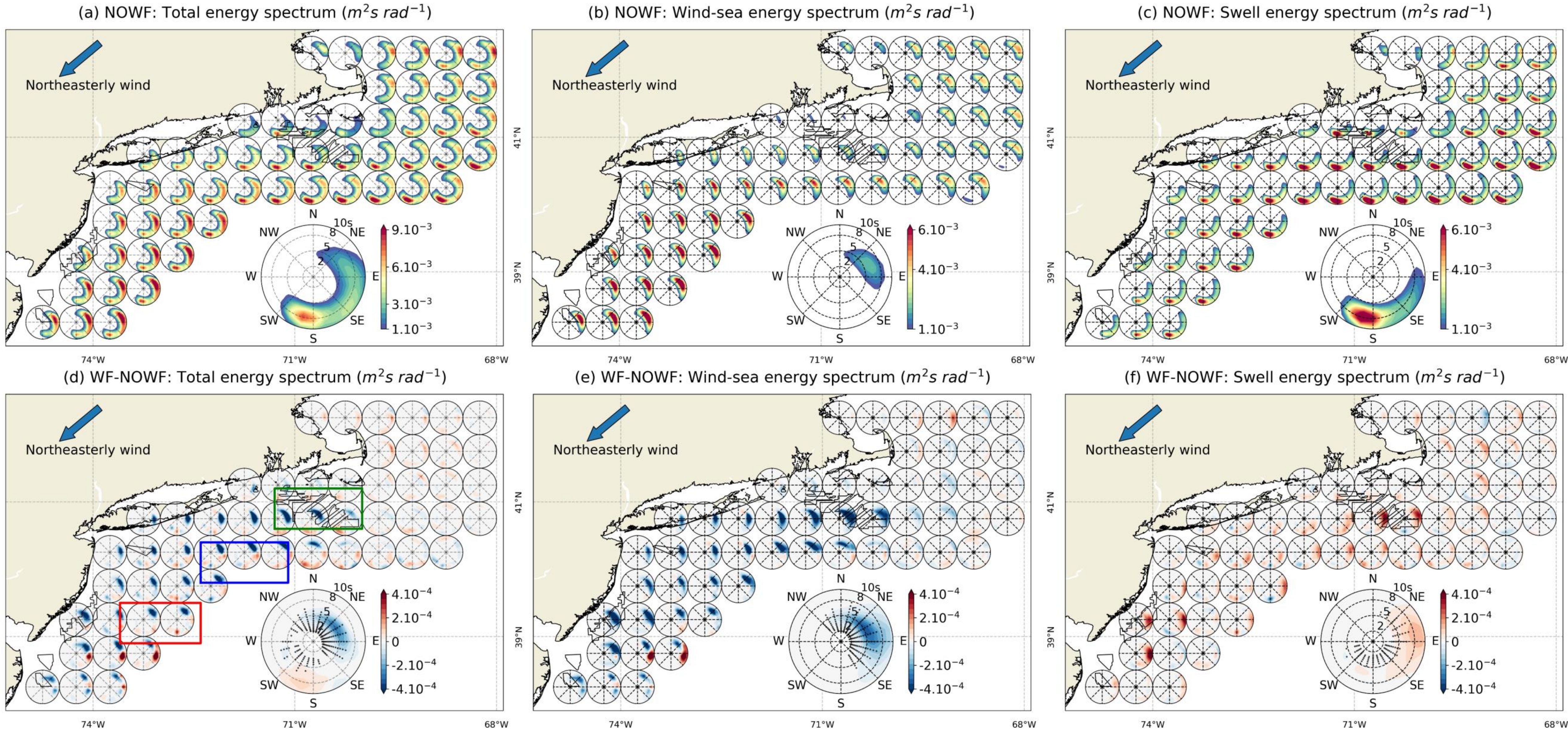

(a) NOWF: Total energy spectrum ($m^2s\ rad^{-1}$)
(b) NOWF: Wind-sea energy spectrum ($m^2s\ rad^{-1}$)
(c) NOWF: Swell energy spectrum ($m^2s\ rad^{-1}$)
(d) WF-NOWF: Total energy spectrum ($m^2s\ rad^{-1}$)
(e) WF-NOWF: Wind-sea energy spectrum ($m^2s\ rad^{-1}$)
(f) WF-NOWF: Swell energy spectrum ($m^2s\ rad^{-1}$)
Northeasterly wind
N
NE
E
SE
S
SW
W
NW
10s
8
5
2
9.10^{-3}
6.10^{-3}
3.10^{-3}
1.10^{-3}
4.10^{-3}
4.10^{-4}
2.10^{-4}
0
-2.10^{-4}
-4.10^{-4}
41°N
39°N
74°W
71°W
68°W

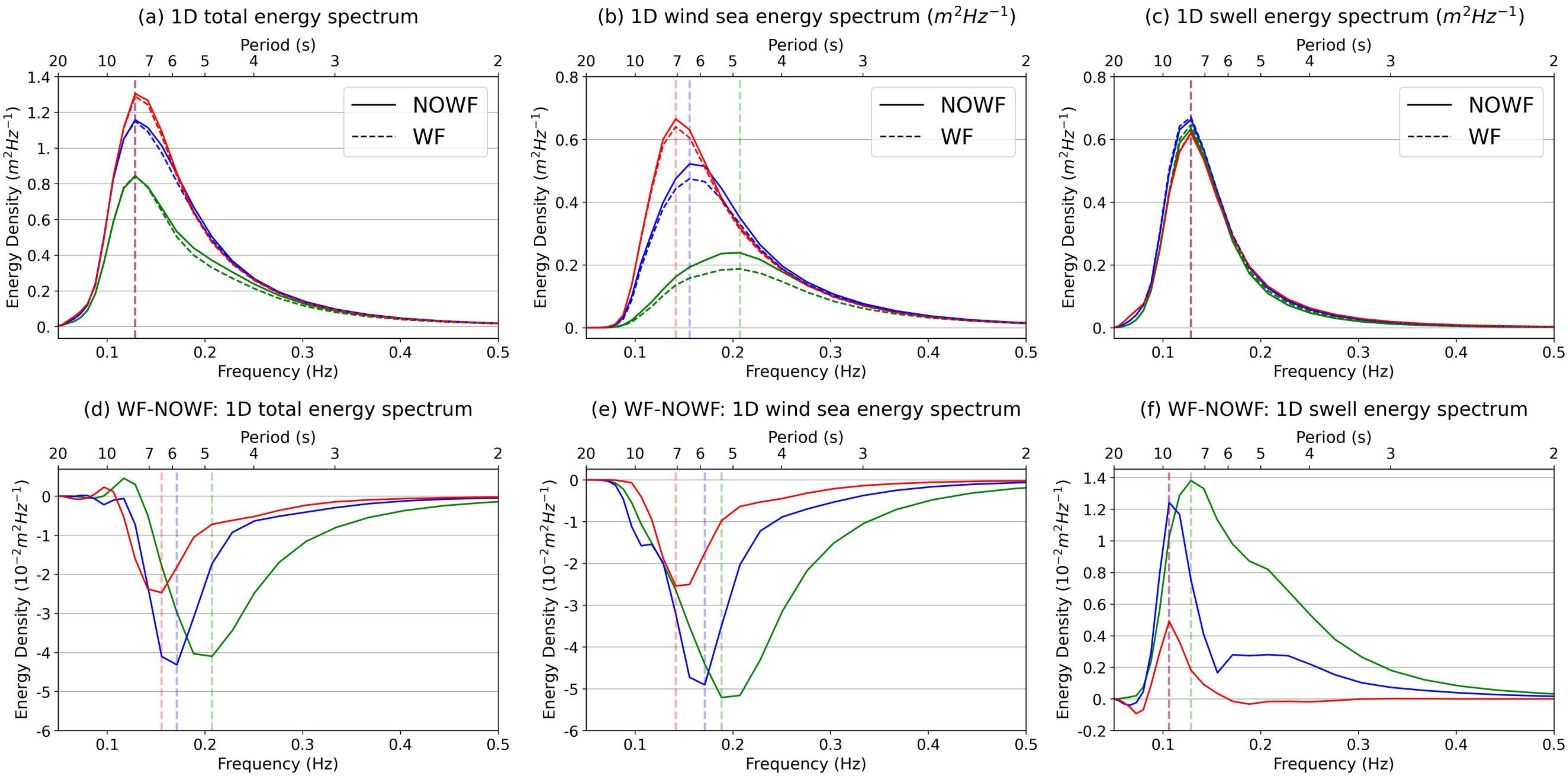

(a) 1D total energy spectrum
(b) 1D wind sea energy spectrum (m^2Hz^{-1})
(c) 1D swell energy spectrum (m^2Hz^{-1})
(d) WF-NOWF: 1D total energy spectrum
(e) WF-NOWF: 1D wind sea energy spectrum
(f) WF-NOWF: 1D swell energy spectrum
Period (s)
Frequency (Hz)
Energy Density (m^2Hz^{-1})
Energy Density ($10^{-2}m^2Hz^{-1}$)
NOWF
WF

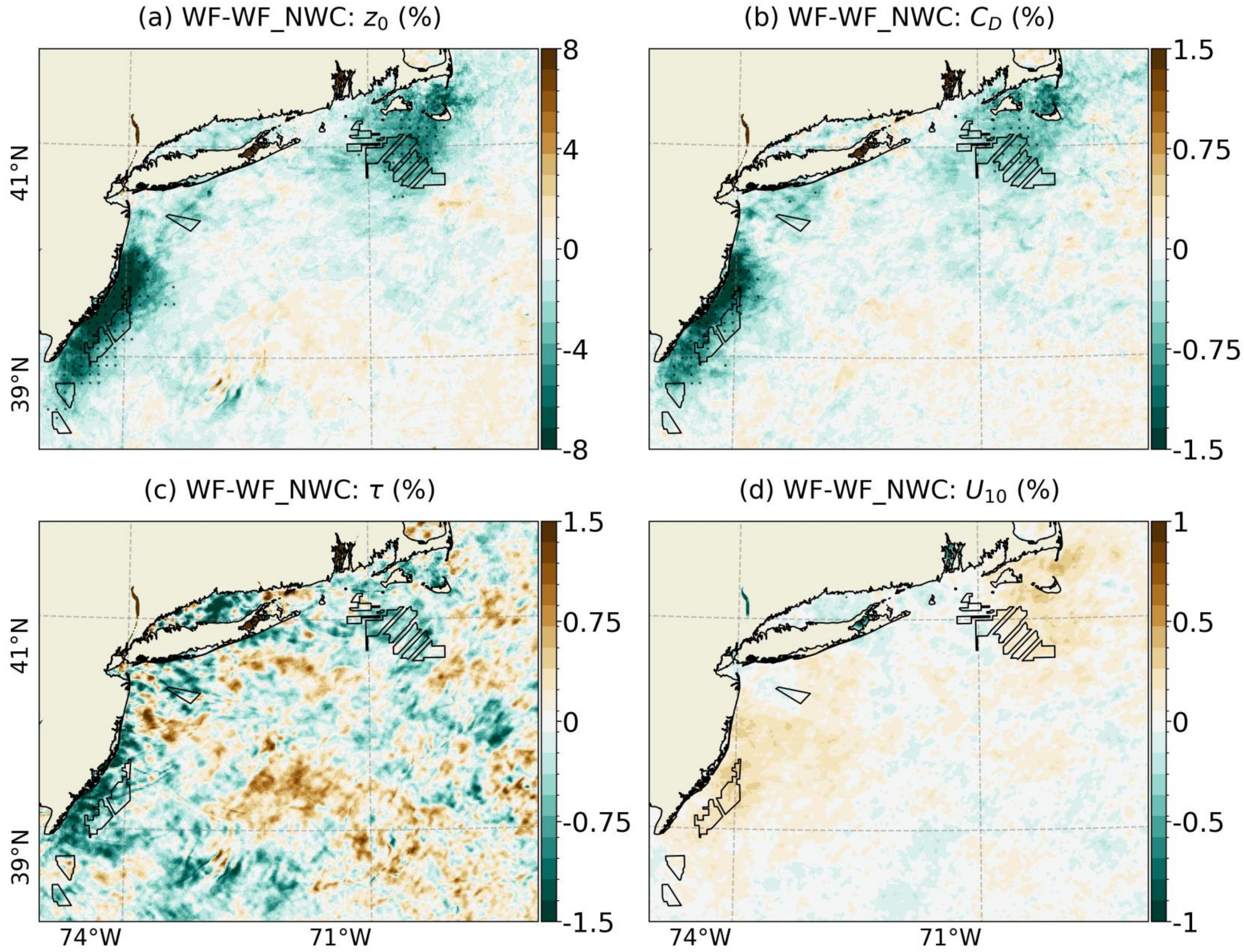

(a) WF-WF_NWC: z_0 (%)
(b) WF-WF_NWC: C_D (%)
(c) WF-WF_NWC: τ (%)
(d) WF-WF_NWC: U_{10} (%)
8
4
0
-4
-8
1.5
0.75
0
-0.75
-1.5
1.5
0.75
0
-0.75
-1.5
1
0.5
0
-0.5
-1
41°N
39°N
41°N
39°N
74°W
71°W
74°W
71°W

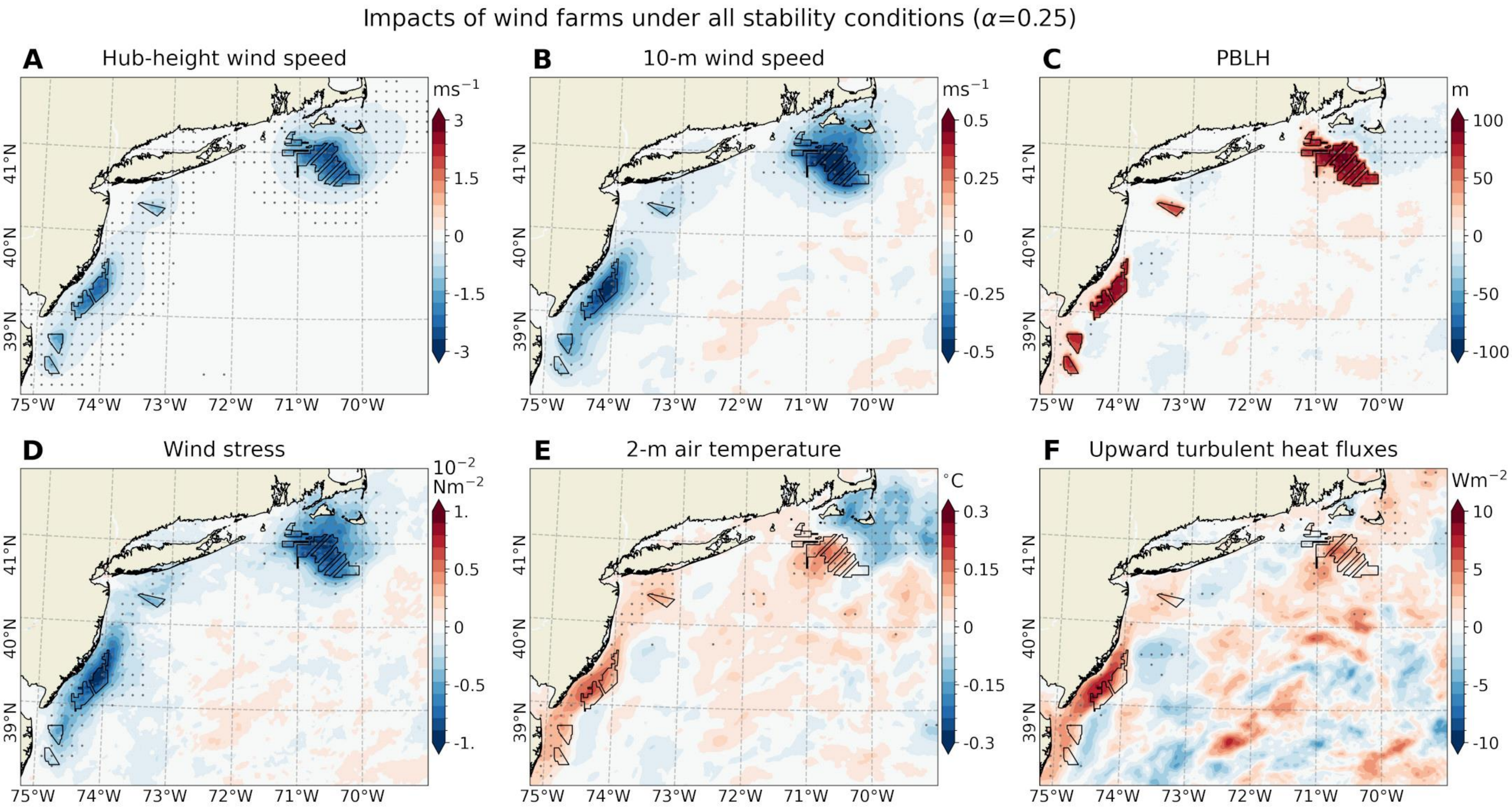

Impacts of wind farms under all stability conditions (α=0.25)
A
Hub-height wind speed
ms⁻¹
3
1.5
0
-1.5
-3
B
10-m wind speed
ms⁻¹
0.5
0.25
0
-0.25
-0.5
C
PBLH
m
100
50
0
-50
-100
D
Wind stress
10⁻² Nm⁻²
1.
0.5
0
-0.5
-1.
E
2-m air temperature
°C
0.3
0.15
0
-0.15
-0.3
F
Upward turbulent heat fluxes
Wm⁻²
10
5
0
-5
-10
41°N
40°N
39°N
75°W
74°W
73°W
72°W
71°W
70°W

Long-term near-surface impacts of wind farms for all stability conditions with $\alpha = 1.0$.

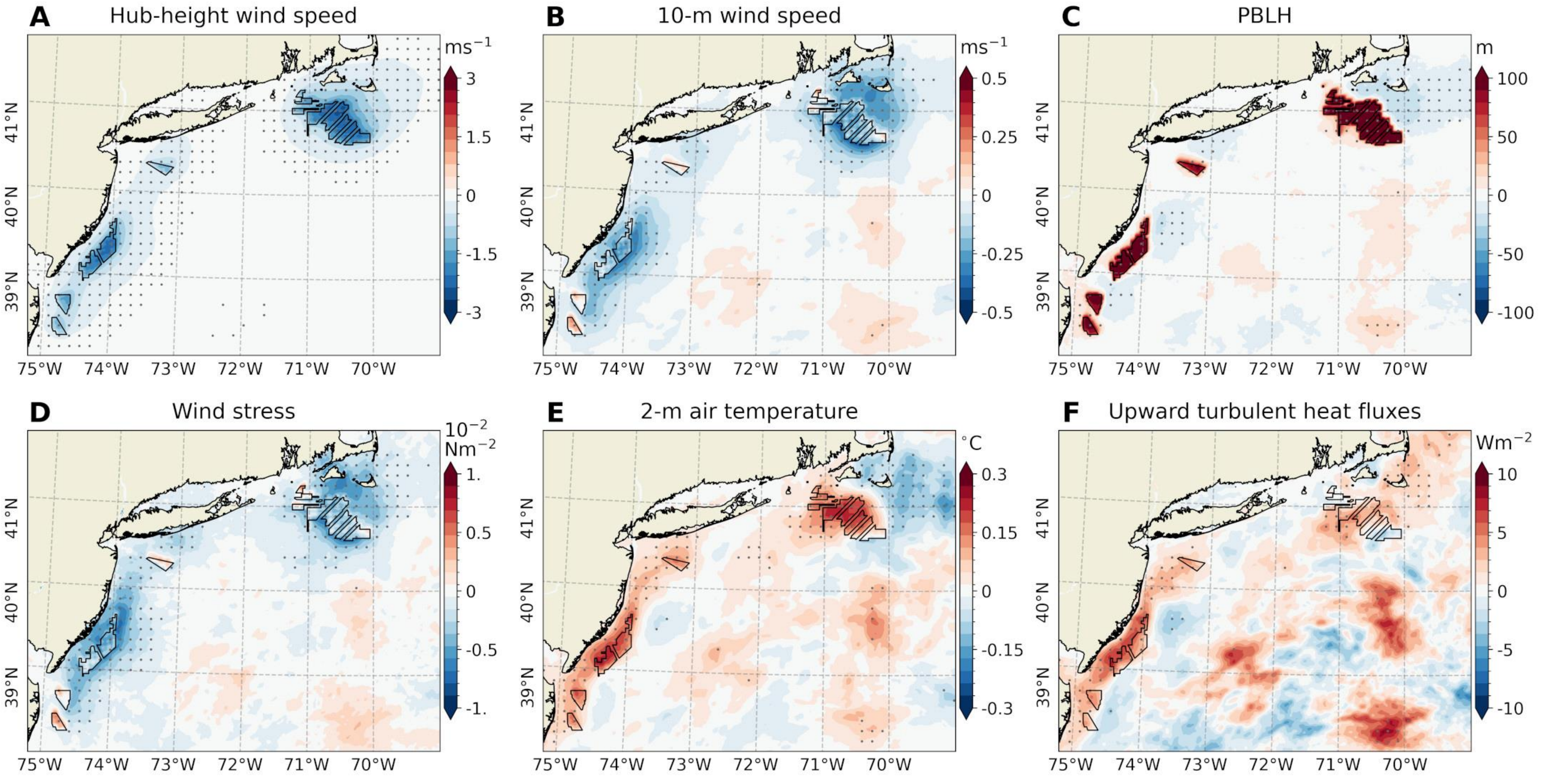

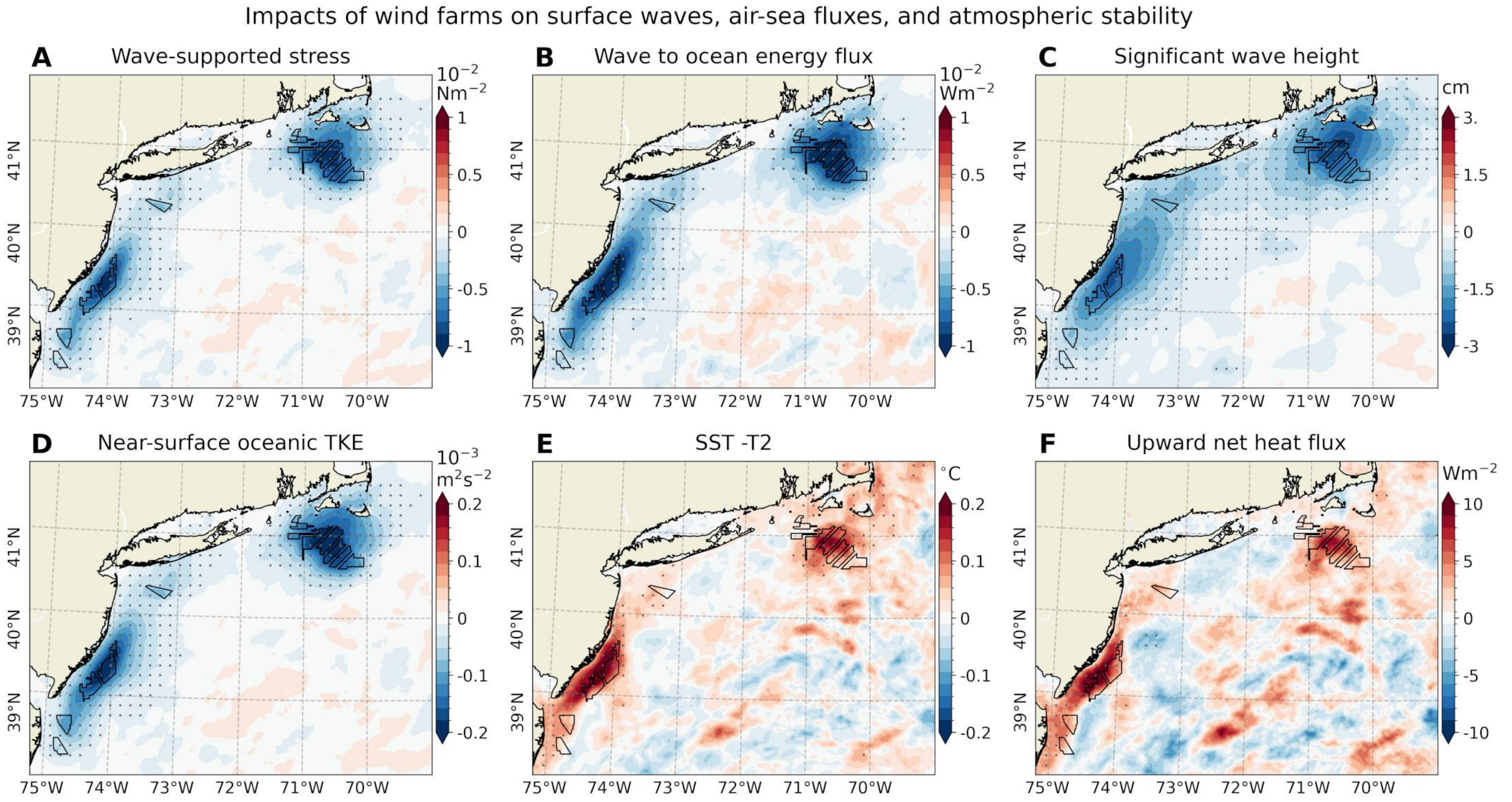

Impacts of wind farms on surface waves, air-sea fluxes, and atmospheric stability
A
Wave-supported stress
10^{-2} Nm^{-2}
B
Wave to ocean energy flux
10^{-2} Wm^{-2}
C
Significant wave height
cm
D
Near-surface oceanic TKE
10^{-3} m^2s^{-2}
E
SST -T2
°C
F
Upward net heat flux
Wm^{-2}
39°N
40°N
41°N
75°W
74°W
73°W
72°W
71°W
70°W

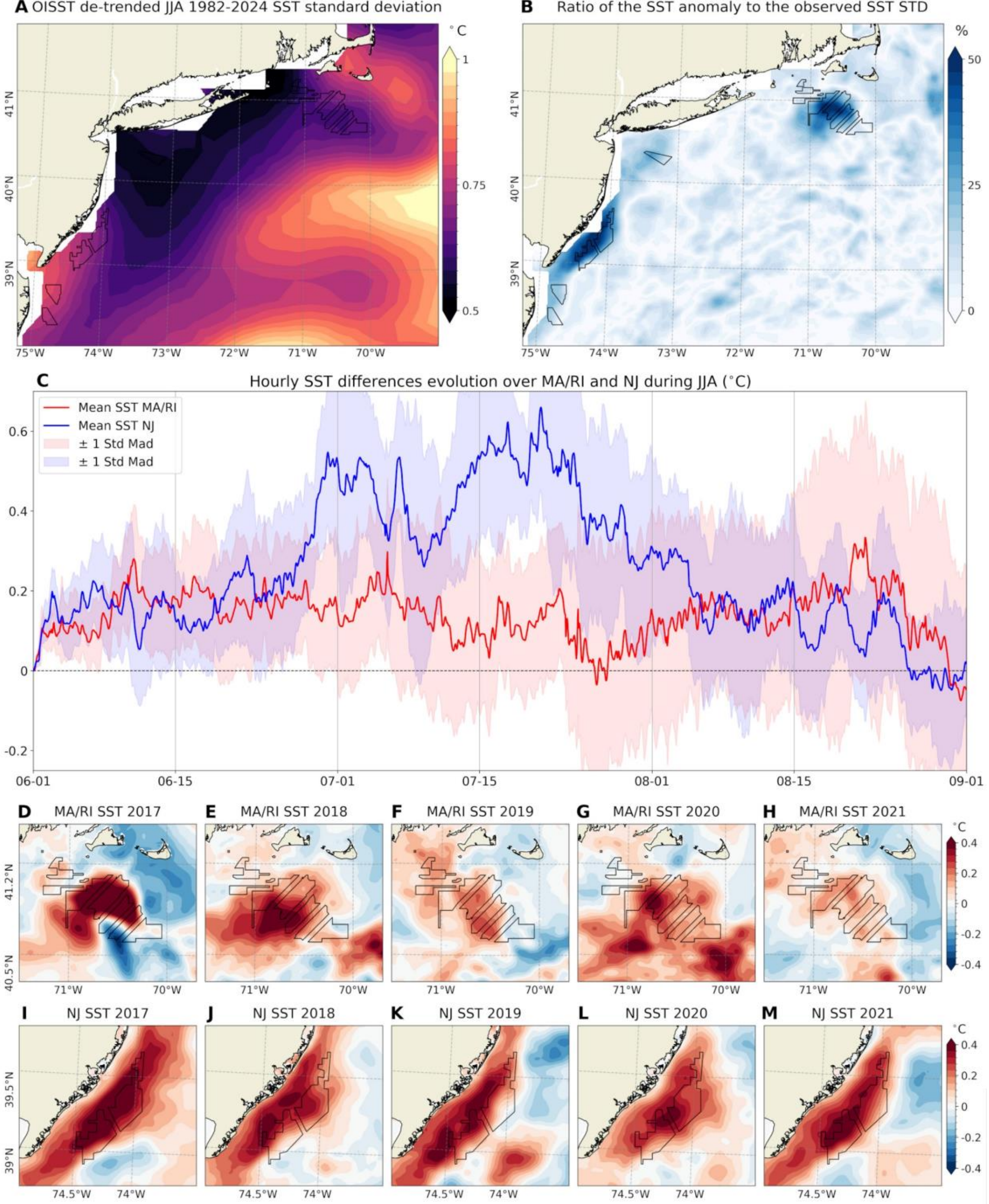

A OISST de-trended JJA 1982-2024 SST standard deviation
°C
1
0.75
0.5
41°N
40°N
39°N
75°W
74°W
73°W
72°W
71°W
70°W
B Ratio of the SST anomaly to the observed SST STD
%
50
25
0
C Hourly SST differences evolution over MA/RI and NJ during JJA (°C)
Mean SST MA/RI
Mean SST NJ
± 1 Std Mad
± 1 Std Mad
0.6
0.4
0.2
0
-0.2
06-01
06-15
07-01
07-15
08-01
08-15
09-01
D MA/RI SST 2017
E MA/RI SST 2018
F MA/RI SST 2019
G MA/RI SST 2020
H MA/RI SST 2021
41.2°N
40.5°N
71°W
70°W
°C
0.4
0.2
0
-0.2
-0.4
I NJ SST 2017
J NJ SST 2018
K NJ SST 2019
L NJ SST 2020
M NJ SST 2021
39.5°N
39°N
74.5°W
74°W

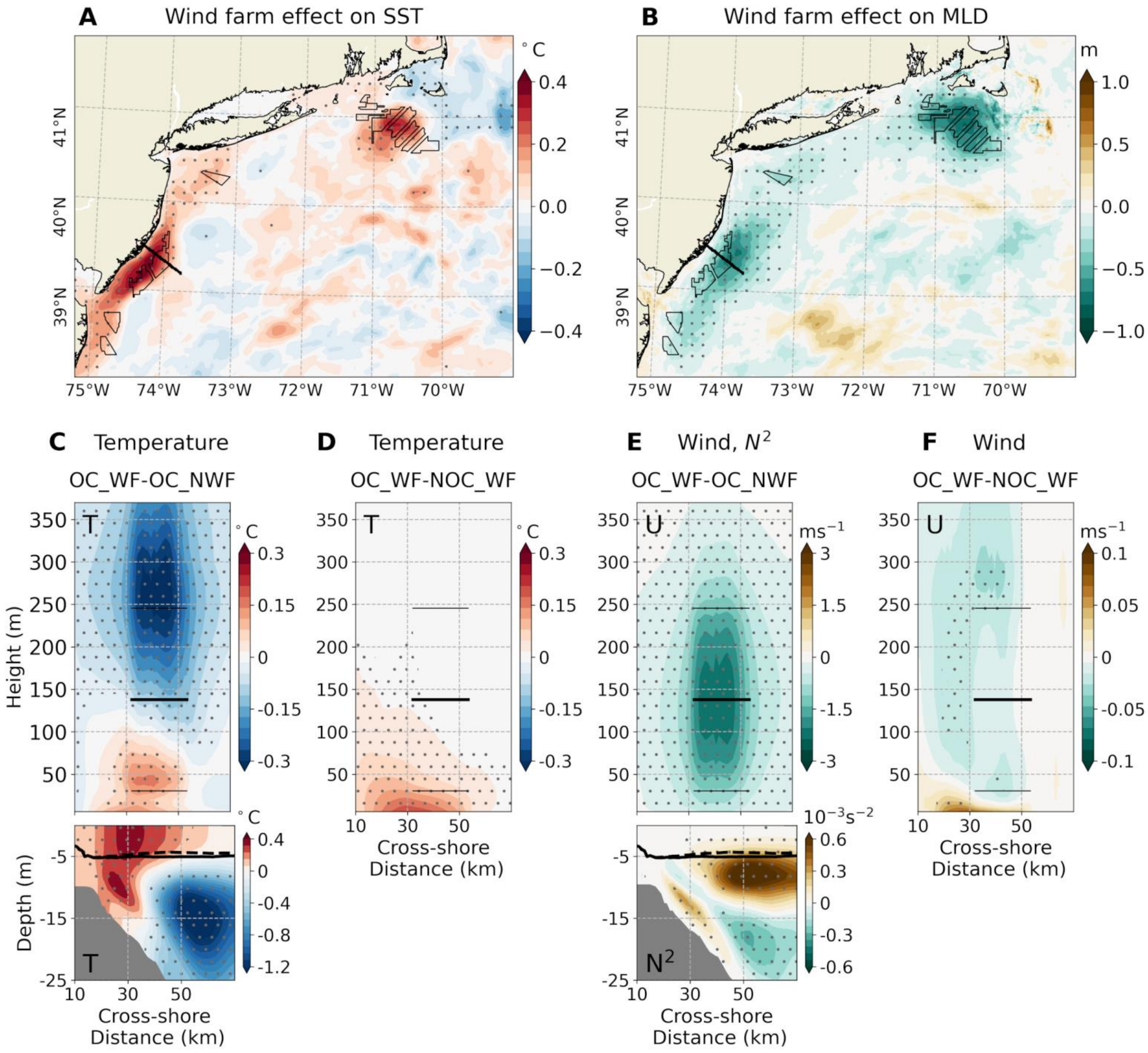

A Wind farm effect on SST
B Wind farm effect on MLD
°C
m
41°N
40°N
39°N
75°W 74°W 73°W 72°W 71°W 70°W
C Temperature
OC_WF-OC_NWF
D Temperature
OC_WF-NOC_WF
E Wind, N^2
OC_WF-OC_NWF
F Wind
OC_WF-NOC_WF
Height (m)
Depth (m)
Cross-shore Distance (km)
ms^{-1}
$10^{-3}s^{-2}$
T
U
N^2

Ocean mixed layer heat budget

$$\underbrace{\frac{\partial \langle T \rangle}{\partial t}}_{\text{TEND}} = \underbrace{-\langle \nabla \cdot (\mathrm{u}T) \rangle}_{\text{HADV}} + \underbrace{\frac{1}{H}(wT)_{z=-h}}_{\text{VADV}} + \underbrace{\left\langle \nabla \cdot \left(\kappa_{\mathrm{h}} \nabla T \right) \right\rangle}_{\text{HMIX}} - \underbrace{\frac{1}{H}\left(\kappa_{\mathrm{v}} \frac{\partial T}{\partial z} \right)_{z=-h}}_{\text{VMIX}} - \underbrace{\frac{\Delta T}{H}\frac{\partial h}{\partial t}}_{\text{ENT}} + \underbrace{\frac{Q_{\mathrm{net}} - Q_{\mathrm{sw}}|_{z=-h}}{\rho c_p H}}_{\text{QFLX}}$$

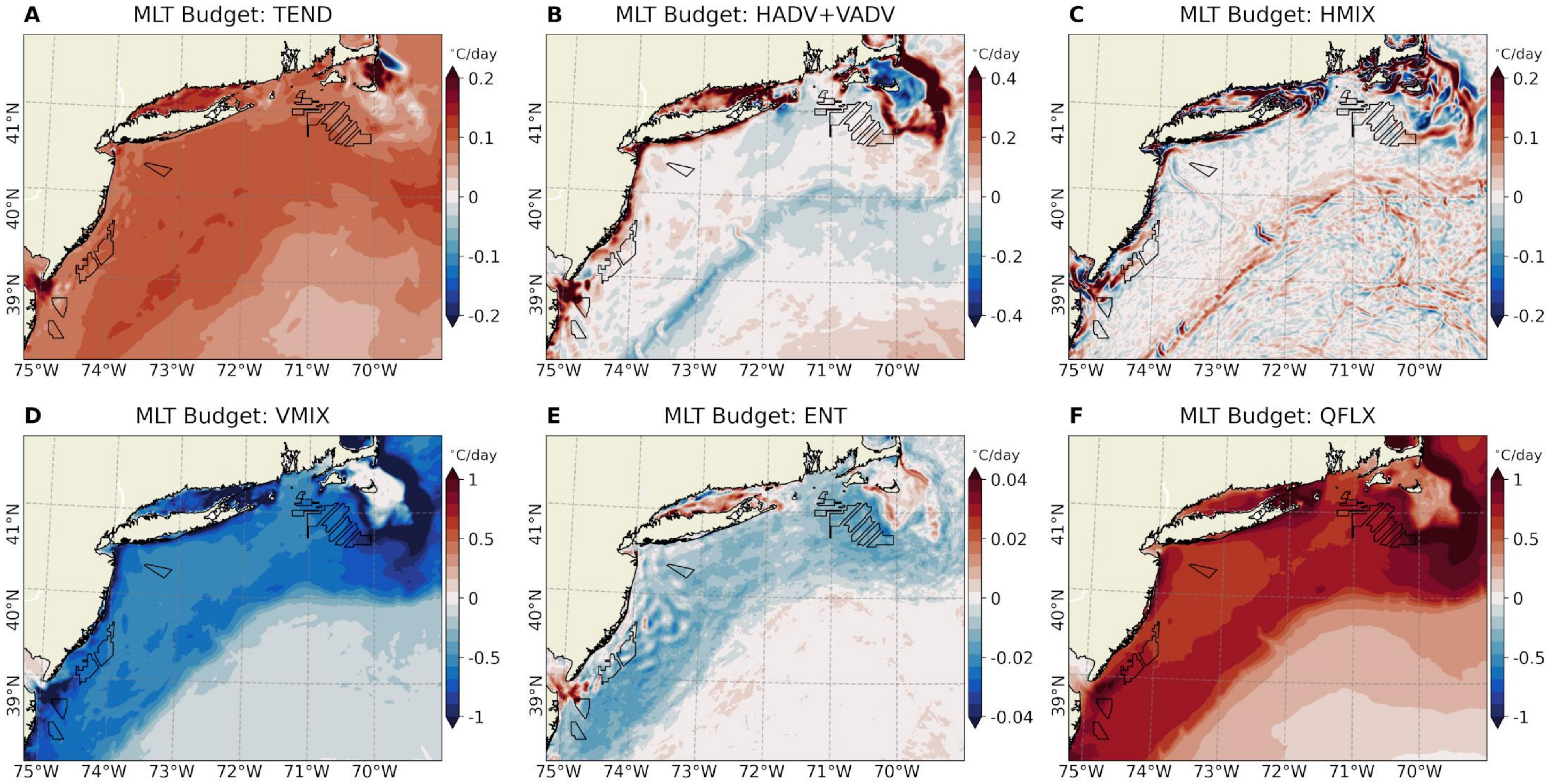

In the unperturbed simulations, the warming of the MLT across the shelf is primarily driven by surface heat flux (QFLX) warming. This warming is partially offset by cooling from VMIX, with a secondary contribution from entrainment (ENT) cooling. Horizontal heat flux divergence (HADV) cools the MLT, which is largely offset by the warming due to vertical temperature advection at the base of the mixed layer (VADV).